UNIVERSITÀ DEGLI STUDI DI NAPOLI FEDERICO II

Scuola Politecnica delle Scienze di Base

CORSO DI LAUREA MAGISTRALE IN
INGEGNERIA STRUTTURALE E GEOTECNICA
CLASSE DELLE LAUREE MAGISTRALI IN INGEGNERIA CIVILE, LM-23

DIPARTIMENTO DI STRUTTURE PER L'INGEGNERIA E L'ARCHITETTURA

TESI DI LAUREA

PROCEDURE TO OPTIMIZE THE STRUCTURAL DESIGN FOR BUILDINGS EQUIPPED WITH HYSTERETIC SLB DEVICES

RELATORE **CANDIDATO** Ch.mo Prof. Ing. Giorgio Serino Riccardo Chianese

Matr. M56/831

CORRELATORI
Ch.mo Prof. Ing. Luis M. Bozzo
Ing. Nuzzo Iolanda

ANNO ACCADEMICO 2019/2020

ABSTRACT

The aim of the thesis is to define a procedure to optimize the structural design of a structure equipped with Shear Link Bozzo (SLB) metallic hysteretic devices taking into account the dissipative effects of the devices through the definition of an equivalent damping calibrated on the results of nonlinear time-history analyses with direct integration.

Part of the work has been carried out during the Erasmus Traineeship at the engineering company*Luis Bozzo Estructuras y Proyectos* in Barcelona (Spain) lasted six months.

The initial part of the thesis is focused on the study of the SLB devices and their mechanical behavior. The Shear Links Bozzo are innovative supplemental energy dissipation devices able to undergo significant plastic deformations when yielding occurs. Widely spread in South America, especially in Perú, Mexico and Ecuador, they are often installed to provide seismic protection of existing and new construction buildings. Their major contribution is to reduce inter-story drifts during an earthquake thus providing an important benefit for non-structural elements and reducing damage to principal framing elements. On the other hand, the possible substitution of the devices after a strong earthquake is easy, cheap and minimally invasive. The SLB metallic hysteretic device is manufactured from a hot laminated steel plate generally modeled so that to obtain a I-shape. Flanges of the device represent the stiffer parts that provide the connection to structural elements. Differently, energy dissipation is concentrated in so-called dissipative windows situated in the web and generated through a milling manufacturing process. Variations of the total width of the device and of the thickness of the dissipative windows allow to obtain devices with quite different stiffness and yielding force, making them suitable for the different shear stresses expected.

The mechanical properties of the SLB device are defined on the basis of a large experimental campaign carried out over the years, particular attention is given to the experimental test of the fourth generation of the SLB devices in which the dissipator shows a great deformation capability passing from a maximum displacement of 30mm

of the previous generation to at least 48mm of the last generation. The increasing deformation capability leads to an increasing in the dissipative capacity.

The two methods commonly used in professional practice for the selection of SLB devices actually are the Direct Iteration and the Inverse Iteration, both are based on response spectrum analysis (RSA). The two iterative procedures lead to the preliminary definition of the dimension of the devices and of the size of the supporting elements (concrete walls or metallic diagonals). A nonlinear time-history analysis is recommended at the end of the process for the assessment of results.

The main focus of the work is on the development of a procedure in order to evaluate the effects of the dissipative capacity of the devices on structural behavior. It is implemented a new procedure in order to evaluate the increase of the total damping of the structure due to the installation of SLB devices. The purpose is to apply the evaluateddamping value to reduce the spectral ordinates and consequently reduce the effects on the structure, thus optimizing the structural design. The procedure provided is based on the comparison of the results in terms of inter-story drift and story shear between linear time-history analysis and nonlinear time-history analysis. The damping value of the linear analysis has to be increase iteratively up to obtain a good correlation of the results between the two analyses. A suite of 11 seismic signals have to be considered, according to ASCE/SEI 7-16, and for each of them the equivalent damping valuehas to be evaluated in order that the results of the linear and nonlinear analysis are compatible. The final modal damping is evaluated reducing the mean value, obtained over the comparison of the 11 nonlinear analysis and the linear one, for the standard deviation, thus allowing the estimation of a conservative value. Theestimated equivalent damping can be applied to the design response spectrum, reducing the ordinates and consequently the effects on the structure, leading to economical advantages in the structural design.

An application of the design procedure and estimation of the equivalent damping has been shown for a complex case study situated in Guadalajara (Mexico). The structure analyzed has been equipped with SLB of fourth-generation designed through the inverse iterative method. The results obtained show an improvement of the structural behavior in terms of inter-story drift and of story shear but because of the not optimal disposition

of the supporting elements on plane due to the architectural restrictions, the structure shows a torsional first mode of vibration. In the specific, it would be preferable to place the walls of concrete symmetrically respect to the center of the building.

The increase of the dissipative capacity of the structure due to the installation of the devices has been considered through the application of the procedure of evaluation of the equivalent damping. The correlation of the results has been done considering the maximum values of the trends of the results for the maximum and the minimum peaks of the acceleration, in both directions. A good correlation of the results has been reached when at least one of the maximum values considered reached a difference range of 10% between the results of the linear analysis and nonlinear analysis. Based on the evidence of the results for 11 seismic signals and considering a restrictive tolerance range, it has been obtained an equivalent damping value of 7%.

The next step was to design the structural elements optimizing the design taking into account the dissipative capacity of the devices installed through the use of the equivalent damping obtained from the previous analyses. To operate in a conservative range it has been decided to adopt the 7% of damping to design only the beams and the conventional 5% of damping to design the columns. For this part of the study, it has been considered a simplified example case, in the specific, it has been considered just one of the frames of the structure, in the most deformable direction, in order to reduce the computational time. The final results led to a reduction of the amount of steel for the beams up to 15% for each floor leading to great economic advantages especially for tall buildings.

The final step of the study was to check the performance of the structural design of the frame considered in the case study through a complete nonlinear time-history analysis considering both geometric and material nonlinearities. In this way it has been possible to have a clear idea of the behavior of the structure designed, checking the development of the plastic hinges and the correct behavior of the devices.

It is important to specify that the definition of a procedure to adopt to optimize the structural design increasing the damping value is in a preliminary phase, it is necessary to analyze much more cases and compare all the results in order to calibrate correctly all

the parameters considered and to define a complete procedure to be implemented in the design process.

TABLE OF CONTENTS

LIST OF FIGURES

LIST OF TABLES

1 INTRODUCTION

Historically, the seismic design has been based upon a combination of strength and ductility. For small, frequent seismic disturbances, the structure is expected to remain in the elastic range, with all stresses well below yield levels, while for strongest earthquake events it is expected upon the inherent ductility of buildings to prevent catastrophic failure while accepting a certain level of structural and nonstructural damage.This philosophy has led to the development of aseismic design codebased on the capacity design leading that the energy dissipation occurs in specially detailed ductile plastic hinge regions of beams and column bases. This design approach is acceptable because structural collapse is prevented and life safety is ensured.

However, alternative design procedures have been developed incorporating earthquake protective systems in the structure.New and innovative concepts of structural protection have been advanced and are at various stages of development. Modern structural protective systems can be divided into three major groups, these can be distinguished by examining the approaches employed to manage the energy associated with the seismic events.

- *Seismic Isolation*:
  A seismic isolation system is typically placed at the foundation of a structure. By means of its flexibility and energy absorption capability, the isolation system partially reflects and partially absorbs some of the earthquake input energy before this energy can be transmitted to the structure.
- *Passive Energy Dissipation*:
  The basic function of passive energy dissipation devices,when incorporated into the superstructure of a building, is to absorbor consume a portion of the input energy,thereby reducing energy dissipation demand on primary structural members and minimizing possiblestructural damage.
- *Semi-active and Active Systems*:

Semi-active and active structural control is an area ofstructural protection in which the motion of a structure is controlled or modified by means of the action of a control system through some external energy supply.

Particularly, this thesis work deals with passive energy dissipation systems focusing especially on metallic hysteretic devices.

In the second chapter have been introduced the basic concepts of passive energy dissipation, focusing the attention on the development and design of the following types of energy dissipation devices: metallic-yielding, friction and viscoelastic. Furthermore, have been described the characteristics of the main devices belonging to this category.

In the third chapter has given particular attention to the Shear Links Bozzo (SLB), a metallic yielding device that represents the main topic of the thesis. It is presented a complete description of the device, regarding its geometry, its behavior under horizontal actions (wind or earthquakes) and its evolution in the years. A great part of the chapter is dedicated to the descriptions of the large experimental campaign carried out over the years paying particular attention to the last that led to the test of the fourth generation of the SLB devices adopted in the case of study. The last part of the chapter has been dedicated to the modeling of the SLB device.

The fourth chapter describes the design procedures for SLB devices commonly used in professional practice, in the specific, the “direct” and “inverse” iterative methods. In the last part, it has been described a new procedure, basedon nonlinear time-history analyses, in order to evaluate the increase of the total damping of the structure due to the installation of SLB devices. The procedure,subject of study of this thesis, has the purpose to reduce the effects acting on the structure increasing the damping value, leading to an optimization of the structural design.

The last part of the work shows an application of the procedures described in the fourth chapter for a complex structure situated in Guadalajara (Mexico). It has been provided theSLB design through the application of the inverse iteration and the evaluation of the equivalent damping according to the procedure described in the previous chapter. A simplified example has been considered in order to verify the results obtained in terms of equivalent damping, designing the structural elements and checking the complete

nonlinear behavior of the simplified structure.The conclusions of the work are provided in the chapter 6 where have been explained the results obtained reporting the final considerations.

2 PASSIVE PROTECTION SYSTEMS

2.1 BASIC PRINCIPLES

In conventional seismic design, acceptable performance of a structure during earthquake shaking is based on the lateral force resisting system being able to absorb and dissipate energy in a stable manner for a large number of cycles. According to the capacity design, energy dissipation occurs in specially detailed ductile plastic hinge regions of beams and column bases. This design approach aims to prevent structural collapse and to ensure life safety.

Alternate design procedures have been developed which incorporate earthquake protective systems in the structure. These systems may take the form of seismic isolation systems or supplemental energy dissipation devices. An examination of the behavior and effects of these systems may begin with the consideration of the distribution of energy within a structure. During a seismic event, a finite quantity of energy is input into a structure. This input energy is transformed into both kinetic and potential (strain) energy which must be either absorbed or dissipated through heat. If there were no damping, vibrations would exist for all time. However, there is always a level of inherent damping which withdraws energy from the system and therefore reduces the amplitude of vibration until the motion ceases. The structural performance can be improved if a portion of the input energy can be absorbed, not by the structure itself, but by some type of supplemental “device”.

This is made clear by considering the conservation of energy relationship (Uang and Bertero, 1988):

$$E = Ek + Es + Eh + Ed$$

- E is the absolute energy input from the earthquake motion,
- Ek is the absolute kinetic energy
- Es is the recoverable elastic strain energy
- Eh is the irrecoverable energy dissipated by the structural system through inelastic or other forms of action
- Ed is the energy dissipated by supplemental damping devices

The absolute energy input **E**, represents the work done by the total base shear force at the foundation on the ground (foundation) displacement. It, thus, contains the effect of the inertia forces of the structure. In the conventional design approach, acceptable structural performance is accomplished by the occurrence of inelastic deformations. This has the direct effect of increasing energy **Eh**. The occurrence of inelastic deformations results in softening of the structural system which itself modifies the absolute input energy. In effect, the increased flexibility acts as a filter which reflects a portion of the earthquake energy. The significant result is that it leads to reduced accelerations and reduced strains in regions away from the plastic hinges. In the case of the presence of seismic protection devices, there will be direct effects of increasing energy **Ed**.

The feature of different passive protection systems is that their operation is activated by the structure's motion: thus they work in feedback, as shown in Fig. 2.1, not requiring any external source of energy.The presence of the external excitation generates the structure's relative displacements that actuate the action of passive energy dissipation systems; consequently their action reduces the structural response.

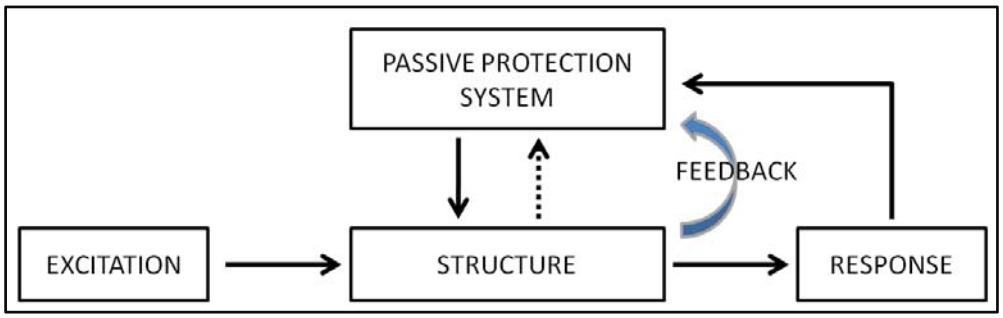

FIGURE 2.1PASSIVE PROTECTION SYSTEM WORKING PRINCIPLE

Modern seismic isolation systems icorporate energy dissipating mechanisms. Examples are high damping elastomeric bearings, lead plugs in elastomeric bearings, mild steel dampers, fluid viscous dampers, and friction in sliding bearings. Another approach to improving earthquake response performance and damage control is that of supplemental energy dissipation systems. In these systems, mechanical devices are incorporated into the frame of the structure and dissipate energy throughout the height of the structure. The means by which energy is dissipated is either yielding of mild steel, sliding friction, motion of a piston or a plate within a viscous fluid, orificing of fluid, orviscoelastic action in polymeric materials addition to increasing the energy dissipation capacity per unit drift of a structure, some energy dissipation systems also increase the strength and stiffness. Such systems are defined as passive control systems and they include the following types of energy dissipation devices: metallic-yielding, friction and viscoelastic.

Energy dissipation systems utilizing fluid viscous dampers will not generally increase the strength or stiffness of a structure unless the excitation frequency is high. In general, the addition of an energy dissipation system will result in a reduction in drift and, therefore, reduction of damage (due to energy dissipation) and an increase in the total lateral force exerted on the structure (due to increased strength and/or stiffness). Reduction of both drift and total lateral force may be achieved only when deformations are reduced to levels below the elastic limit.
Seismic isolation and energy dissipation systems are classified as earthquake protection systems since their function is to mitigate earthquake hazard. Mitigation is defined as the action taken to reduce the consequences of earthquakes, such as seismic strengthening or upgrading, installation of a seismic isolation or energy dissipation system, etc. However, energy dissipation systemsare also useful in reducing dynamic response under wind and other types of service loads. Thus in general, seismic isolation and energy dissipation systems may be termed motion control systems.

Examples of hysteretic systems include devices based on yielding of metals or through sliding friction. Figure 2.2 shows typical force-displacement loops of hysteretic energy

dissipation systems. The simplest models of hysteretic behavior involve algebraic relations between force and displacement.

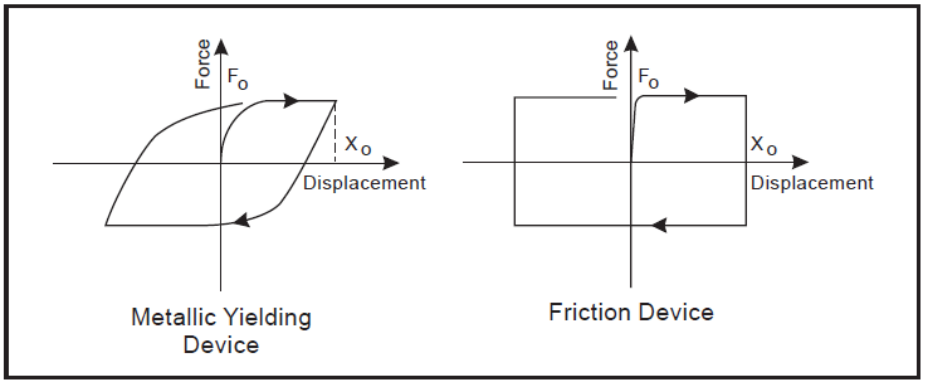

FIGURE 2.2 IDEALIZED FORCE-DISPLACEMENT LOOPS OF HYSTERETIC ENERGY DISSIPATION DEVICES

Viscoelastic energy dissipation systems include devices consisting of viscoelastic solid materials, devices operating on the principle of fluid orificing (e.g. viscous fluid dampers) and devices operating by deformation of viscoelastic fluids. Figure 2.3 shows force-displacement loops of these devices. Typically, these devices exhibit stiffness and damping coefficients which are frequency dependent. Moreover, the damping force in these devices is proportional to velocity, that is, the behavior is viscous. Accordingly, they are classified as viscoelastic systems. A purely viscous device is a special case of a viscoelastic device with zero stiffness and frequency independent properties.

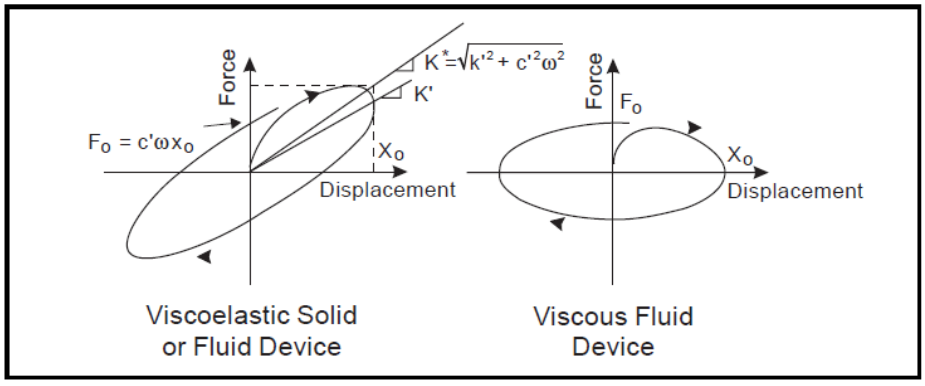

FIGURE 2.3 IDEALIZED FORCE-DISPLACEMENT LOOPS OF VISCOELASTIC ENERGY DISSIPATION DEVICES

Energy dissipation systems which cannot be classified by one of the basic types depicted in Figure 2.2 and 2.3 are classified as other systems. Examples are friction-spring devices with recentering capability and fluid restoring force and damping

devices. Figure 2.4 illustrates the behavior of these devices. While the illustrated loops appear very different from those of Figures 2.2 and 2.3, in reality these devices originate from either hysteretic devices (a friction device with an innovative re-centering mechanism) or fluid viscous devices (a pressurized device to develop preload and re-centering capability, together with fluid orificing for energy dissipation).

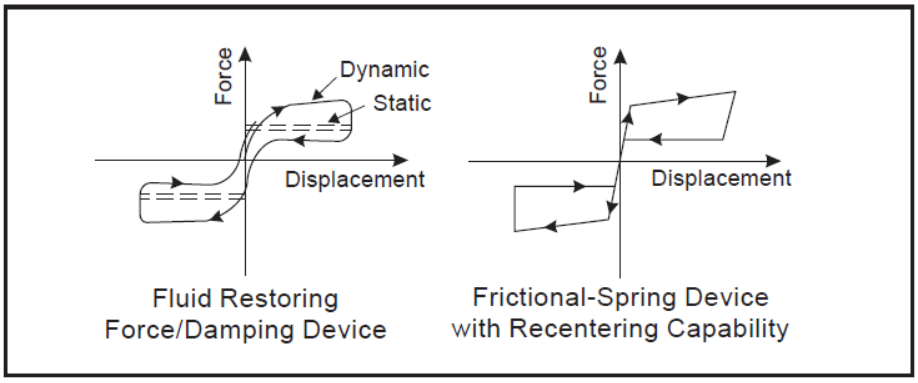

FIGURE 2.4 IDEALIZED FORCE-DISPLACEMENT LOOPS OF OTHER ENERGY DISSIPATING DEVICES

Shape memory alloy devices are also classified as hysteretic (or displacementdependent) systems despite the fact that their force-displacement loops resemble those of Figure 2.4 for other systems, rather than those of Figure 2.2 for hysteretic systems.

	Viscous Fluid Damper	Viscoelastic Solid Damper	Metallic Damper	Friction Damper
Basic Construction		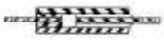	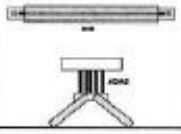	
Idealized Hysteretic Behavior	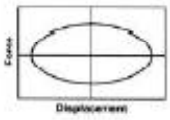	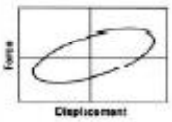	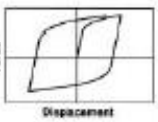	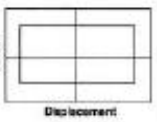
Idealized Physical Model	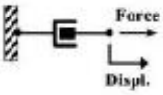	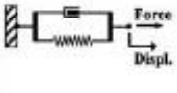	Idealized Model Not Available	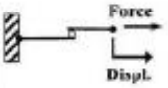
Advantages	- Activated at low displacements - Minimal restoring force - For linear damper, modeling of damper is simplified. - Properties largely frequency and temperature-independent - Proven record of performance in military applications	- Activated at low displacements - Provides restoring force - Linear behavior, therefore simplified modeling of damper	- Stable hysteretic behavior - Long-term reliability - Insensitivity to ambient temperature - Materials and behavior familiar to practicing engineers	- Large energy dissipation per cycle - Insensitivity to ambient temperature
Disadvantages	- Possible fluid seal leakage (reliability concern)	- Limited deformation capacity - Properties are frequency and temperature-dependent - Possible debonding and tearing of VE material (reliability concern)	- Device damaged after earthquake; may require replacement - Nonlinear behavior; may require nonlinear analysis	- Sliding interface conditions may change with time (reliability concern) - Strongly nonlinear behavior; may excite higher modes and require nonlinear analysis - Permanent displacements if no restoring force mechanism provided

TABLE 2-1SUMMARY TABLE OF THE PRINCIPAL ENERGY DISSIPATION DEVICES

2.2 PASSIVE PROTECTION SYSTEMS DEVICES

A large number of passive control systems devices have been developed and installed in structures for performance enhancement under earthquake loads. Discussions presented below are centered around some of the more common devices which have found applications in passive energy dissipation.

2.2.1 METALLIC YIELDING DEVICES

These devices dissipate the energy input to a structure from an earthquake through inelastic deformation of metals. They use mild steel plates with triangular or X shapes so that yielding is spread almost uniformly throughout the material.

Other materials, such as lead and shape-memory alloys, have also been evaluated. Some particularly desirable features of these devices are their stable hysteretic behavior, low-cycle fatigue property, long term reliability, and relative insensitivity to environmental temperature. Hence, numerous analytical and experimental investigations have been conducted to determine these characteristics of individual devices. After gaining confidence in their performance based primarily on experimental evidence, implementation of metallic devices in full-scale structures has taken place.

The earliest implementations of metallic dampers in structural systems occurred in New Zealand and Japan. More recent applications include the use of metallic yielding dampers in the seismic upgrade of existing buildings in Mexico and in the USA.

2.2.1.1 ADAS DISSIPATORS

ADAS (Adding Damping And Sitffness) device is another well-known system developed in the 1980s. This device consists of X-shaped metal plates placed in parallel, as shown in the following figures. Plasticisation occurs at the same time on each plate and the variation in height of the number of plates used allows the structural response to be optimised. Each plate is embedded at both ends and its X-shape optimises energy dissipation throughout its volume.

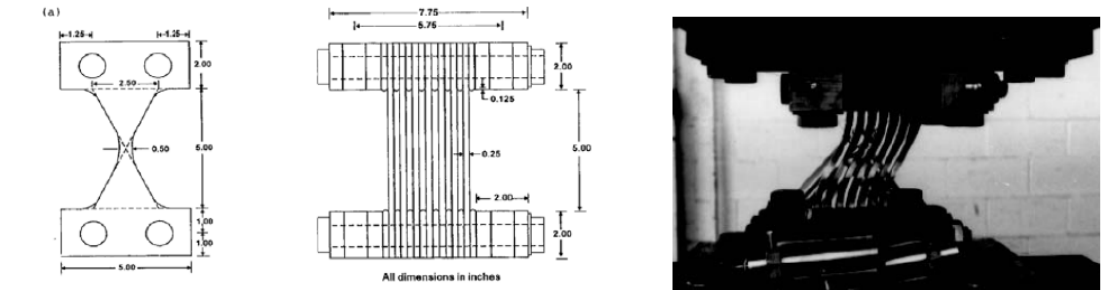

X-shaped mild steel plates device (ADAS) [Perry et al., 1993]

FIGURE 2.5 ADAS DEVICE

These connections are predominantly installed at the junction of the diagonals below the beams but their application has a wide range of alternatives, for example, they can be located in coupled reinforced concrete walls.

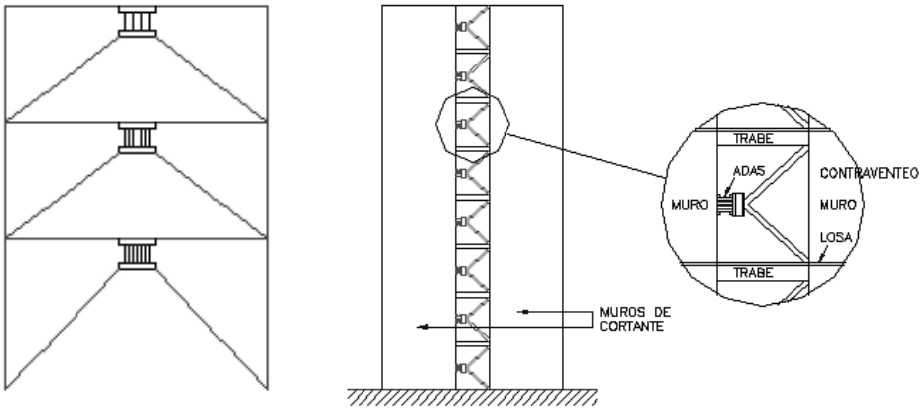

FIGURE 2.6 APPLICATIONS OF ADAS DEVICES

The typical hysteretic response of these connections is stable and without significant degradation after many load cycles.

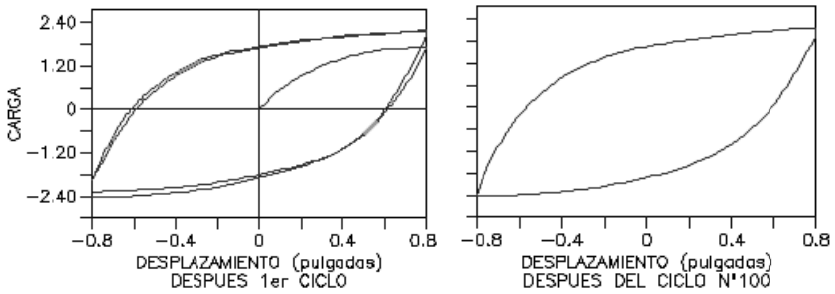

FIGURE 2.7 ADAS HYSTERETIC CYCLES

2.2.1.2 TADAS DISSIPATORS

Another example of dissipator is known as the TADAS system. These devices consist of a set of metal plates, of constant thickness and trapezoidal section, parallel to each other, which are welded to a common base plate and the acting forces are perpendicular to the plane shown.

FIGURE 2.8 TADAS DEVICE

The TADAS dissipator is recessed at the top and hinged at the bottom, so that the plates are deformed by bending in a simple curvature. The TADAS systemis recessed at the top and hinged at the bottom, so that the plates are deformed by bending in a simple curvature. Moreover, the curvature is uniformly distributed and, therefore, plastification can occur simultaneously over the entire height of the plates without concentration of the curvature (Tsai et al. 1993).

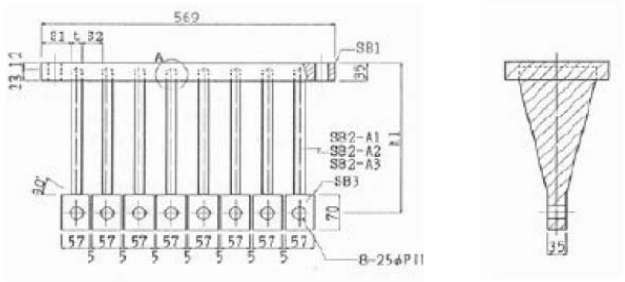

Triangular steel plates device (TADAS) [Tsai et al. 1993]

FIGURE 2.9TADAS GEOMETRY

The following figures show the hysteretic cycles of the dissipator which, as can be seen, are approximately rectangular, which makes it very efficient since the energy dissipated is the enclosed area and is maximum if it is rectangular.

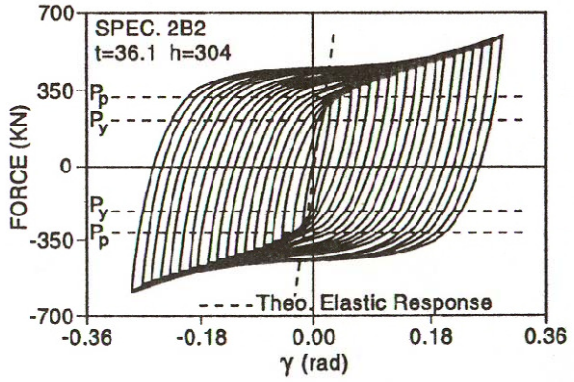

FIGURE 2.10 FORCE-DISPLACEMENT CURVES FOR TADAS DEVICE

2.2.1.3 BUCKLING RESTRAINED BRACE (BRB)

A variation of the devices described above but operating on the same metallic yielding principle is the tension/compression yielding brace, also called the unbonded brace [16,17], which has found applications in Japan and the USA.

Steel braces are lateral load-carrying members used in structures against the wind and earthquake forces. Steel braces carry lateral forces applied to the braced frame in proportion to their axial rigidity. Since the axial rigidity of the brace members is high, they are the most widely used framing systems in seismic zones. One of the largest challenges in the design of these braces is that their tension and compression capacities are not equal. Black et al. [1] found that when the braces are subjected to large tension forces they yield but they exhibit buckling deformation under compressive forces and their axial load-carrying capacity drops suddenly. This unsymmetrical hysteretic behavior in tension and compression causes unstable seismic performance of the steel braced frames. The axial compression capacity of the brace members can be shifted from unstable to stable if they are prevented from buckling.

The BRBs consist of a core steel plate (CP) encased in a concrete-filled steel tube (casing member). A special coating is provided between the core plate and concrete in order to reduce friction.

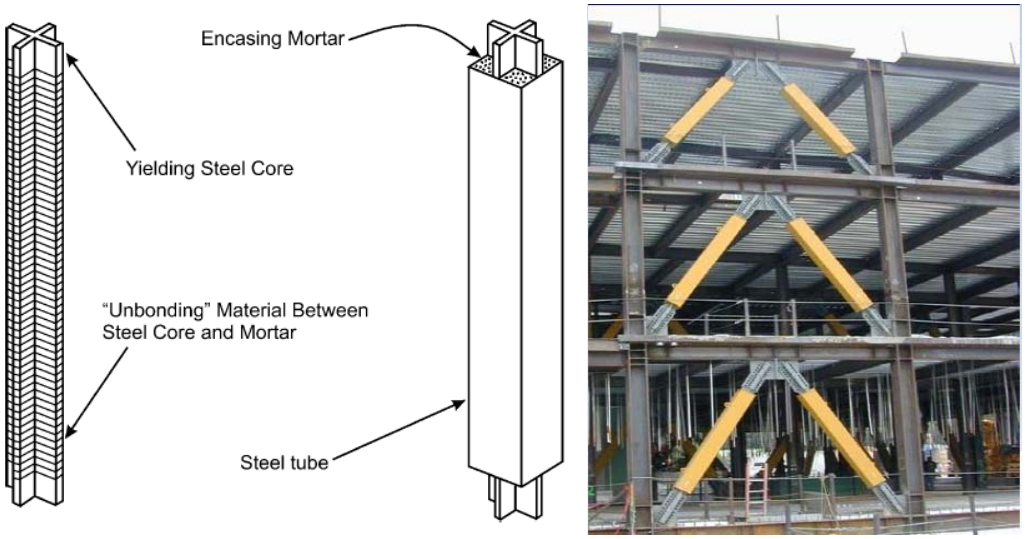

FIGURE 2.11UNBONDED BRACES

Although the CP has negligible compression capacity, its capacity can be increased by using a CM or by restraining its buckling. In this case, the CP may yield in tension or compression or may buckle in high buckling modes. BRBs generally have three parts, namely an unrestrained elastic zone, a restrained elastic zone, and a restrained plastic zone. The unrestrained elastic zone is designed to provide a connection between the BRB and the gusset plate. This zone is also capable of resisting axial demands without buckling when the restrained plastic zone yields in tension and compression. The restrained elastic zone is a transition part of the CP between elastic and plastic behavior. Although this zone has elastic behavior under tension and compression demands, the CM prevents it from buckling. The restrained plastic zone carries the tension and compression forces elastically and plastically.

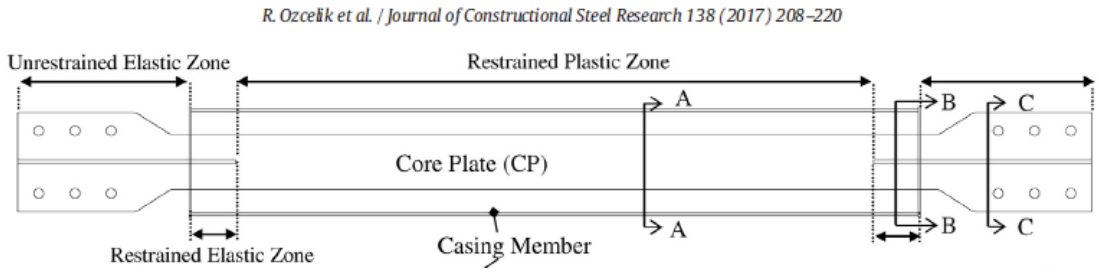

FIGURE 2.12DETAILS OF BRB

Since the purpose of BRBs is to dissipate lateral forces from columns and beams, the connection between the devices and the columns can greatly affect their performance

during an earthquake. Typically the BRB is attached to a gusset, which in turn is welded to the beam and/or column.

For BRBs, there are three types of connections are typically used:

- Welded connection: The BRB is welded to the gusset on site. Although this procedure involves additional hours on site, it can improve the energy transfer mechanism and potentially require smaller BRBs.
- Bolted connection: The BRB is bolted directly on site. It does not require a lot of time or skilled personnel to do so, which greatly simplifies the connection.
- Pin connection: Both the arm and the gusset are designed to accept a pin. This pin connects them together and allows free rotation of the connection.

2.2.1.4 BOZZO SHEAR-LINK DEVICES

Shear Link Bozzo (SLB) is a low-cost hysteretic device, made from a vertical metal profile with horizontal stiffeners to avoid buckling problems and is made of steel. It should be noted that the dissipative part is formed by milling, which allows the stiffeners to be of small dimensions and no elements have to be welded in the plasticizing zone, thus eliminating the residual stresses that this would generate (Bozzo, Part 2, et al 2001).It has been already adopted for several applications in South America, both for new constructions and seismic retrofit of existing buildings.

FIGURE 2.13 BOZZO SHEAR-LINK

The previous image, fig. 2.13, shows an “SLB” device with its crenelated or comb-type connection that transmits shear but no axial or bending force. The stability of the device and its connection to structural elements is provided by vertical stiffeners (VS) and external flanges (EF) respectively, whereas energy dissipation is concentrated on the ‘dissipative windows’ (DWs) of the web. Moreover, thanks to small transversal dimensions of the milled areas, uniform energy dissipation is ensured for very low values of shear stresses, since the device requires low shear forces to yield. Consequently, it has the advantage of starting to dissipate energy at very small deformations with the potential of reducing inter-storey drifts for buildings, thus providing an important benefit for non–structural elements. Stable hysteretic curves imply that the shear link energy dissipation device must be designed so that yielding is reached before the buckling critical load, since it causes a significant reduction of the dissipative capacity (Rai and Wallace, 1998).

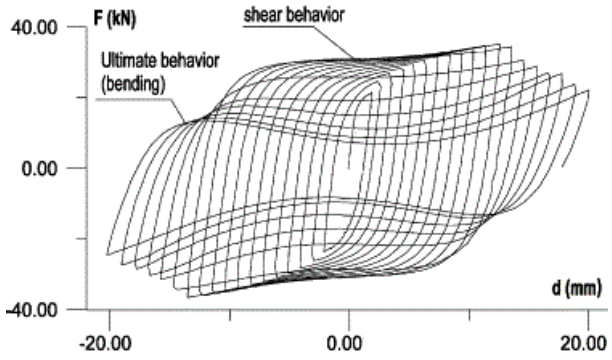

FIGURE 2.14FORCE-DISPLACEMENT CURVES FORSLB DEVICES

Shear link's properties make it suitable to be used in non-standard dual systems to protect the structural and non-structural elements. It may be used as a link between the flexible frame and a conventional steel braced system, or it may be used as link between flexible frames and concrete walls (Figure 2.15). These shear energy dissipation devices have the characteristic of not transferring axial load, being hinged at one end thanks to a special connection intrinsic to the dissipator itself.

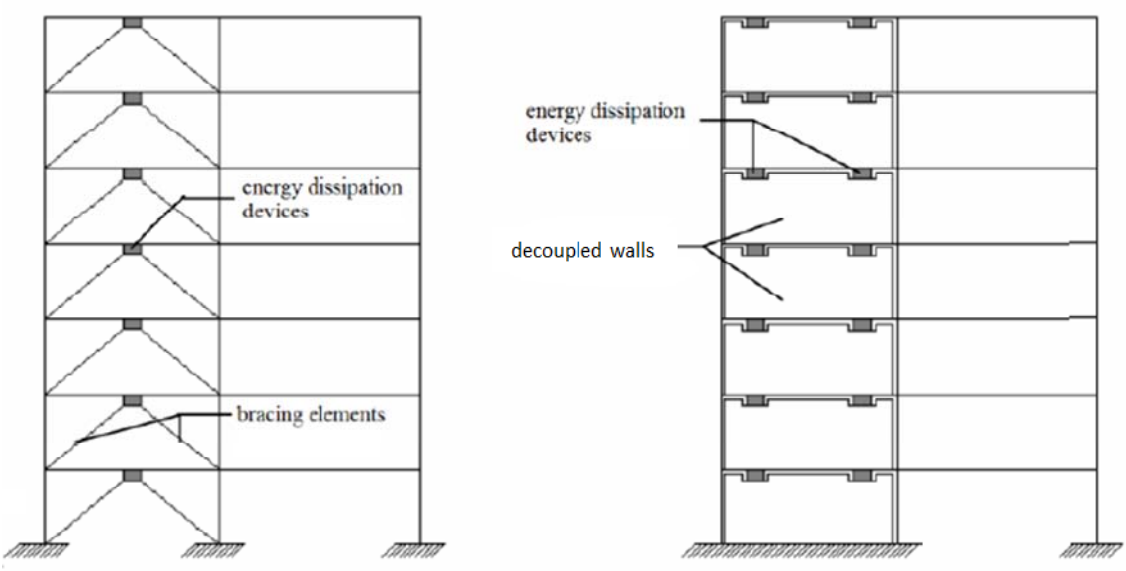

FIGURE 2.15 POSSIBLY APPLICATIONS OF "SLB"DEVICES

The "SLB" devices will be discussed in more details in the next chapter.

2.2.2 SHAPE MEMORY ALLOYS (SMA)

In recent years, a new class of materials referred to as shape memory alloys (SMA) have been considered for application in passive dampers. These metals collectively exhibit somewhat counter-intuitive behavior as a result of reversible temperature or stress induced transformations between martensitic and austenitic crystalline phases. Consider, for example, the shape memory effect. An SMA specimen in its low temperature martensitic phase is first distorted in an apparently permanent manner. The temperature of the specimen is then elevated above a critical level, inducing a transformation to the austenitic phase. As a consequence, the specimen returns to its original undistorted shape.

Of more direct interest for passive energy dissipation, however, is the characteristically large hysteresis loop that is obtained during cyclic loading of SMA materials in the martensitic phase, and the so-called superelastic behavior that occurs for loading above the critical temperature.

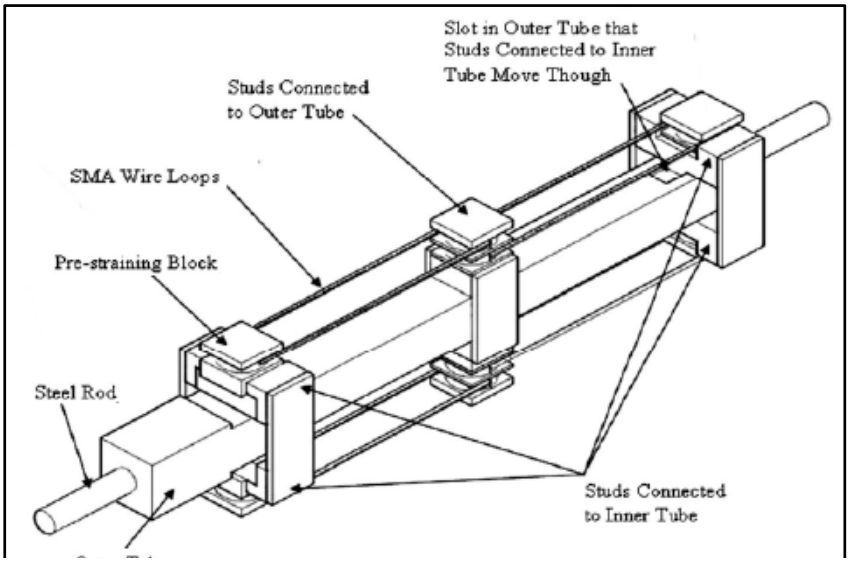

FIGURE 2.16 SMA DEVICE

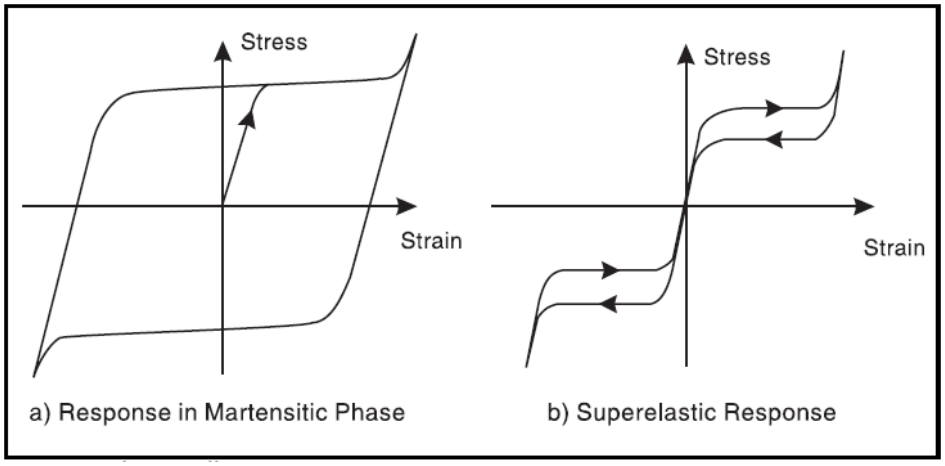

FIGURE 2.17STRESS-STRAIN RESPONSE OF SHAPE MEMORY ALLOYS

The most important application is the restoration of the Basilica of San Francesco inAssisi - Italy, which was severely damaged during the earthquake of 1997.

FIGURE 2.18BASILICA OF SAN FRANCESCO IN ASSISI – ITALY

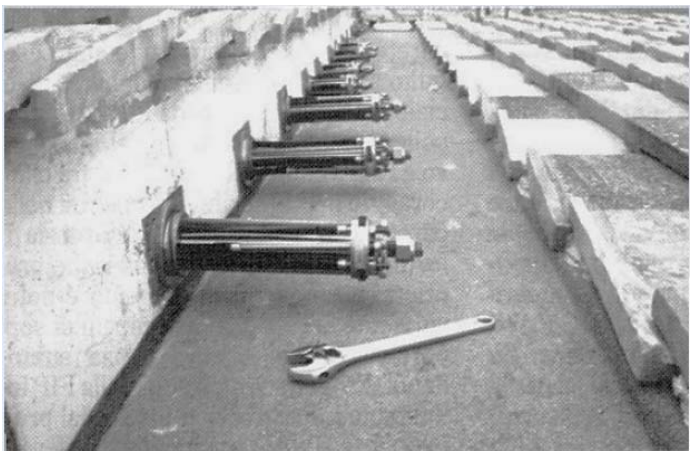

FIGURE 2.19 INSTALLATION OF SHAPE MEMORY ALLOY DEVICES

Shape memory alloy devices were used to connect the roof to the walls of the two tympana of the transepts.

2.2.3 FRICTION DAMPERS

Friction dampers utilize the mechanism of solid friction that develops between two solid bodies sliding relative to one another to provide the desired energy dissipation. Several types of friction dampers have been developed for the purpose of improving seismic response of structures. During cyclic loading, the mechanism enforces slippage in both tensile and compressive directions. Generally, friction devices generate rectangular hysteretic loops, similar to the characteristics of Coulomb friction, guaranteeing large energy dissipation and, moreover, they are insensitive to environmental temperature's excursions. It is also important to consider that the behavior of the devices could change with time due to the interface condition; Consequently it is difficult to ensure a friction coefficient independent by time and by device's status, although, it has been observed that if the structure remains in the elastic field the friction coefficient variation with time does not influence significantly structural response (Bozzo and Barbat 1995). A further disadvantage is that if restoring forces are not provided, a structure equipped with friction dampers may present permanent displacements after a strong ground motion.
In recent years, there have been a number of structural applications of friction dampers aimed at providing enhanced seismic protection of new and retrofitted structures.

2.2.3.1 X-BRACED FRICTION DAMPER

The Pall friction damper is made of a set of special steel plates, which can create the convenient frictional performance. These plates are bolted together with a high strength screws and they are designed not to slip during wind. These dampers slide over each other at the determined optimum slip load prior to yielding of structural members and dissipate the big portion of the earthquake energy. This makes the structure remain in the elastic range or delay the yielding of the structural member during major earthquake.

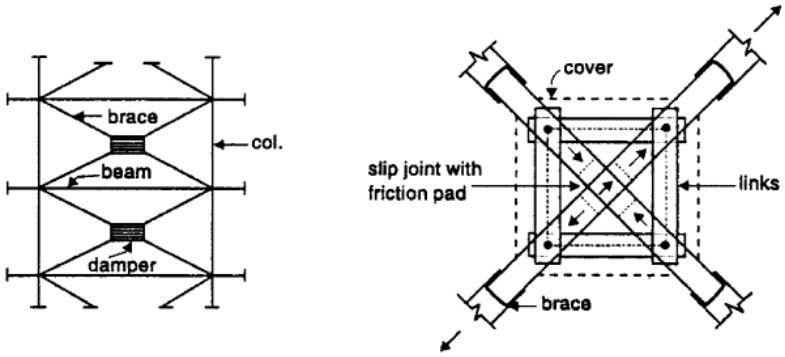

FIGURE 2.20 X-BRACED FRICTION DAMPER

2.2.3.2 WIRE ROPE ISOLATORS

Wire rope isolators consist of wire rope strands held between two metal retainer bars in the form of helix shape or polycal shape (Figure 2.21). As the name implies, wire rope isolators use metal wire rope made up of individual wire strands that are in frictional contact with each other. WRI can provide flexibility in all directions and possess inherent damping characteristic derived from rubbing and sliding friction between the intertwined cables. It is therefore a kind of friction-type damper which adopts stranded wire rope as the elastic component and utilities friction damping (Coulomb damping) between the individual wire strands. This friction dominant property causes the viscous damping in WRI to be relatively insignificant. The advantages of WRI include wide temperature range operations between -100°C to +250°C and less susceptible to the detrimental effects of environmental conditions like extreme temperature, salt, fog, grease, radiation, dust and low manufacturing cost. The polycal type of WRI is primarily used for micro mechanical and electronic applications. For heavy machinery applications the helical WRI is used.

FIGURE 2.21 WIRE ROPE ISOLATORS

2.2.3.3 DAMPTECH FRICTION DEVICE

This friction damper device consists of several steel plates rotating against each other in opposite directions. The steel plates are separated by several shims of friction pad material producing friction with the steel plates. When an external force excites a frame structure the girder starts to displace horizontally due to this force. The damper will follow the motion and the central plate will rotate around the hinge. The horizontal plates will rotate in opposite direction to the central plate because of the tensile forces in the bracing elements. When the applied forces are reversed, the plates will rotate in opposite way. During this process the damper is dissipating mechanical energy by means of friction between the sliding surfaces in to thermal energy (heat) and thus minimizing the vibration of the frame structure.

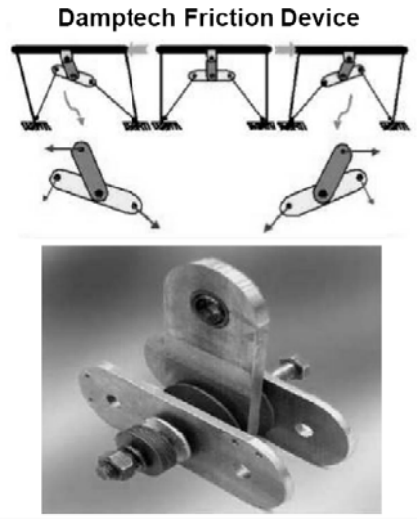

FIGURE 2.22DAMPTECH FRICTION DEVICE

2.2.3.4 SUMITOMO FRICTION DAMPER (SFD)

The friction damper was designed and developed by Sumitomo Metal Industries, Ltd., Japan.It is a cylindrical device with friction pads that slide directly on the inner surface of the steel casing of the device.

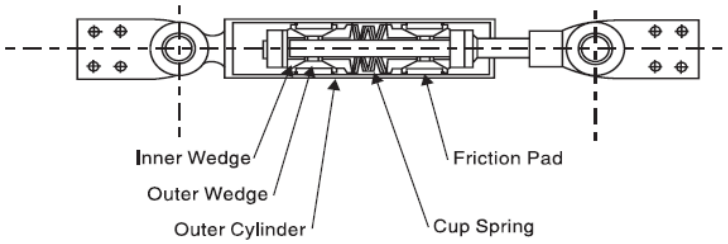

FIGURE 2.23 UNIAXIAL FRICTION DAMPER

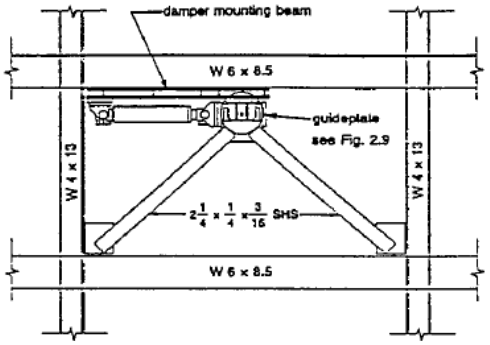

FIGURE 2.24INSTALLATION OF UNIAXIAL FRICTION DAMPER

2.2.4 VISCOELASTIC DAMPERS

This grouping includes viscoelastic solid dampers and viscoelastic fluid dampers, with the latter expanded to incorporate devices based upon both fluid deformation and orificing.

Viscoelastic materials used in structural applications are usually copolymers or glassy substances that dissipate energy through shear deformation. The response of these viscoelastic materials under dynamic loading depends upon the frequency of vibration, the level of strain, and the ambient temperature. Viscoelastic dampers have no threshold or activation force level, and thus they dissipate energy for all levels of earthquake excitation. This contrasts with the behavior of the friction dampers, which, for forces less than the slip force, do not slip and thus do not dissipate energy.

Significant advances in research and development of VE dampers, particularly for seismic applications, have been made in recent years through analyses and experimental tests. However, in many applications, the behavior is confined to the linear range. This often greatly simplifies the required analysis procedures. Furthermore, since energy dissipation occurs even for infinitesimal deformations, viscoelastic devices have potential application for both wind and seismic protection.

2.2.5 VISCOELASTIC SOLID DAMPER

A typical viscoelastic (VE) damper, which consists of viscoelastic layers bonded with steel plates, is shown in Figure 3.12. When mounted in a structure, shear deformation and hence energy dissipation takes place when the structural vibration induces relative motion between the outer steel flanges and the center plate.

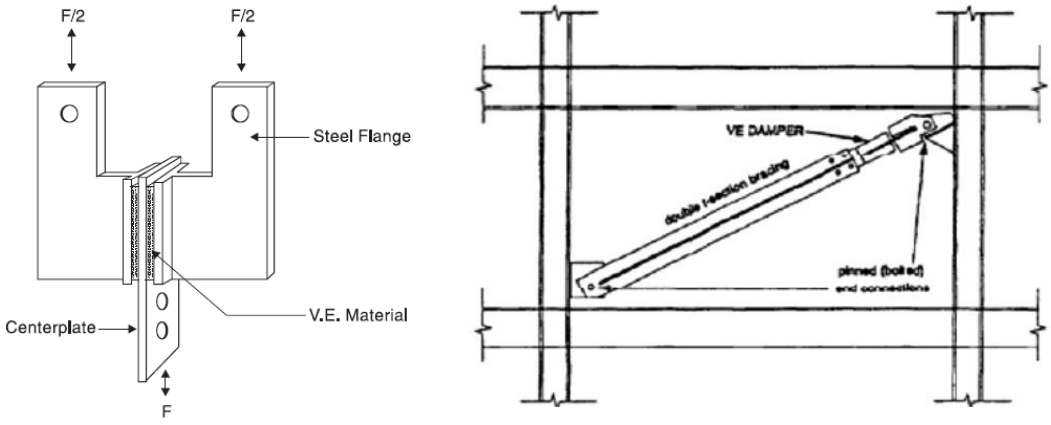

FIGURE 2.25TYPICAL VISCOELASTIC SOLID DAMPER CONFIGURATION

2.2.6 VISCOELASTIC FLUID DAMPER

A VF damper generally consists of a piston within a damper housing filled with a compound of silicone or similar type of oil, and the piston may contain a number of small orifices through which the fluid may pass from one side of the piston to the other. Thus, VF dampers dissipate energy through the movement of a piston in a highly VF based on the concept of fluid orificing.

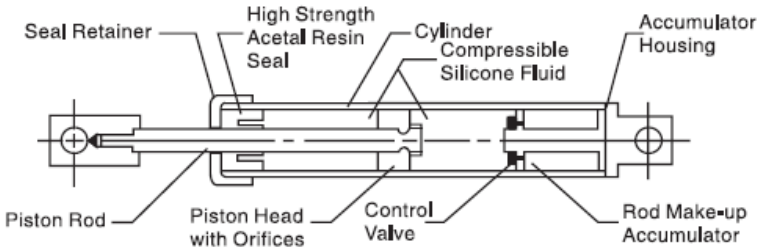

FIGURE 2.26 ORIFICED FLUID DAMPERS

2.2.6.1 VISCOUS DAMPING WALL

In this design, the piston is simply a steel plate constrained to move in its plane within a narrow rectangular steel container filled with a viscous fluid. For typical installation in a frame bay, the piston is attached to the upper floor, while the container is fixed to the lower floor. Relative interstory motion shears the fluid and thus provides energy dissipation.

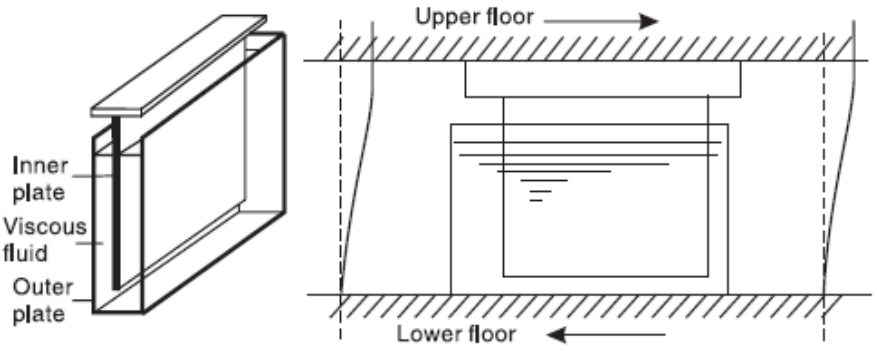

FIGURE 2.27 VISCOUS DAMPING WALL

3 SHEAR LINKS BOZZO DEVICES

3.1 DESCRIPTION OF THE SLB SYSTEM

The “Bozzo Shear link” (SLB) consists of a metallic yielding device first developed at the University of Girona, Spain, in 1997, belonging to the family of hysteretic passive control devices. They can provide additional source of energy dissipation through metals yielding mechanism, when properly introduced within a frame structure.The SL device system ismadefrom a hot laminated steel plate which is generally modeled so that to obtain an I-shape.

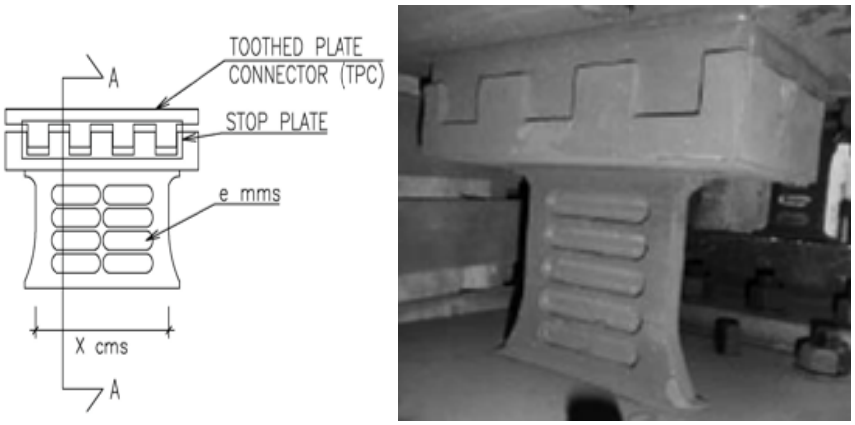

FIGURE 3.1 SHEAR LINK BOZZO

The flanges of the device represent the stiffer parts and are employed to make the connection to structural elements.Differently, energy dissipation is concentrated at the web where “dissipative windows” with reduced thickness are generated through a milling manufacturing process. Wide ranges of SL’s dissipation capacities can be obtained simply varying the height, width and thickness of the dissipative windows and web stiffeners.Initially, it works according to a “shear mode”, with uniform shear distribution in the web and an almost linear deformation (see Figure 3.2 a). As a result,

energy dissipation is mainly concentrated in the latter. After web's degradation, stiffeners continue dissipating energy in a flexural mode, leading to a robust system able to dissipate energy also after web's degradation. At this step the element behaves like a Vierendeel beam, characterized by a typical frame deformation (see Figure 3.2 b).

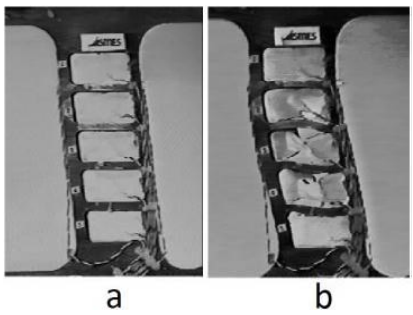

FIGURE 3.2 WORKING MODES OF SLB DEVICE: (A) SHEAR AND (B) BENDING STAGES

Generally, the energy dissipation provided by the "bending mode" is not taken into account, ensuring an additional safety factor. It is worth noticing that after milled areas failure, stiffness is quite reduced and so hysteretic curves are characterized by larger displacements and lower forces than the ones proper of the "shear mode" (see Figure 3.3).

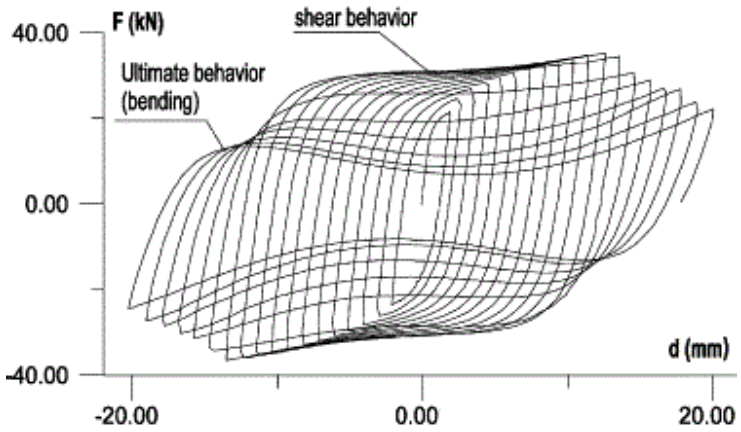

FIGURE 3.3 SHEAR LINK TYPICAL HYSTERETIC CURVES

Designing a shear link energy dissipation device means todefine several parameters, apart from steel class, i.e.: totalheight, dissipative height, width, thicknesses, position anddimension of stiffeners. This variability allows to obtaindevices with quite different

stiffness and yielding force,making them suitable for the different shear stresses expectedin several points of the structure or at different stories. Stable hysteretic curves imply that the SL energydissipation device must be designed so that yielding is reachedbefore buckling of the thinner "windows" takes place, since it causes a significant reduction of the dissipative capacity. For this reason these devices are usually characterized by horizontal and vertical stiffeners (corresponding to the thicker elements of the device) between milled areas. Design of devices has to properly consider the web buckling check.

Different generations have been proposed and investigated both numerically and experimentally during last 20 years (Fig. 3.4), aiming at optimizing their mechanical performance.

FIRST GENERATION,2002 SECOND GENERATION,2016

THIRD GENERATION,2019 FOURTH GENERATION,2020

FIGURE 3.4SLB GENERATIONS

- The first device was characterized by two columns of dissipative windows in the web and a bolted connection, the role of the tolerance between holes and bolts was analyzed through a parametric analysis.

- The second SL generation, characterized by heights, as well as stiffeners' thickness, mainly unvaried with respect to the previous geometry. The connection is totally bolted, in order to avoid welding and make easier installation and replacement process during lifetime of the building. As a difference with respect to previous generation, the number of dissipative windows, always distributed intwo columns, is increased from 2 to 4, reducing their height but significantly increasing their width, in order to enhance ductility as well as to improve web buckling resistance. A further innovation is the adoption of slotted holes for connection on one side, with the aim to avoid axial load transferred from the upper beam to the device and vice versa.
- The third generation has the peculiarity of being installed by means of flanged connections that prevent axial load transfer to the dissipator allowing the devices to be freely incorporated into the structure both in plan and in height. However, fixing the device at one end, while providing a variety of benefits, reduces the total energy dissipated compared to a system fixed at both ends.
- The prototype of the fourth generation has the prupose to increase the deformation capacity of the devices, to reach this a first option is to increase their height and a second option is to increase the height of the dissipative windows.The height of the SLB3 devices is 155mm, so in order to increase the deformation capacity without compromising the stability, a height of 270mm was set and the windows were enlarged from 25mm to 50mm. It is important to highlight that also the SLB of fourth generation presents a "toothed" connection in order to prevent axial loads transfer.

Design parameters for the devices are defined in the designing table provided by SLBs' manual [ANÁLISIS Y DISEÑO UTILIZANDO DISIPADORES SÍSMICOS TIPO SLB EJEMPLOS DE APLICACIÓN - 2019.](Table 2):

The standard devices are currently manufactured with ASTM A36 steel (Fy 2530kg / cm^2). Each specimen is denoted as 'SLB*NX_Y*,' where*N* represents the generation of the

device,*X* represents the web width (in cm), and*Y* represents the thickness of the "dissipative windows" (in mm).

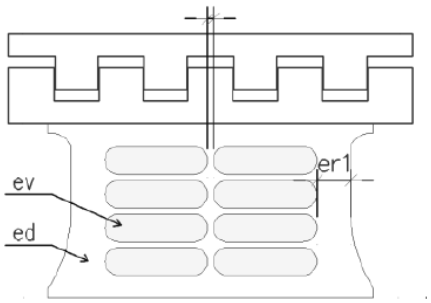

FIGURE 3.5 GEOMETRIC PARAMETERS

Mechanical parameters are reported in the columns of the table where K1 and K2 refer, respectively, to the initial stiffness (elastic stiffness) and post-elastic stiffness expressed in kN/cm, Fy refers to the yielding force expressed in kN, Dy is the displacement at yielding point expressed in mm, Fmax refers to the maximum strength of the device expressed in kN, and, finally, EDrefers to the dissipated energy within a complete cycle.

Parámetros de diseño para los disipadores SHEAR LINK BOZZO										
Dispositivo	ed (mm)	er1 (mm)	er2 (mm)	ev (mm)	K_1 (KN/cm)	K_2 (KN/cm)	D_y (mm)	F_y (KN)	$F_{Máx}$ (KN)	E_D (KN.cm)
SLB2 6_2	19	13	-	2	363.33	9.75	0.980	35.60	69.01	87.08
SLB2 6_3	19	13	-	3	397.80	10.75	1.031	41.00	79.21	99.25
SLB2 6_4	19	13	-	4	421.73	11.65	1.065	44.90	88.58	108.31
SLB2 6_5	19	13	-	5	439.60	12.78	1.078	47.40	96.67	115.18
SLB2 8_2	19	15	-	2	592.87	13.86	0.811	48.10	92.76	119.78
SLB2 8_3	19	15	-	3	676.27	15.38	0.858	58.00	107.57	141.77
SLB2 8_4	19	15	-	4	737.00	16.28	0.900	66.30	120.87	159.39
SLB2 8_5	19	15	-	5	784.27	17.43	0.927	72.70	133.29	173.71
SLB2 10_2	19	20	-	2	893.40	19.15	0.761	68.00	128.71	168.89
SLB2 10_3	19	20	-	3	1039.13	21.57	0.780	81.10	148.63	198.84
SLB2 10_4	19	20	-	4	1149.53	22.96	0.809	93.00	166.26	224.54
SLB2 10_5	19	20	-	5	1237.80	14.93	0.906	112.20	182.26	246.55
SLB2 15_2	19	20	-	2	1571.47	31.17	0.648	101.80	199.61	258.66
SLB2 15_3	19	20		3	1961.47	37.36	0.643	126.10	240.15	319.16
SLB2 15_4	19	20	-	4	2290.27	42.03	0.654	149.70	276.57	373.16
SLB2 15_5	19	20	-	5	2575.60	45.69	0.670	172.50	310.13	424.52
SLB2 20_2	19	25	5	2	2073.33	37.83	0.601	124.60	243.14	316.64
SLB2 20_3	19	25	5	3	2630.13	46.27	0.597	156.90	298.30	396.26
SLB2 20_4	19	25	5	4	3105.53	53.03	0.606	188.30	348.53	470.63
SLB2 20_5	19	25	5	5	3520.20	58.63	0.620	218.40	395.71	540.18
SLB3 25_2	25	30	5	2	3214.07	58.98	0.606	194.80	383.50	494.69
SLB3 25_3	25	30	5	3	4046.67	70.69	0.589	238.20	457.15	602.54
SLB3 25_4	25	30	5	4	4783.20	81.04	0.585	279.60	526.49	703.70
SLB3 25_5	25	30	5	5	5447.47	90.85	0.586	319.00	592.39	799.88
SLB3 25_6	25	30	5	6	6064.13	99.65	0.590	357.10	655.63	891.40
SLB3 25_7	25	30	5	7	6644.13	107.41	0.594	394.50	716.83	979.51
SLB3 25_8	25	30	5	8	7191.47	114.57	0.599	430.70	776.40	1064.12
SLB3 25_9	25	30	5	9	7711.07	120.73	0.605	466.40	834.90	1145.71
SLB3 30_2	25	30	5	2	3666.73	64.22	0.578	212.10	415.33	539.19
SLB3 30_3	25	30	5	3	4717.00	78.76	0.563	265.70	507.23	672.79
SLB3 30_4	25	30	5	4	5661.33	92.21	0.560	316.90	594.62	799.16
SLB3 30_5	25	30	5	5	6525.67	104.93	0.561	366.10	678.62	920.34
SLB3 30_6	25	30	5	6	7336.60	116.45	0.565	414.20	759.77	1036.63
SLB3 30_7	25	30	5	7	8106.07	126.92	0.569	461.30	838.79	1149.06
SLB3 30_8	25	30	5	8	8840.00	135.93	0.575	508.00	915.50	1257.99
SLB3 30_9	25	30	5	9	9542.20	145.74	0.579	552.50	992.12	1363.80
SLB3 40_2	25	30	5	2	4571.07	76.44	0.543	248.30	482.60	634.54
SLB3 40_3	25	30	5	3	6043.67	97.23	0.531	321.00	609.64	817.79
SLB3 40_4	25	30	5	4	7393.67	116.17	0.530	391.60	732.20	993.03
SLB3 40_5	25	30	5	5	8650.00	133.79	0.533	460.80	851.48	1162.82
SLB3 40_6	25	30	5	6	9843.00	149.92	0.537	528.70	967.95	1327.13
SLB3 40_7	25	30	5	7	10988.00	165.19	0.542	595.40	1082.30	1487.38
SLB3 40_8	25	30	5	8	12091.27	179.81	0.547	660.90	1195.00	1643.93
SLB3 40_9	25	30	5	9	13156.07	194.00	0.551	725.10	1306.30	1797.11
SLB3 50_2	25	30	5	2	5479.60	88.67	0.520	284.90	551.27	730.67
SLB3 50_3	25	30	5	3	7367.13	114.64	0.512	377.50	713.65	963.00
SLB3 50_4	25	30	5	4	9110.00	130.30	0.513	466.10	871.40	1180.77
SLB3 50_5	25	30	5	5	10759.13	160.81	0.518	557.00	1025.70	1404.77
SLB3 50_6	25	30	5	6	12328.67	181.80	0.523	644.40	1177.30	1616.83
SLB3 50_7	25	30	5	7	13844.20	202.03	0.528	730.30	1326.80	1824.38
SLB3 50_8	25	30	5	8	15312.67	221.80	0.532	814.70	1474.50	2028.05
SLB3 50_9	25	30	5	9	16737.00	241.37	0.536	897.70	1621.20	2228.57

TABLE 3-1 DESIGN TABLE SLB DEVICES

The simplicity of SL damper's geometry makes them particularly suitable tobe adapted to different arrangement within the structure. The typical and most used installation mode for SLs is between chevron braces and upper beam, as schematically shown in Fig. 3.6.Significant feature is that the battlement connection, characterizing the most recent generations, which avoids transferring axial force to the device. This no-axial-force-transferred characteristic has the advantage that the walls or supporting braces do not necessarily have to be aligned in height so they could be added where the architectonical project allows. Besides under vertical seismic movements they dissipate energy.

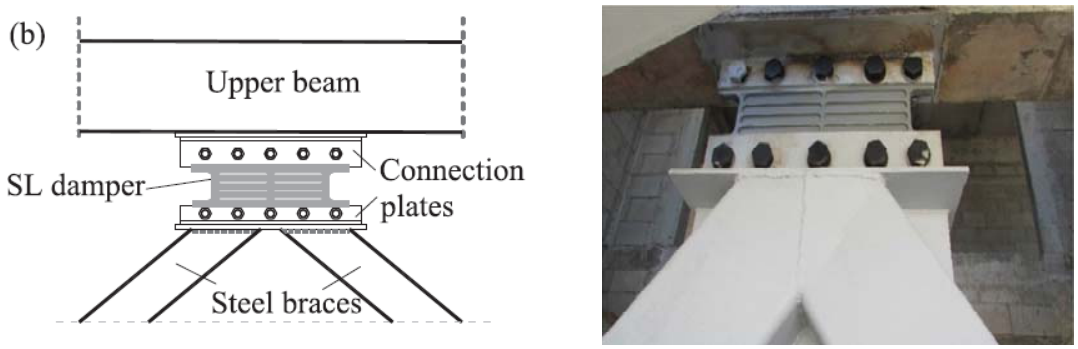

FIGURE 3.6INSTALLATION MODE BETWEEN CHEVRON BRACES

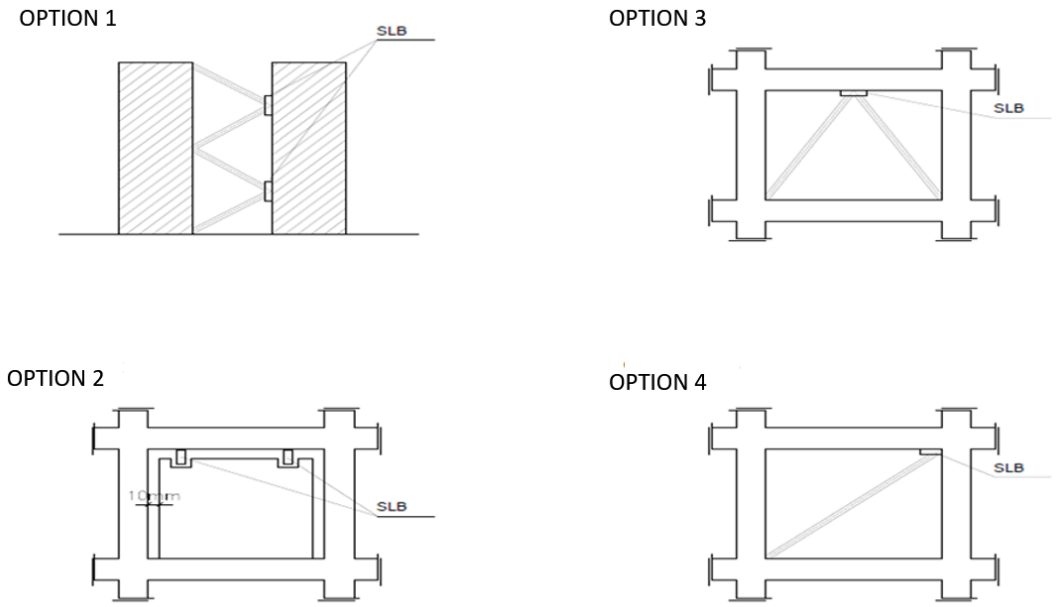

FIGURE 3.7 OPTIONS OF INSTALLATIONS OF SLB DEVICES

Although, the first use of such devices was to protect infill masonry walls. The authors also investigated the alternative use of SL dampers to protect precast RC structures, inserting devices within diagonal braces (Fig. 3.8).

FIGURE 3.8 APPLICATION OF SLB DEVICES IN DIAGONAL BRACES

Nowadays, several applications have been developed and carried out using these devices: more than one thousand of SL dampers havebeen installed worldwide, mainly

in RC buildings in Mexico, Peru and Ecuador, for new constructions as well as for seismic retrofitting of existing ones.

FIGURE 3.9TORRE PARADOX – MEXICO

FIGURE 3.10 TORRE IXTAPA - MEXICO

3.2 EXPERIMENTAL CAMPAIGN

A large experimental campaign has been carried out over the years in order to check the real behavior of the deviceunder cyclic loads and allowing to identify any critical points. Each generation of the SLB device has been tested leading to the calibration of the analytical and numerical model on the results obtained from the tests.

3.2.1 FIRST GENERATION OF "SLB"

The first experimental studies were performed at ISMES S.p.A., in Bergamo (Italy) in 1997, where the prototype of the first generation of SL devices was tested.

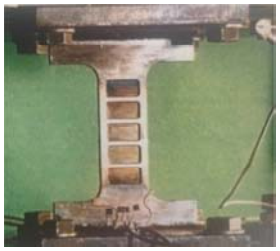

FIGURE 3.11 PROTOTYPE FIRST GENERATION

The flanges of the devices were welded to horizontal thick plates, constituting elements of connection to the machine, through high strength bolts. In the web, there was a unique column of dissipative windows with thicknesses between 1.5 and 2.0 mm, while flanges and other stiffeners were 15mm thick. Four devices with different types of transition zone between the web and stiffeners were cyclically tested, all performing stable hysteretic behavior with significant strain hardening. It is worth to note that after severe damage of the dissipative windows, the SL devices continued to exhibit a stable behavior even with lower hysteretic curves corresponding to a flexural dissipative behavior.

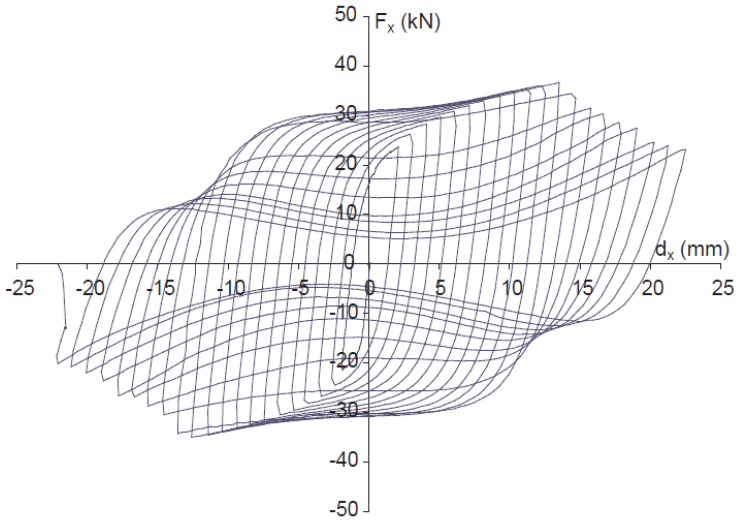

FIGURE 3.12 EXPERIMENTAL FORCE-DISPLACEMENT HYSTERETIC CURVE (ISMES, 1997)

A further device belonging to the first SL generation was examined at the Laboratory of the University of Girona. Its shape was more stockythan the previous and the main investigation was concerning web buckling. It was observed that the distortion angle γ, analytically evaluated as the ratio between the head displacement and the total dissipative windows' height, was quite close to the experimental strainangle γ' assumed as twice the linear strain orientated at 45° in the hypothesis of a pure shear strain state.

The first SL generation (Fig. 3.13) was tested cyclically again at ISMES S.p.A in 2004, with the main aim of generalizing its mechanical properties for many different yielding force levels.

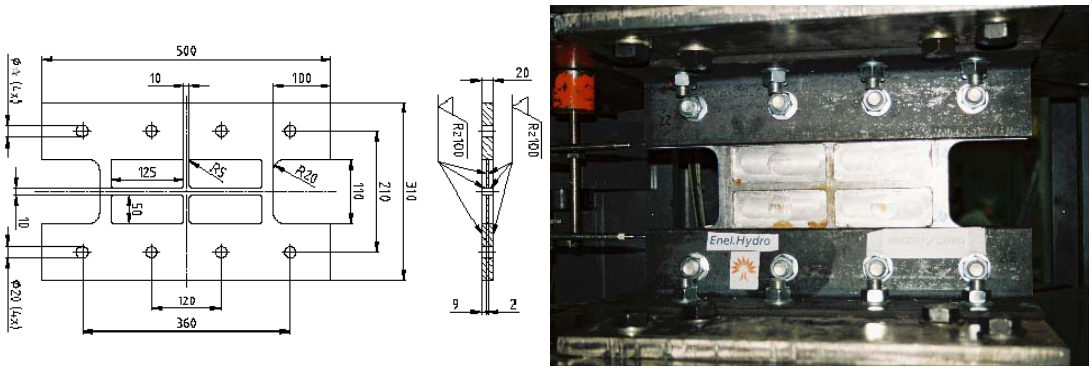

FIGURE 3.13DIMENSIONS FOR EXPERIMENTAL MODEL TESTED7

To define the optimum shape and characteristics of the dissipator, four basic preliminary devices called Disip1SL30_2, Disip2SL30_2, Disip3SL30_2 and Disip4SL30_2, have been compared. The first device has 200 mm height and just one 10 mm vertical stiffener. Consequently this device has two milled areas of 125x200 mm. The second device adds an horizontal 10 mm stiffener, so the milled areas are 125x95 mm. The aim is to increase their strength against web buckling. In this line the third device has two horizontal stiffeners, so the milled areas are 125x60 mm. The last preliminary device reduces the vertical height up to 110 mm maintaining a horizontal stiffener. All have in common two vertical stiffeners (20 mm width) at both lateral ends, the width is 300 mm, the web thickens 2mm and the initial plate thickness 20 mm.

The numerical model has been made using the computer program ANSYS. The model for all the cases corresponds to the isotropic hardening one giving the complete stress – strain material relation. This relation was obtained experimentally for a typical material. Figure 3.14 shows the Von Mises stresses for a given imposed relative displacement of 20 mm for the devices Disip3SL30_2 and Disip4SL30_2.These stresses are uniformly distributed in all the dissipative windows, indicating a maximum profit of the material. Besides this indicates that the stiffeners do not affect significantly the dissipation.

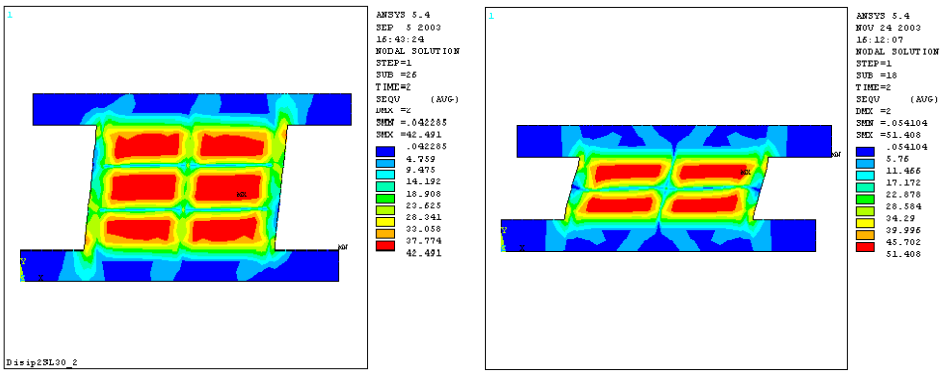

FIGURE 3.14VON MISES STRESSES FOR THE DISIP3SL30_2 AND DISIP4SL30_2 DEVICES

Figure 3.15 presents the force–displacement relation-ship for the preliminary 200 mm vertical height proposed devices. The aim is to study the influence of the stiffeners in the yielding strength and post-yielding slope. The increase in stiffeners originates a small increment in the yielding strength, although the post-yielding slope is maintained

constant in all the cases. Consequently, the total dissipated energy is increased as the number of stiffeners increases, although the milled area is reduced by them. This result is explained by the stiffness increase. For design purposes, however, all these devices have very similar performances regarding the force–displacement relation-ship.

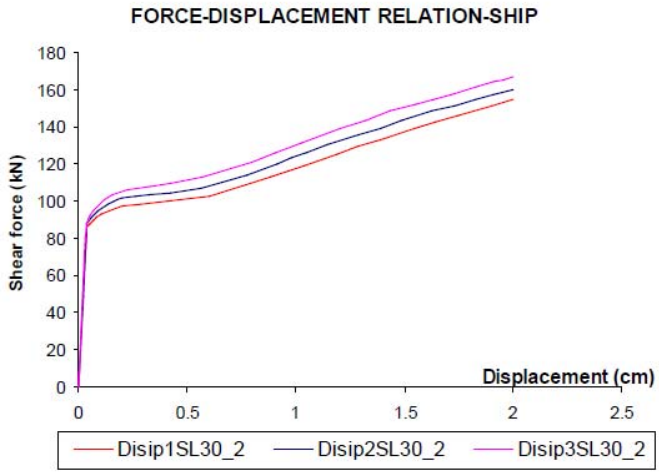

FIGURE 3.15 NONLINEAR MONOTONIC FORCE–DISPLACEMENT RELATION-SHIP

The device, indicated as SL30_2, has been compared to the previous generation and has been characterized by two columns of dissipative windows in the web. The connection to the equipment was just bolted and the role of the tolerance between holes and bolts has been analyzed through a parametric analysis. In the case of tolerances of 2 or 4 mm, tests were not concluded successfully because the slippage was too high. Conversely, specimens with 1mm of hole tolerance showed again stable hysteretic curves with strain hardening, performing shear and flexural mode behaviors, similarly to what shown in Fig. 3.3. Anyway, even in this case, significant slippage was registered, observing collapse in correspondence of the vertical bolted connection. In order to continue the test,the damaged connection was welded to the horizontal plate, butafter a high number of cycles even the weld connection failed. However, slippage is not considered a good response characteristic since it is difficult to predict. Consequently the tolerance is reduced as much as possible just for installing the devices.

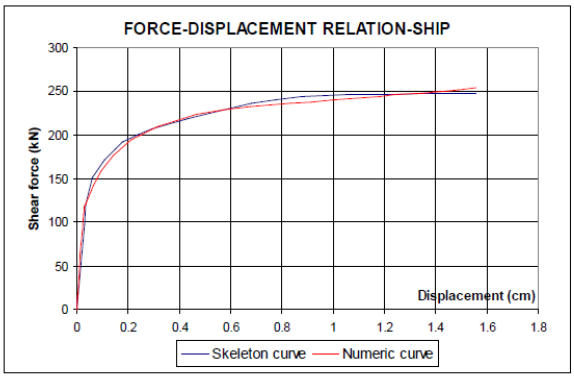

FIGURE 3.16 EXPERIMENTAL AND NUMERICAL MONOTONIC FORCE-DISPLACEMENT RELATION-SHIP

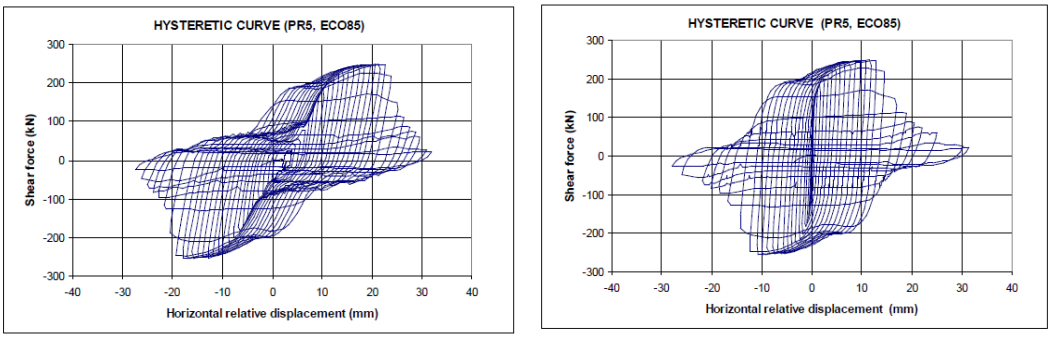

A) INCLUDING SLIPPAGE OF THE BOLTSB) WITHOUT SLIPPAGE OF THE BOLTS
FIGURE 3.17 HYSTERETIC CURVE FOR DEVICE SL30_2

The calibration of the force-displacement relationship of the numeric model with respect to the backbone of the experimental model showed a good correlation using a relatively simple isotropic hardening plasticity model. A numerical interpretation of these experimental tests was used to deduce mechanical properties of 32 devices of different dimensions (web height fixed at 110 mm) that could even be combined in parallel, so providing a wide range of performance parameters to designers.

A further device was later tested at the laboratory of the Pontificia Universidad Católica del Perú (PUCP) in Lima, in 2015. The geometry was similar to the SL30_2, but smaller, with a total web's width L of 25 cm (SL25_2). An horizontal actuator was used to apply a quasi-static load history to the device through the interposition of a square hollow element under controlled displacement. During this test, the specimen suffered an out-of-plane failuremechanism, probably due to torsion in correspondence of the head tubular component, causing a premature interruption of the experiment.

3.2.2 SECOND GENERATION OF SLB

The performance of the newest SL version has been tested at the Laboratory of Structures at the University of Naples Federico II in collaboration with University of Naples Parthenope, Italy in 2016. Five different geometries have been investigated, testing two specimens for each of them, for a total of ten tests. Seven specimens were tested cyclically, while three of them were subjected to monotonic load, measuring reaction forces up to 1000 kN.

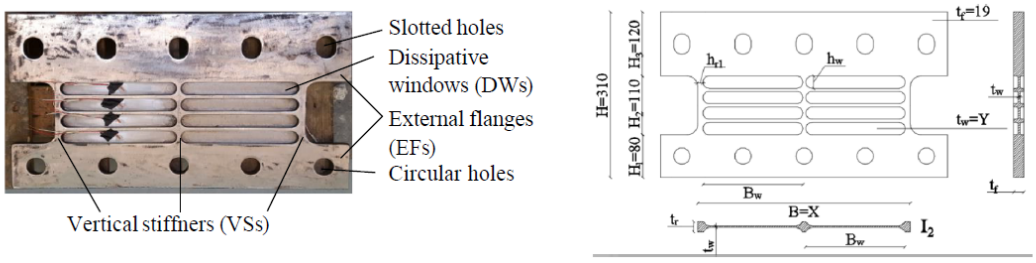

FIGURE 3.18 FIGURE 3.13 DIMENSIONS FOR EXPERIMENTAL MODEL TESTED

Actually, due to free or restrained rotations at slotted holes, the device can be roughly thought as a cantilever in the FNF configuration and as fixed at both ends in the FF configuration.

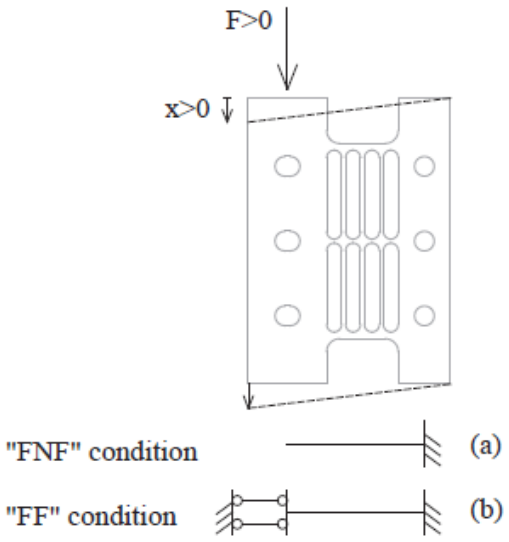

FIGURE 3.19BOUNDARY CONDITIONS FOR SLB DEVICES

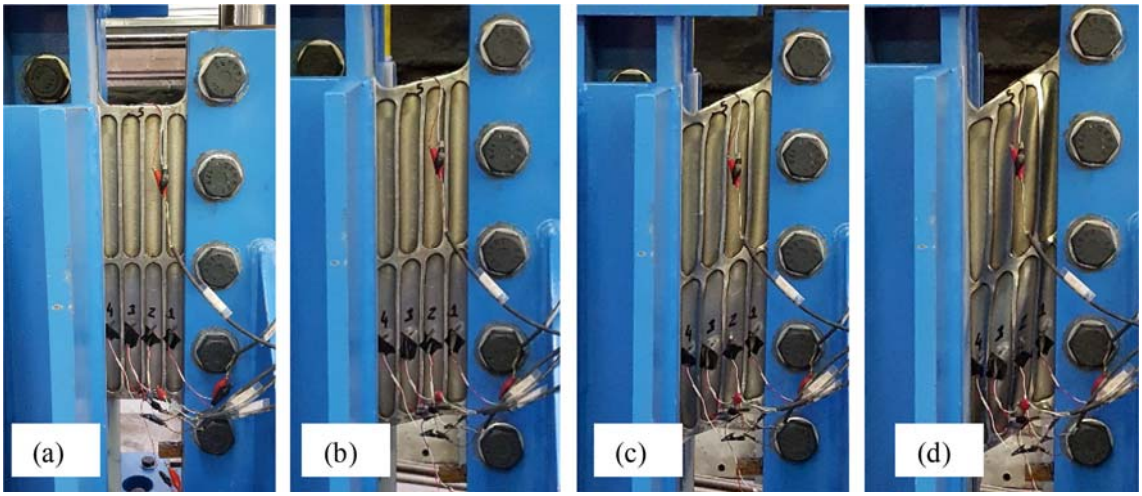

FIGURE 3.20 MONOTONIC TEST # 4 DAMAGE SCENARIO: (A) INITIAL CONDITION, (B) YIELDED PHASE, (C) ONSET OF BUCKLING, (D) GLOBAL BUCKLING

Results in terms of force-displacements (F–x) response are shown inFig. 3.21.Smoother curves are those related to tests performed in the FF configuration (#1, 3, 4, 7), as expected. The others referred to FNF testsare more irregular due to the sliding of bolts within the slotted holes.Due to different boundary conditions, it can be observed that SLs inFF configuration usually provide higher values of initial stiffness and yielding force than FNF case, although with no significant discrepancy.The same SL device provided almost the same maximum peak force for both cyclic and monotonic tests. However, they occurred for different amount of displacement. Actually, the envelope of the loops registered for cyclic tests provided higher values of force with respect to the monotonic test on the same device.

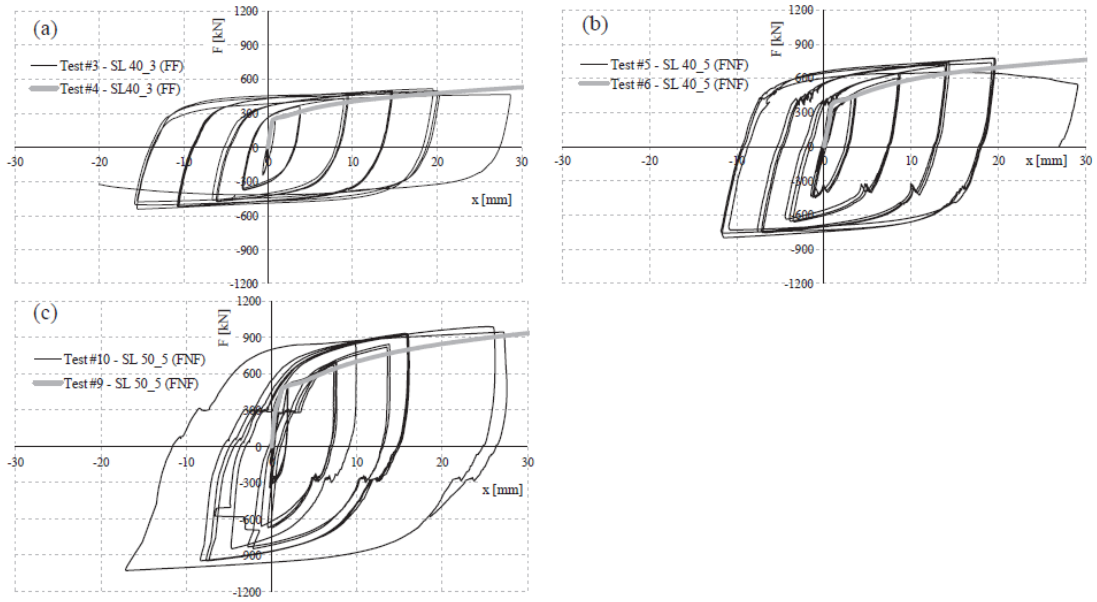

FIGURE 3.21CYCLIC AND MONOTONIC F–X CURVES

Collapse phenomenon in the cyclic tests was due to tearing in the external stiffeners, while in monotonic tests samples suffered from web buckling.

The FEA of the SL device is performed using ABAQUS/Standard, which is a general-purpose FEA program. The SL is modelled as a deformable planar shell and discretised using a four-node doubly curved general purpose shell S4, which considers finite membrane strains. The basic material is A36 steel, which is characterised through a tensile test. Both the FF and FNF configurations and both monotonic and cyclic load conditions are analysed. For cyclic analysis the plastic behaviour is modelled in a different way because the experimental hysteretic behaviour is affected by both kinematic hardening (KH) and isotropic hardening (IH), which are responsible for the translation and expansion of the yielding surface, respectively. This behaviour is well represented by Chaboche model, which is implemented in ABAQUS and defined as a “combined hardening model”.

A comparison of the analytical, numerical, and experimental results confirmed the accuracy of the models for the prediction of the mechanicalbehaviour of SL devices.

The stress distribution at failure for one of the specimens is presented in Fig. 3.22.The experimental behaviour is confirmed by the numerical simulation, where normal stress concentrations at the bottom and top of the external stiffeners are obtained, as shown in Fig. 3.22(a). At the same time, the windows are characterised by a uniform shear stress distribution, Fig. 3.22(b), confirming a global energy-dissipation mechanism through the windows.

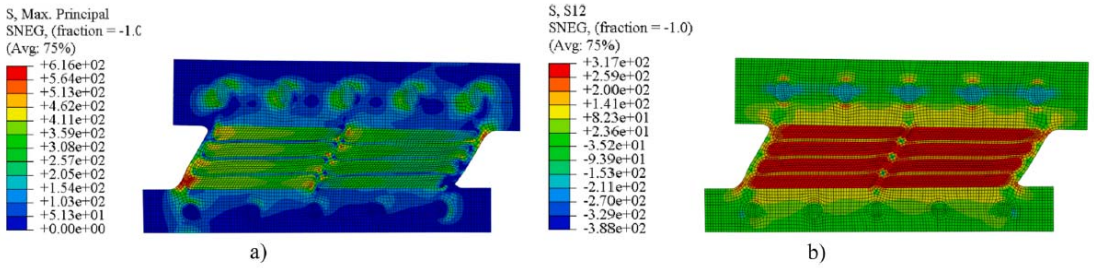

FIGURE 3.22 STRESS DISTRIBUTION IN SL50_5 FNF AT FAILURE:
(A) PRINCIPAL MAXIMUM NORMAL STRESS; (B) SHEAR STRESS

Fig. 3.23 shows the strain distribution at failure (i.e. when the ultimate strain of the material is reached). In the FNF configuration, Fig. 3.23(a), the maximum strain occurs in the stiffeners, whereas in the FF configuration, Fig. 3.23(b), it is concentrated in the windows; this is consistent with the experimentally observed failure mechanisms.

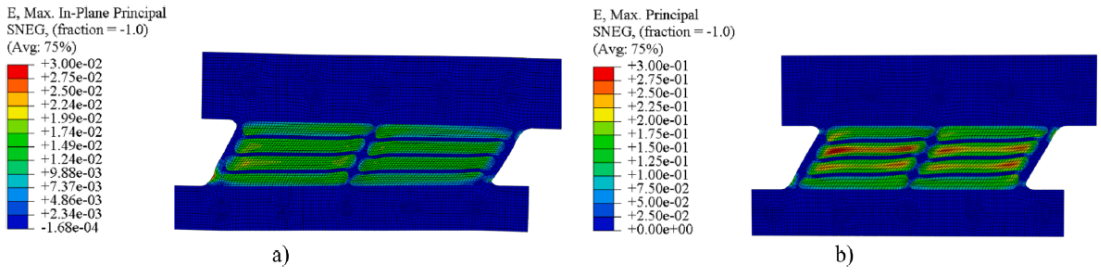

FIGURE 3.23 STRAIN DISTRIBUTION AT FAILURE: (A) 50_5 FNF CONFIGURATION; (B) 40_3 FF CONFIGURATION

3.2.3 THIRD GENERATION OF SLB

The third generation of Shear Link Bozzo (SLB) was tested at the UNAM laboratory in Mexico - 2019. The test was focused over the behaviour of the SLB connection with an uncoupled reinforced concrete wallunder a cyclic loading.

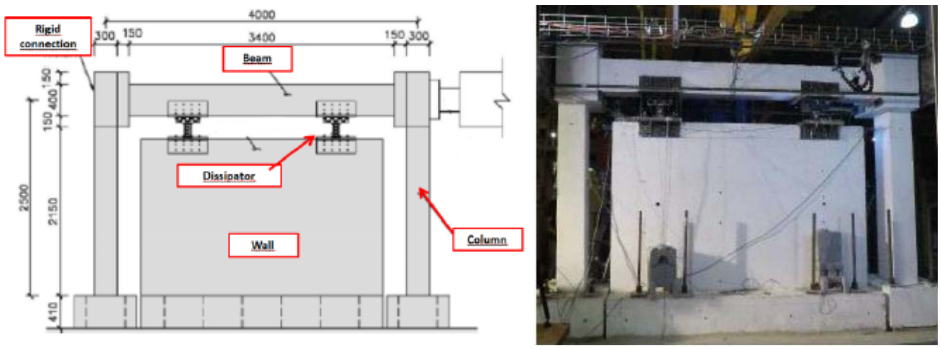

FIGURE 3.24 GEOMETRY OF THE REINFORCED CONCRETE FRAME

In order to understand the structural behavior of the SLB connections, three 1:1-scale tests were performed: (1) a bare reinforced concrete frame, (2) a reinforced concrete frame with 50kN SLB devices (Type 1) on uncoupled walls and (3) a reinforced concrete frame with 100kN SLB devices (Type 2) in the same uncoupled walls. These test results are used to validate numerical simulations of the system through Finite Element Analysis software; in this case, ABAQUS CAE.

The main characteristic of the SLB device tested is the upper connection called “hair comb” or “Almena”. These connections transfer only displacements significantly avoiding the transmission of axial load over the devices and, consequently, through the structural global configuration. The material of the steel connections is, in general, structural steel ASTM A36, with a nominal strength of 250 MPa. Figure 3.25 shows dimensions of SLB connection type 1.

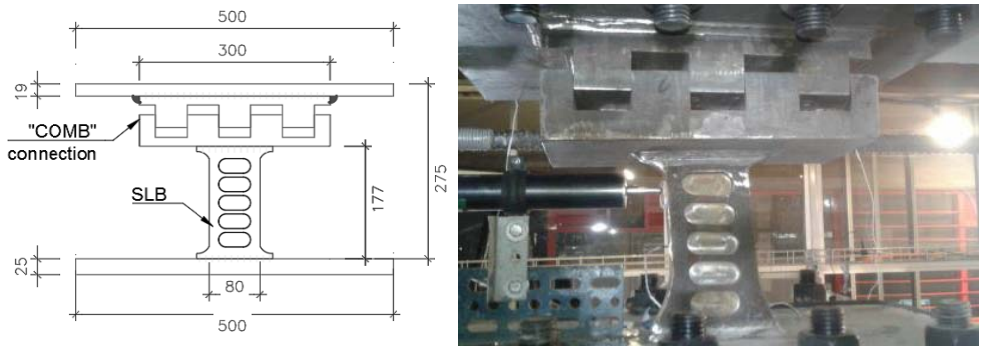

FIGURE 3.25DIMENSIONS (MM) OF SLB CONNECTION TYPE 1

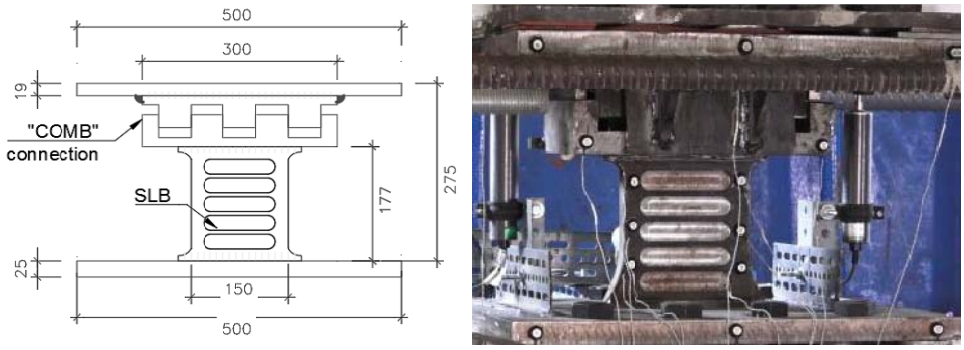

FIGURE 3.26 DIMENSIONS (MM) OF SLB CONNECTION TYPE 2

The experimental results of the frame without SLB connections exhibits an approximately linear elastic behavior without significant dissipated energy by concrete frame plasticity, whilefor the concrete frame with SLB connections through the un-coupled reinforced concrete wall, the results showhysteresis curves with evident dissipation of energy. The figure 3.27shows that SLB connections exhibited a linear-elastic behavior up to achieving the yielding lateral displacement.

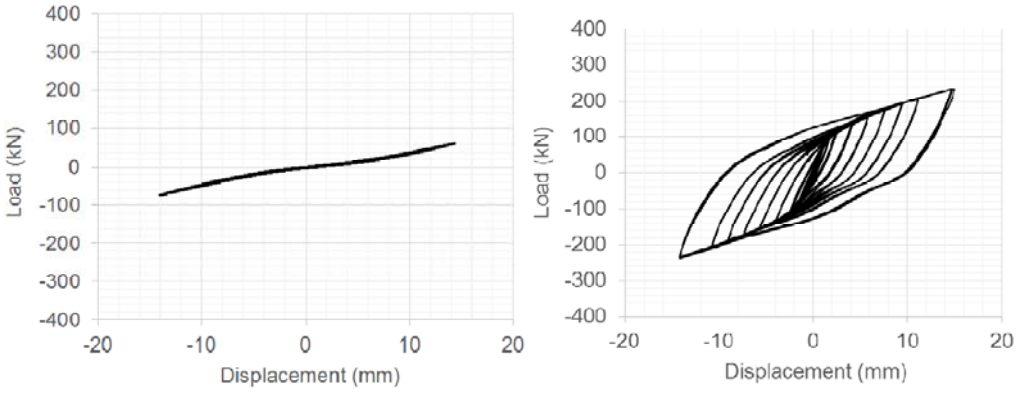

[A] [B]

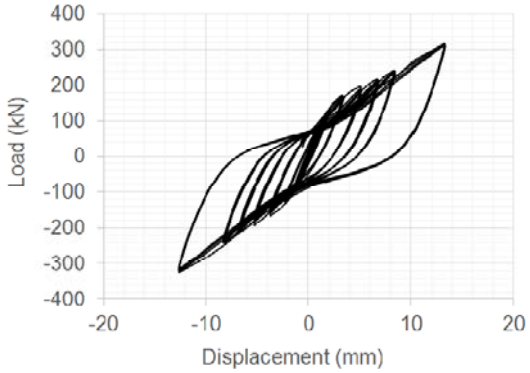

[C]

FIGURE 3.27HYSTERESIS CURVE CPNCRETE FRAME:
A) WITHOUT SLB; B)WITH SLB TYPE 1; C) WITH SLB TYPE 2

The hysteresis curve shows that structural behavior of concrete frame with SLB connections type 1, fig. 3.27 [B], exhibit steady hysteresis loops without loss of strength and stiffness degradation.

The hysteresis curve referred to connection Type 2, fig. 3.27 [C], shows an initial practically linear-elastic behavior but pinching of hysteresis curve appears as soon as relative displacements between connecting plates of the SLB connections and concrete shear wall occur. The origin of this “pinching of hysteresis curve” was due to the excessive displacements of the bolted connections of the devices that were unwittingly omitted in the laboratory.

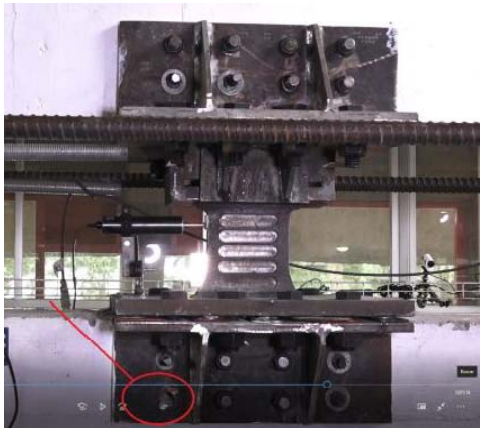

FIGURE 3.28 UNWITTINGLY OMITTED IMPORTANT BOLT NOT DISPOSED IN THE TESTS

The finite element analysis software ABAQUS CAE was used to simulate the experimental results of the tests through modeling, analysis, assembling, and visualization of structural components. Only the frame without SLB connections and the frame with SLB connections Type 1 are modelled since the frame with SLB connections Type 2displayed an unexpected behavior due to the assembly errors in the test. Consequently, the reaction wall on ABAQUS CAE model was not included. Because of the response of the reaction wall was effected by some unwitted errors,alternatively, simpler linear springs were used in order to simulate the response.

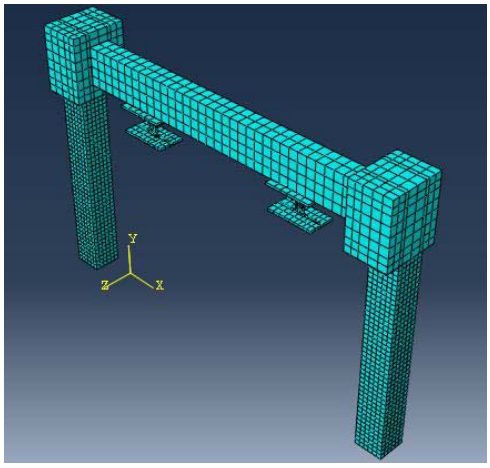

FIGURE 3.29 FE MODEL OF THE TEST

First the concrete frame without SLB connections was modeled in order to calibrate the model, the experimental response of the concrete frame without SLB connections behaved displaying stiffness of a cracked section. Consequently, a complete cracked section was used in the numerical model. Drawing a trend line of both, the results of the

experimental test (green line) and the cracked behavior of the numerical model (blue line), it can be seen that the results display a highly similar stiffness.

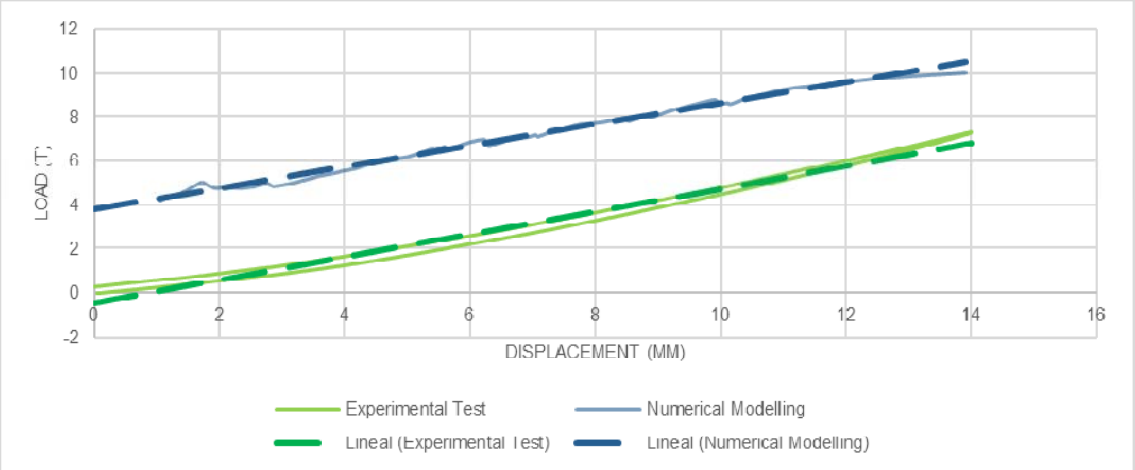

FIGURE 3.30CONCRETE FRAME WITHOUT SLB CONNECTIONS
EXPERIMENTAL TEST – NUMERICAL MODELLING

The uncoupled frame with SLB connections type 1 was modeled until achieving the right behavior of the SLB connections. Linear springs were used in order to simulate the response of the reaction wall. In total 36 springs were used under the plates where the SLB connections were welded to the reaction wall with lineal stiffness in direction “x” and “z”. Through several iterations to get the spring stiffness,it was possible to obtain a numerical model that displays a similar behavior tothe experimental test. Fig. 3.31 shows comparisons between experimental and numerical hysteresis loops.

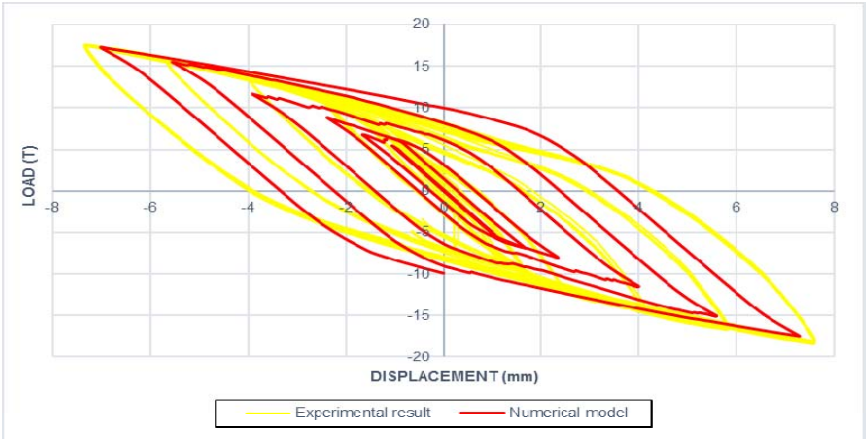

FIGURE 3.31 COMPARISON BETWEEN EXPERIMENTAL AND
NUMERICAL HYSTERESIS LOOP OF SLB CONNECTIONS TYPE 1

Furthermore, a model using fixed supports was implemented and it shows that using good connections between the reaction wall and the SLB devices, the behavior of the SLB connections is improved significantly, being an effective way to improve the behavior of the structure.

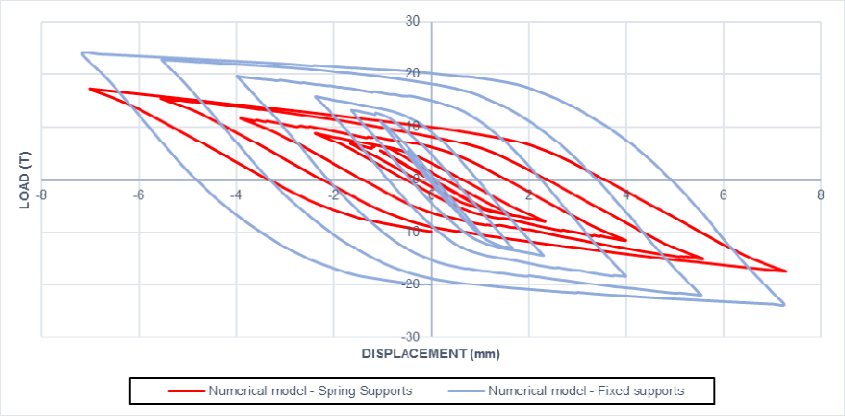

FIGURE 3.32 COMPARISON BETWEEN SPRING SUPPORTS (RED LINE) AND FIXED FUPPORTS NUMERICAL MODEL (BLUE LINE)

As shown in Fig. 3.33, the stress distribution in the SLB connection type 1 is mainly distributed in the "windows" which are the thinner sections; however, the upper part of the frames also presents high stress levels. Furthermore, the welding sections are subject to minimum levels of stress. On the other hand, sections like steel plate and steel teeth (located over the SLB connection) do not display significant stress distribution.

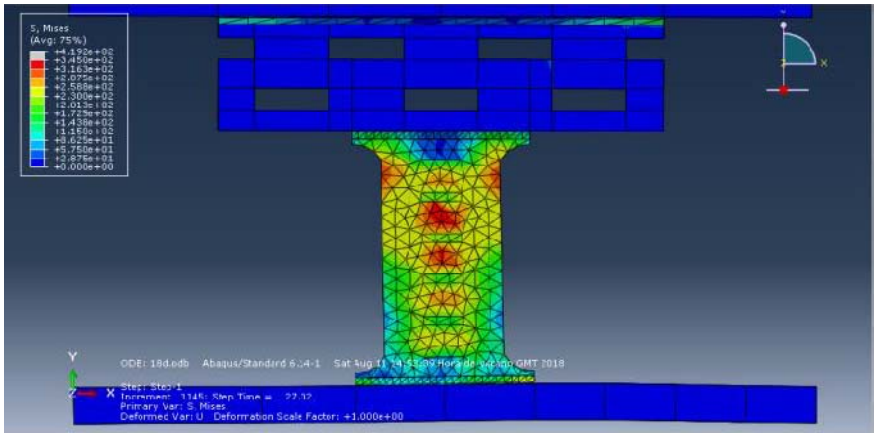

FIGURE 3.33VON MISES STRESS DISTRIBUTION

3.2.4 FOURTH GENERATION

The fourth generation of Shear Links Bozzo has been tested in the laboratory LADICIM of the University of Cantabria (2020). The main aim of the new generation is to increase the deformation capacity of devices and for this purpose the solution adopted was to increase their height, passing to a height of 270mm instead of the 155mm of the previous generation causing probably problems of global instability,and to increase the height of the dissipative windows or, in other words, to reduce the horizontal stiffeners of the devices, which also has the potential drawback of generating buckling in the web for thin milled windows. Considering this, two alternativeshave been proposed for this generation, a first option shown in figure 3.34 [A], characterized by aratio between thickness and height of the dissipative windows equal to 0.1, a second option, shown in figure 3.34 [B], characterized by two lateral wings welded to the device. These wings increase considerably the torsional capacity of the device and prevent its buckling failure. Of this second alternative have been proposed two versions varying the thickness of the dissipative windows obtaining for the first a ratio of 0,08 and for the second a ratio of 0.1. The dimensions of the devices considered are referred to the SLB4 20_5 and to the SLB4 20_4.

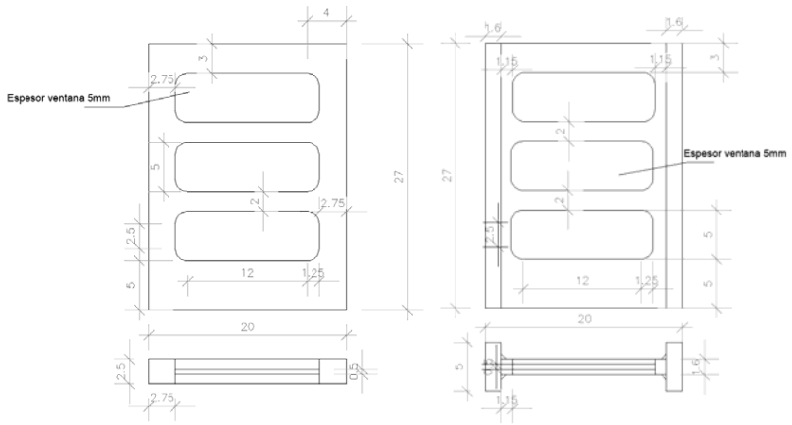

FIGURE 3.34 GEOMETRY OF EXPERIMENTAL MODEL TESTED:
A) ALTERNATIVE 1; B) ALTERNATIVE 2

One of the objectives of these tests is to satisfy the requirements of the American code AISC (American Institute of Steel Construction).The code requires that the devices must provide a deformation capacity significant through creep of the dissipator in

tension and compression. These deformations must correspond to the maximum between two times the inter-storydrift of design or, a drift of 2% (AISC, 2016).

The configutation of the samples for testing consists of a dissipator anchored to a concrete wall, as it is in the reality, submitted to cyclic loads applied at the free end of the device. The device is welded to a steel plate connected to the wall through rebars with headaccording to the American Code ACI-19, fig 3.36.

FIGURE 3.35 SCHEME OF THE EXPERIMENTAL TESTS

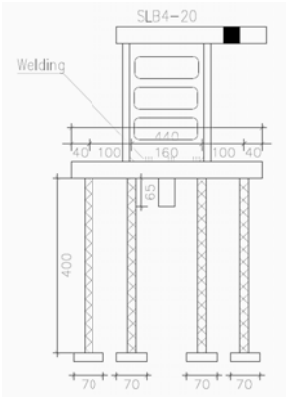

FIGURE 3.36 CONNECTION DETAILS

All the supporting walls of concrete considered in the test have the same geometry and the same quantity of reinforcements calculated according to the American Code ACI-19, only the reinforcements of the concrete wall of the fourth test have been reduced, as shown in fig. 3.37, in order to test the connection.

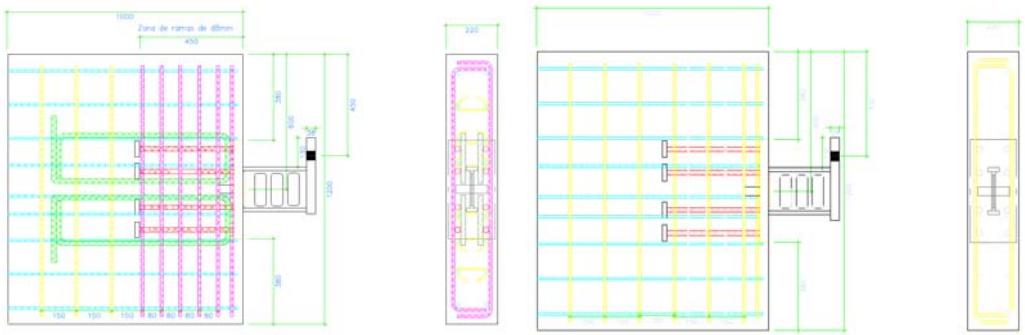

REBARS OF THE FIRST THREE TESTS REBARS OF THE FOURTH TEST

FIGURE 3.37 DETAILS OF THE REBARS OF THE CONCRETE WALLS IN THE TESTS

Material Properties	
ConcreteR_{ck}=35Mpa	
Reinforcing Steel	B500S
Laminated Steel	ASTM A36

A total of four experimental tests were planned,testing the two alternatives of SLB described before.

In order of execution:

1st test: Alternative 1, SLB20_5 without wings, submitted to cyclic loads according to AISC 16

2nd test: Alternative 2, SLB20_5 with welded lateral wings, submitted to cyclic loads according to AISC 16

3rd test:Alternative 1, SLB20_5 without wings, submitted to cyclic loads according to AISC 16 modified, in fact this sequence is modified by adding five more charge cycles but with lower deformations.

4th test:Alternative 2, SLB20_4 with welded lateral wings, submitted to cyclic loads according to AISC 16. The fourth test was principally based on the study of the failure of the connection between the device and the concrete wall, at the same time this test was also useful to check the effects of the thickness reductionof dissipative windows for the new devices SLB4.

In the first test that was carried out, the free extreme of the device has rotated during the application of theload because of some mistakes in the setting of the test, so the results

obtained in this test are not representative. However, the other three tests were successful in order to calibrate the mathematicalmodel as an auxiliary structure was used to prevent the twist.Both proposed devices (Alternative 1 and 2) can verify cycles loadrequired from ASC16but has to be considered that the alternative 2, with welded wings,failed in a fragile wayduring the second test due to insufficient weld, figure 3.39, this can be avoided in futureadopting welding at complete penetration. In the third test, the alternative 1 reached a deformation of 48mm without present a reduction of the stiffness in its hysteretic cycle, fig.3.38but the test has been stopped because of signals of global buckling. Considering that the maximum displacement has to be considered in correspondence of the reduction of the maximum force of 20%, it could be possible to assert that the maximum displacement of the device could be much higher. For this reason, in future it will be necessary to fix the lateral buckling problem considering also the use of lateral stiffeners.

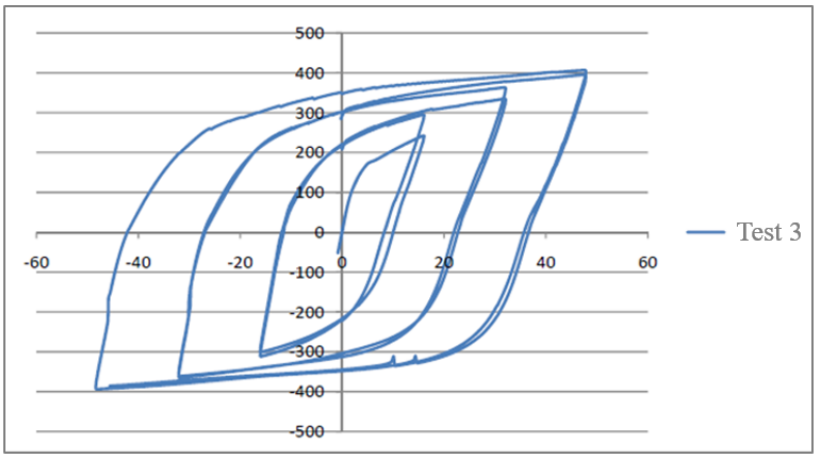

FIGURE 3.38 HYSTERETIC CYCLE THIRD TEST

Furthermore, thanks to the third and fourth tests it can be confirmed that the ratio (thickness/height) of the dissipativewindow of SLB devices must be greater than 0.1 to ensure that there is nolocal buckling. During the fourth test, the dissipative windows characterized by a ratio of 0.08 (thickness of the milled area 4mm, heightdissipative 50mm) presented a starting local buckling, fig. 3.39, while for the other three tests, with a ratio of 0.1 (thickness of the zonemilled 5mm, dissipative height 50mm), there were no sign of buckling. The fourth test showed also no failure in the anchorage despite the lower amount of rebars for the connection, but it needs more experimentations to analyze this aspect with a better set up of the test.

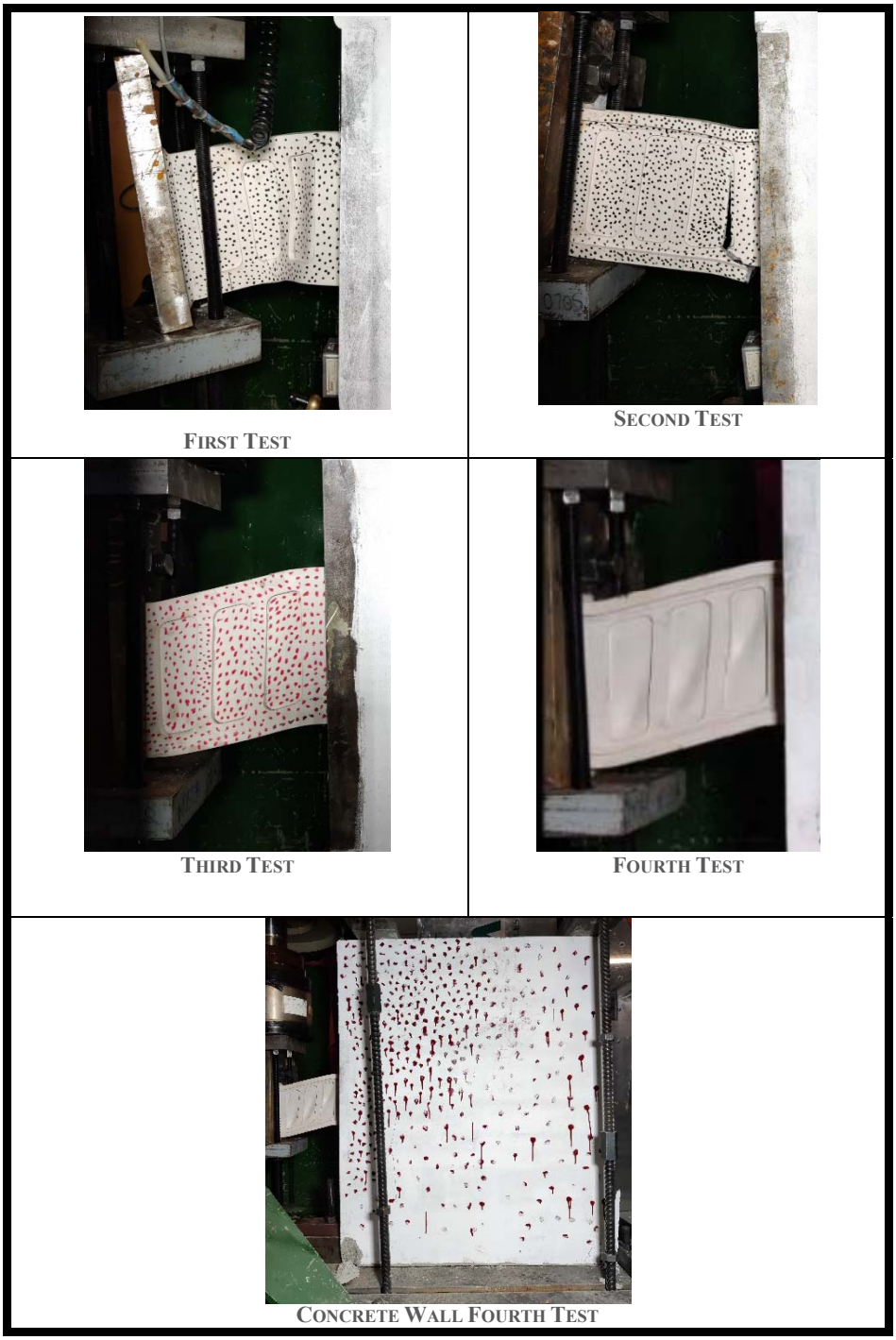

FIGURE 3.39 IMAGES OF TESTS

To simulate the behavior of the devices in the tests, both alternatives have been modeled with the Diana FEA finite element software. After the tests, a parametric analysis has been carried out to adjust the models with the empirical values and, thus, be able to

obtain the parameters with which to model the devices of different sizes without needing to test them.

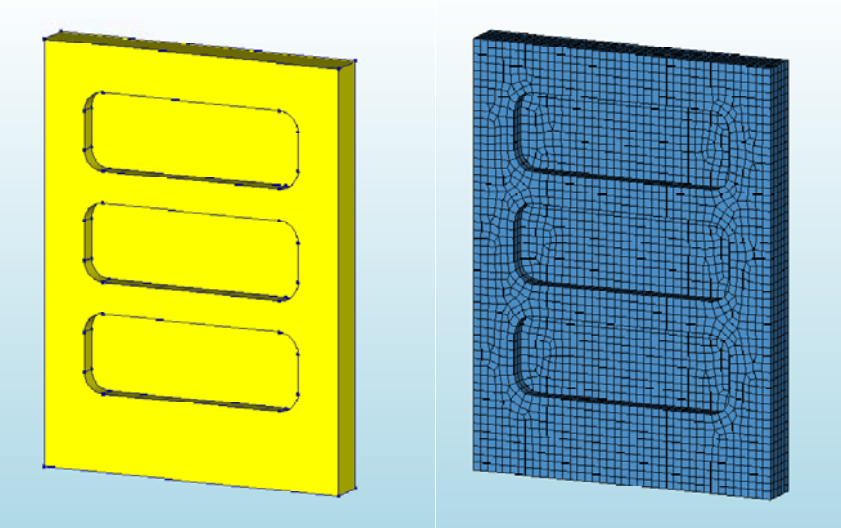

FIGURE 3.40 F. E. MODEL OF THE ALTERNATIVE 1 IN DIANA

Although four tests have been performed, the numerical-experimental correlation has only been performed just for the second and the third test, because they are the two that present representative results on both proposed alternatives. To carry out the correlation, it is intended to fit the hysteretic stress-strain curves obtained numerically with the Diana FEA software to the experimental ones obtained in the laboratory. In addition, for the third test, a nonlinear eigenvalue analysis has also been performed to check the lateral buckling that occurred during the testtrying to predict the failure of the device.

The solid 3D elements of the DIANA FEA software, together with the Nadai approximation to define the actual stress-strain curve of the steel, provide a good approximation for the cyclical behavior of the devices. Using the DIANA FEA software, it has been observed that the isotropic model gives a very good experimental numerical correlation.

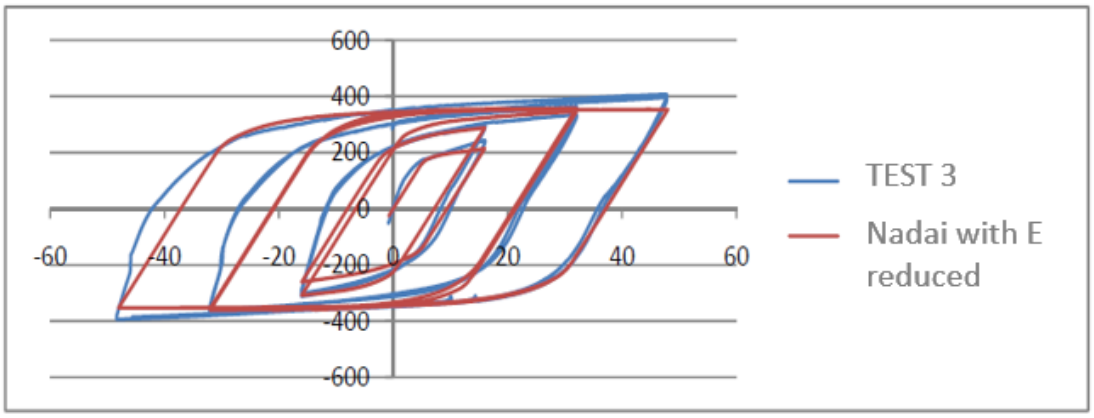

FIGURE 3.41 HYSTERETIC CURVE OF THE TEST (BLUE) VS MODEL WITH THE NON-LINEAR BEHAVIOR (RED)

Figure 3.41 presents the numerical-experimental correlation obtained by reducing the modulus of elasticity by 85%. Therefore, it is the same isotropic model with the same material curve including its yield stress except modifying the linear modulus of elasticity. When calibrating the numerical model with the discharge slope, significant differences can be observed with respect to the slope of the load branches this was due to the wall that was lifted during these phases.

In the same way, it was obtained the numerical-experimental correlation also for the second test which reached a fragile crisis due to the failure of the weld between the device and the steel plate of connection. The failure occurred for a maximum displacement of 32mm, for this reason, the numerical correlation has been obtained up to a deformation equal to 32mm, fig. 3.42.

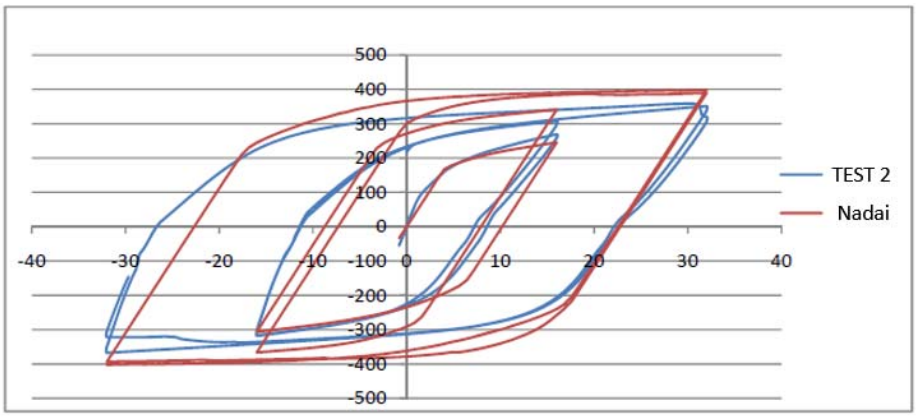

FIGURE 3.42HYSTERETIC CURVE OF THE TEST (BLUE) VS MODELWITH THE NON-LINEAR BEHAVIOR (RED)

3.3 SLB MODELING

The SLB device can be modelled as an elasto-plastic element through the definition of the elastic stiffness K_1 and post-elastic one K_2.

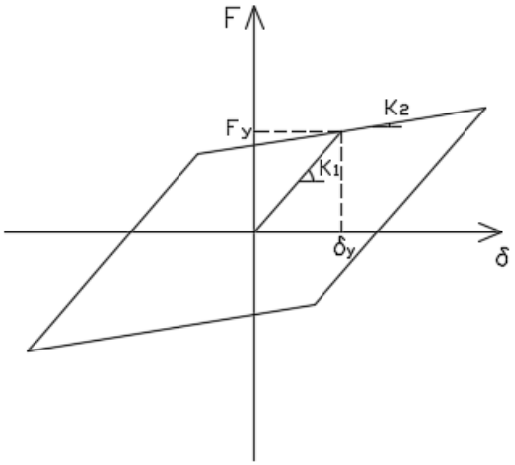

FIGURE 3.43FORCE-DISPLACEMENT RELATION OF SLB DEVICE

The dissipative device (SLB) can be modelled by two springs in parallel that represent respectively the elastic stiffness K_1 and the post-elastic one K_2 (associated to the yielding of the dissipative "windows").

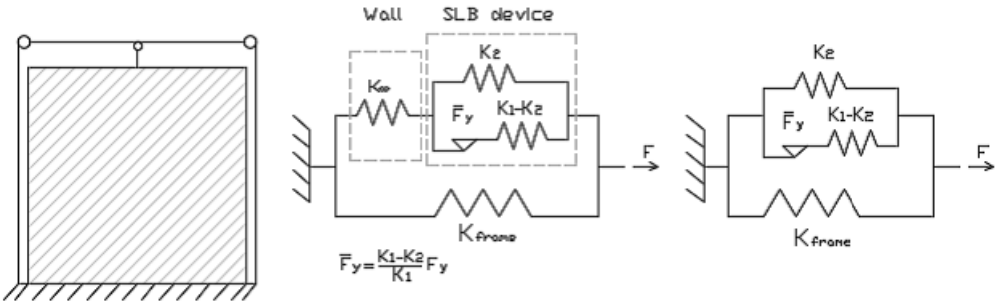

FIGURE 3.44 RHEOLOGICAL MODEL OF THE DISSIPATIVE SYSTEM WITH THE FRAME STRUCTURE

The SLB device works as a parallel system therefore the equivalent stiffness of system is the sum of the stiffnesses. Before the "windows" yield the equivalent stiffness of the SLB is equal to the elastic stiffness K_1, while after yielding it reduces to K_2.

Therefore, two different cases can be considered:

1. $F < F_y$: $K_{eq}=K_2+(K_1-K_2)=K_1$
2. $F > F_y$: $K=K_2$

The decoupled walls can be considered as a spring that works in series with the SLB devices. The equivalent stiffness of system is:

$$\frac{1}{K_{eq}} = \frac{1}{K_{SLB}} + \frac{1}{K_{wall}}$$

But the elastic stiffness of the walls can be considered infinite compered to the stiffness of the devices, for this reason it can be neglected because its contribution is null.
The rigid behavior of the structure is related to the initial elastic behavior of the SLB device that works in parallel with the supporting element, therefore the equivalent stiffness is governed by the stiffness of the SLB.
Before the SLB yields the structure has low displacement exhibiting a rigid behavior. Successively, increasing the seismic intensity the dissipative system adds damping to the structure by dissipating the seismic energy through the yielding of SLB devices. In conclusion, when the structure is subjected to a seismic action the dissipative system works in parallel with the frames of the structure by providing stiffness to the global structure through the limitation of the horizontal displacement and contemporary it adds ductility, dissipating the energy generated by the shear deformation through the yielding of SLB devices. After yielding, the SLB stiffness reduced to K2 reason why the equivalent stiffness of the system is governed by the stiffness of the frames of the structure.

3.3.1 PLASTICITY MODEL OF WEN

The SLBs devices aremodeled as link-type elements, the plasticity model is based on the hysteretic behaviour proposed by Wen (1976) and displayed in Figure 3.45.
The nonlinear force-deformation relationship is given by:

$$f = \alpha \cdot k \cdot x + (1 - \alpha) \cdot f_y \cdot z$$

Where k is the elastic spring constant, fy is the yielding force, α is the post-to-elastic stiffness ratio, and z is a non-dimensional hysteretic variable described by the following differential equation (Wen, 1980):

$$\dot{z} = A\dot{x} - \beta z|\dot{x}||z|^{n-1} - \gamma\dot{x}|z|^{n}$$

where **A** is a scale factor, **β** and **γ** are parameters which define the curve's shape, **n**is a parameter which defines the smoothness of the transition between the linear and nonlinear region.

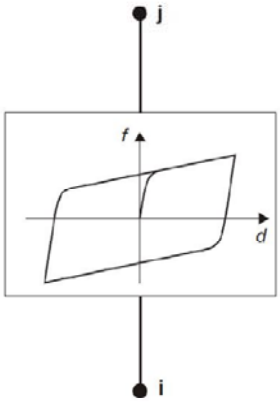

FIGURE 3.45 WEN'S PLASTICITY MODEL

The equation to determine **z** is equivalent to the one belonging to Wen's model with **A**=1 and α=β=0.5 (CSI, 1997). Therefore, "**n**" is the only arbitrary parameter to identify within the definition of the behaviour of the dissipator,"**n**" belongs to the interval [1, +∞) and, as displayed in Figure 3.46, when increasing its value, the transition from linear to nonlinear region is sharper. Commonly, to best describe SLB devices' elastoplastic behaviour, n=1 or n=2 is adopted to better represent experimental results.

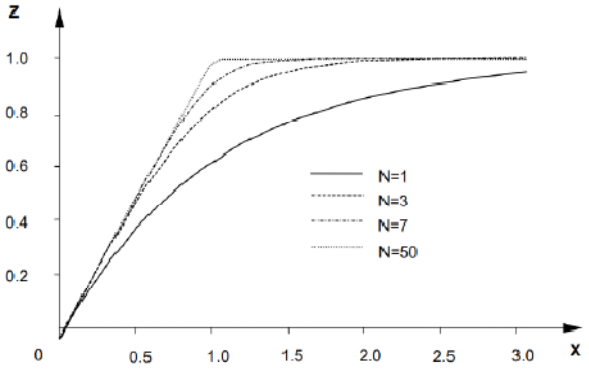

FIGURE 3.46 CURVES FOR DIFFERENT "N" VALUES (A=1, α=β=0.5)

3.3.2 LINK PROPERTIES

When defining the SLB devices in the model as NLINK connections within the ETABS software, a fundamental parameter is the so-called "shear deformation point" or "shear deformation location" or "null moment point". It is defined in the indicated program, as the distance to the point where the moment due to the shear in the link is zero, but, measured from point J or END knot of the link. This point in the SLB dissipators corresponds to the TCP “toothed” connection where the bending moment is zero and, therefore, this distance is zero or the total length of the dissipator (depending on the connection is defined or inserted, but it is important to remember that in automatically charged devices, this distance is define as zero).

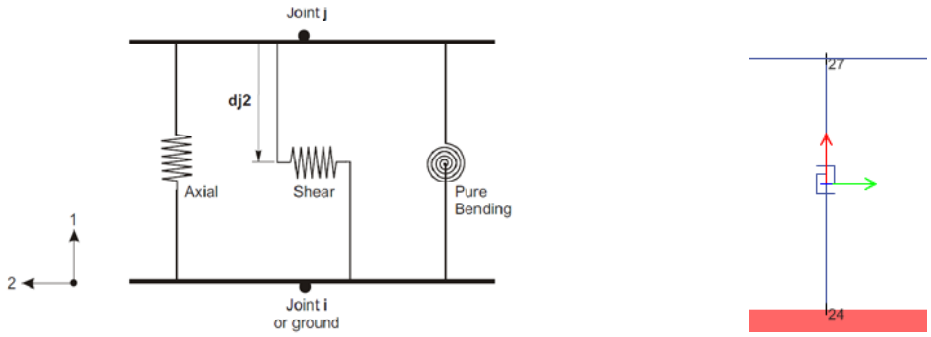

FIGURE 3.47 DEFINITION OF THE SLB DEVICES AS NLINK CONNECTION

Properties	M3	V2
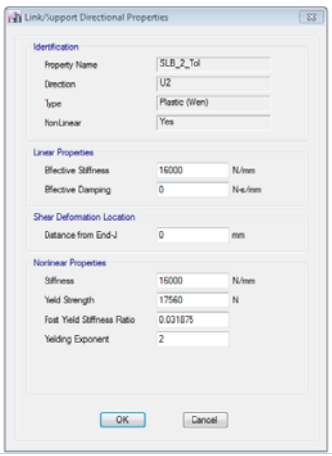	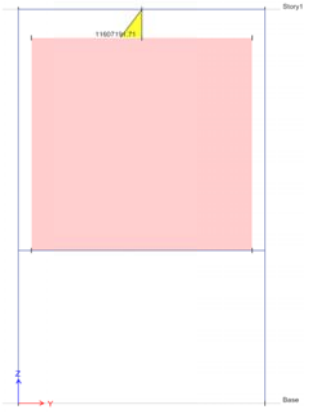	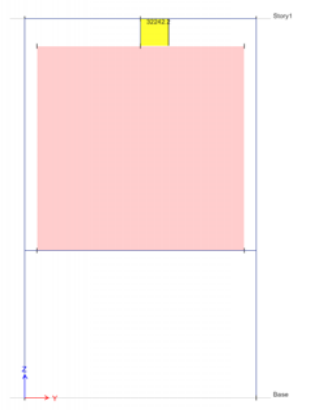

TABLE 3-2PROPERTIES, BENDING MOMENT M3 AND SHEAR FORCE

Nlink is defined with local axes one (red) in the vertical direction and local axes two (green) in the same plane as the wall. Therefore, the SLBs are modeled as a link with properties on local axis 2 and its insertion point or “point i” of the NLINK is the upper end of the wall and point “j” is the beam base (where the TPC “toothed” connection has zero moment). The “distance from node j” to the zero-moment point would therefore be zero. While, for dissipators supported by metallic diagonals, since these are normally bi-articulated, the “toothed” connection is arranged at the junction of the diagonals (and NOT as in the walls at the base of the beam). Since every loaded devices have the null moment distance defined as "zero", their insertion point or point "i" has to be the beam base and the "j point" of the NLINK the end where the diagonals intersect (where the “toothed” connection or zero moment point is). In this case the local axis is directed downwards. In each case, it is important that the distance between the nodes “i” and “j” respect the real hight of the device, that in case of SLB belonging to the third generation is equal to 155mm, for SLB of fourth generation the hight of the devices is equal to 270mm.

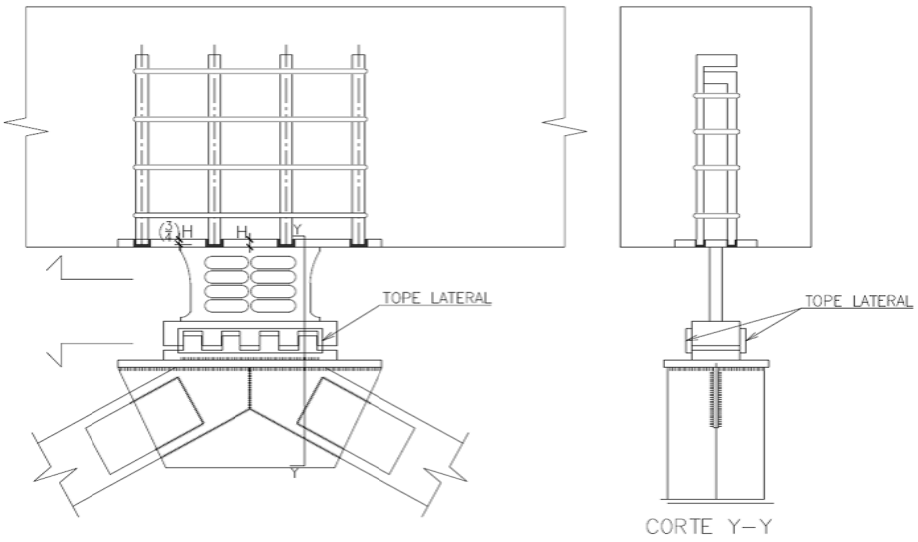

FIGURE 3.48 SLB DISSIPATORS INSTALLED WITH DIAGONALS IN CHEVRON

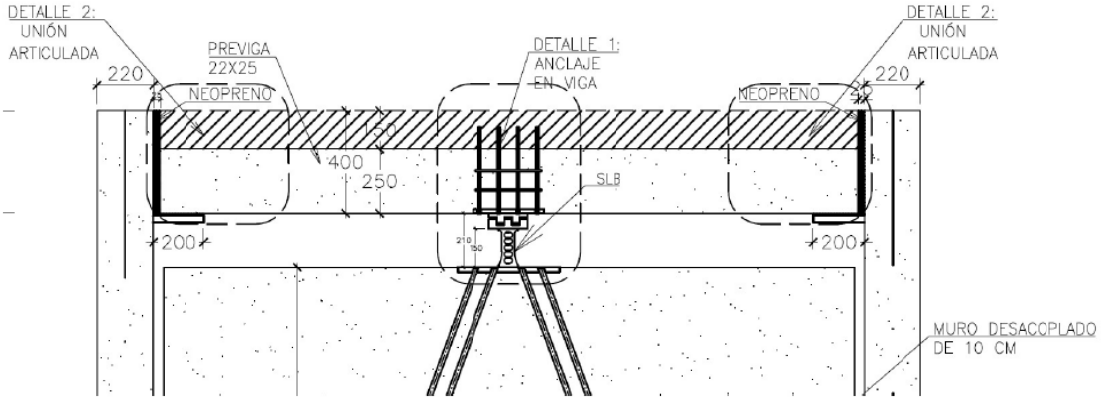

FIGURE 3.49 SLB CONNECTION WITH UNCOUPLED WALL

The properties of the links are aressigned in the local direction 2, defining the linear properties and the nonlinear properties of the link that the program will consider depending on the type of the analysis. The software considers the effective stiffness in case of linear analysis and, the elastic and post yeld stiffness, for the nonlinear analysis, according to the plasticity model of Wen.

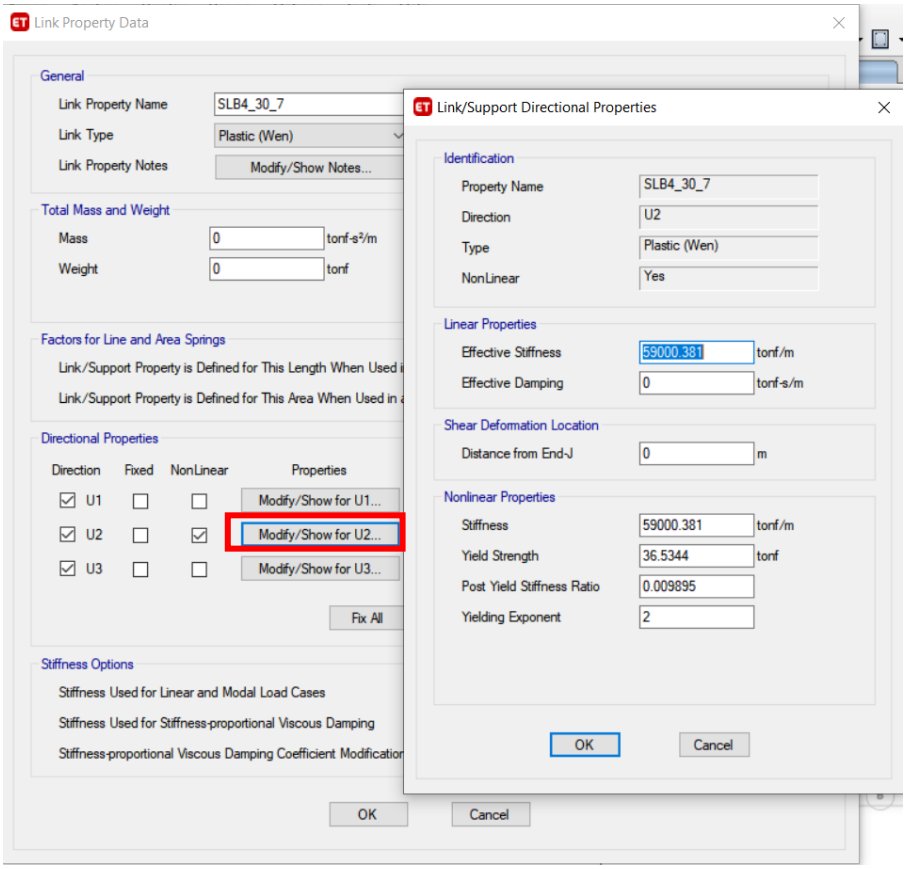

FIGURE 3.50 ASSIGN OF THE LATERAL STIFFNESS FOR THE LOCAL AXIS 1 OF THE DEVICE - ETABS

The elements of support have to be modeled in the software as shell elements, in the case of walls of concrete, assigning the thickness and the material property, or as frames elements, in the case of metallic diagonals, assigning the properties of the section and of the material.It is necessary leave a distance, between the upper part of the element of support and the upper beam, equal to the hight of the dissipator, in order that the link has the real hight of the device. It is also important that the local axes 2 of the link is parallel with the main dimension of the element of support.

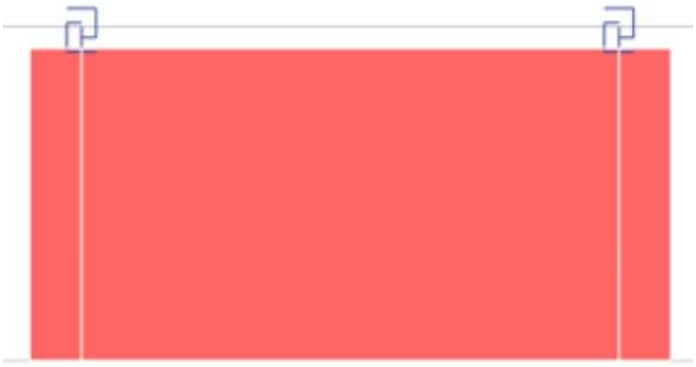

FIGURE 3.51 MODEL OF UNCOUPLED CONCRETE WALL

4 PROCEDURE FOR THE DESIGN OF SLB

The situations where the use of SLB devices are highly efficents are:

- Structures with high torsion of plan in which these devices can be located opposite to the elements that generate the torsion but without the need to carry the elements to their base or at full height.
- Structures with soft or flexible floors, the elements don't need to be continued up to the foundation. In other words, the walls are added in the precise locations where they are needed.
- To increase stiffening and/or ductility in general on existing structures

It is important to highlight that because of the "toothed" connection that doesn't transfer axial forces, the devices can be freely placed on plane and in height, stiffening them specifically whereit is needed and where architecturally possible.

There are two methods for the selection of SLB devices actually incorporated in an ETABS application. Both are based on elastic modal analysis, which reducing the use of the nonlinear time history analysis only to check the right behavior of the devices, thus achieving significant savings in computational time for the solution (see Figure 4.1). This is particularly useful in preliminary design where most important decisions are taken.

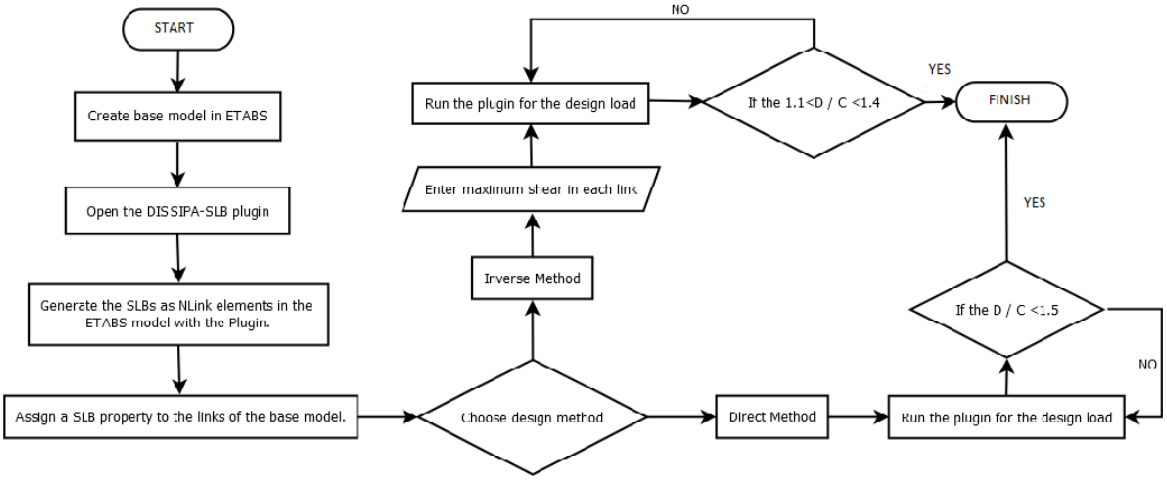

FIGURE 4.1 FLOW-CHART FROM THE MANUAL OF DESIGN OF THE SLB DEVICES

These two processes have been automated through the implementation of a plug-in for the software ETABS, DISSIPA SLB plug-in. This application requires the results of the seismic analysis process iterating in ETABS model by accurate information transfer betweenthe analyses. The plug-in currently supports two automated selection procedures: (1) Direct and (2) Inverse iteration methods, as well as the automatic loading of the property of the dissipators from the design tables.

4.1 "DIRECT ITERATION" PROCEDURE

The direct method consists in iterating a group of devices previously defined by means of a series of seismic analysis, of the modal response spectrum type, until reaching a shear demand compatible with the capacity of the device.It is recommended to create an envelope in the load combinations defined in the model, so the dissipators are designed with the maximum stresses.

In order to implement the iterative design procedure, a target drift must be initially fixed according to local code and a first try SLB suit must be considered. The basic principle is to compare the shear in the links with the yielding force of the SLB device assigned(Fy from SLBs manualtable) and, in order to ensure proper functioning of dissipator, Fy shall result minor than shear force, thus allowing dissipation to occur through yielding of the device. It is required that the ratio between the acting shear and the yield force of the device be less than a certain demand/capacity ratio typically assumed as 1.5. This ratio is considered by various cumulative factors such as the kinematic hardening of the steel or its greater resistance to dynamic loads as well as for the linear modal analysis procedure. These factors can only be considered precisely through a nonlinear time-history analysis, which is recommended, as verification, at the end of the procedure. The direct method requires an iterative procedure because, changing the SLB type, there is a redistribution of the stiffness that leads to a change of the shear force in the links, so the procedure shall be repeated until a convergence condition is reached. The procedure is performed automatically for several devices using DISSIPA SLB plug-in.

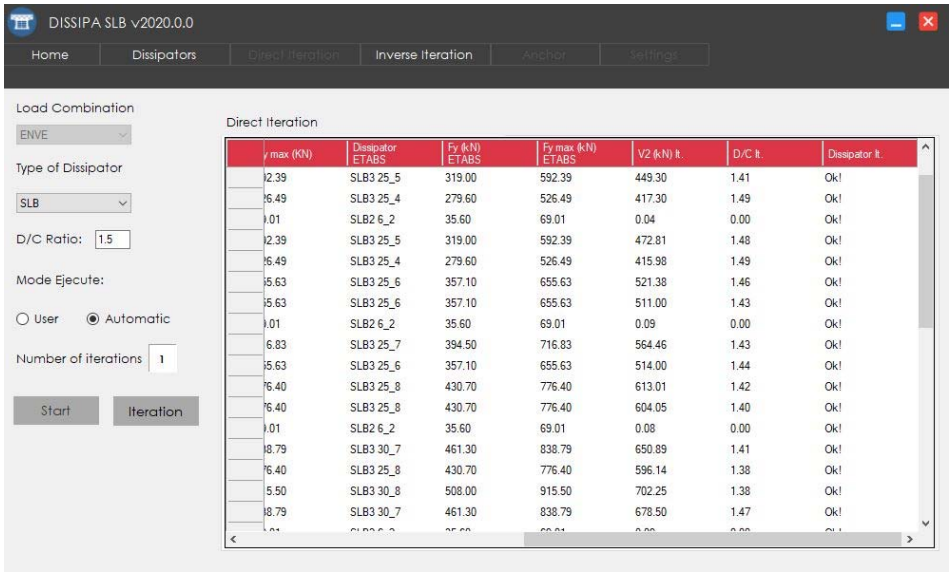

FIGURE 4.2 DIRECT ITERATION PROCEDURE IMPLEMENTED IN THE PLUG-IN ETABS

Once devices dimensions have been set, uncoupled supporting wall must be designed accordingly. In particular, depending on the number of devices supported by each wall and on its yielding force (Fy, from SLB's manual), a shear design force for the wall will be computed through the following expression:

$$Vd = 1.5 \cdot Fy \cdot n_{SLB}$$

It can be noticed that direct procedure usually delivers greater dimensions of SLB devices at each iteration. Therefore, as a negative aspect, response spectrum linear analyses could lead to oversized the supporting elements like the diagonals or the uncoupled reinforced concrete supporting walls which might not correspond to architectural needs.It is for this reason, and in order to fix a size of diagonals or decoupled walls, that the following method of devices selection was developed.

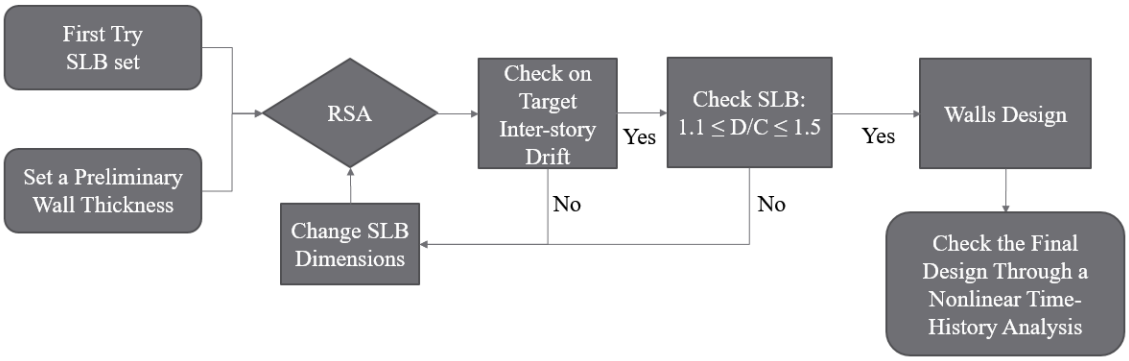

FIGURE 4.3 FLOW-CHART DIRECT ITERATION

4.2 "INVERSE ITERATION" PROCEDURE

The "fixed force" procedure or "inverse" iterative procedure is a procedure ofalternative design to the "direct iteration" to limit the thickness of the decoupled walls andsize of the devices given that said "direct" procedure consecutively increases theirdimensions. Decoupled wall values greater than 300mm are usually excessive due toarchitecture and cost. The shear capacity of a structural wall (obtained considering a certainvalue of fck, length and thickness) is fixed, and according to this capacity, is defined the value of themaximum force that could act on the devices. Unlike the direct iteration procedure, in which the size of the dissipator typically increases with each iteration, as well as itsshear force, in the "inverse" iterative procedure the aim is to set the value of the shear forceof the dissipator and therefore the iteration is to reduce the size of the device in the numerical model (and not in reality) in order to calibrate such transferred shear force.

The selection procedure for the SLB devices is always carried out by linear analysisspectral modal that allows a reduced computation time and can be summarized in the following steps:

1. Definition of a type of SLB device(for example SLB3 30_3) and a preliminary wall thickness (for example150mm).
2. Implementation of a direct iteration procedure verifying theparameters to be controlled, usually the inter-story drift. Increase the number of devices or the thickness of the decoupled walls would reduce the inter-story drift to meet design requirements.In some cases, it may be necessary to increase the number of decoupled walls themselves. On the other hand, it is necessary always to

check the capacity ratio limits (ρ) in the range 1.1-1.4 to proceed to modify the devices selected in the analysis.

3. Verifythe total shear force in the decoupled wall at each step according to the expression:

$$Vd = 1.5 \cdot Fy \cdot n_{SLB}$$

where Fy is the yield strength of each device, 1.5 is a factor of safetyadditional to those corresponding to ELUs and"n_{SLB}" is the number of devices on the wall.

4. The maximum shear in the wall must comply with the provisions of the ACI which depends onits length, thickness and characteristic resistance of concrete according to the expression (unitsMpa):

$$\frac{V_d}{L \cdot t} \leq 0.75 \cdot 0.83 \cdot \sqrt{f_{ck}}$$

For metallic diagonals, the expression is similar but depends on the buckling force of the diagonals so the system is similar to the BRB or "Buckle Restrained Braces" or "Restricted Buckling Diagonals".

5. If the wall thickness "t" cannot be increased, as in the second instance the characteristic resistance of the wall, it is necessary to proceed to the inverse iteration procedure by limiting the force on the decoupled wall.

6. The capacity of the decoupled wall is set as previously established and based on this, the following expression is developed for the maximum force in each device of the wall:

$$F_{max,SLB} = \frac{(0.75 \cdot 0.83 \cdot \sqrt{f_{ck}}) \cdot (L \cdot t)_{wall}}{1.5 \cdot n_{SLB}}$$

This is the maximum "target" force which corresponds to a certain type ofdevice and that it would be the one finally used in the design.

7. Therefore the device is selected by means of the table of SLB devices in such a way that its $F_y$is the one immediately below$F_{max,SLB}$. There is usually more than one optionfor this selection and it is recommended to choose the device with the thickest window for its lowest cost. At this point, the inter-story drift must be checked again because the force could be too low and the drift limit of the local code is not met.

8. Since the spectral modal analysis is linear, the acting force has no limit in each device so selecting the device through step 7 and repeating the analysis it is

certain that the acting shear changes and most likely exceeds the limit demand/capacity established from 1.1-1.4. One solution is to reduce "fictitiously" in the RSA numerical model the size of the device and repeat the analysis until obtaining a shear force within the stated range. This iterative procedure is automatized in the ETABS plug-in, Dissipa SLB. It is recommended to consider an envelope of the load combinations defined in the model, so the dissipators can be designed with the maximum stresses.

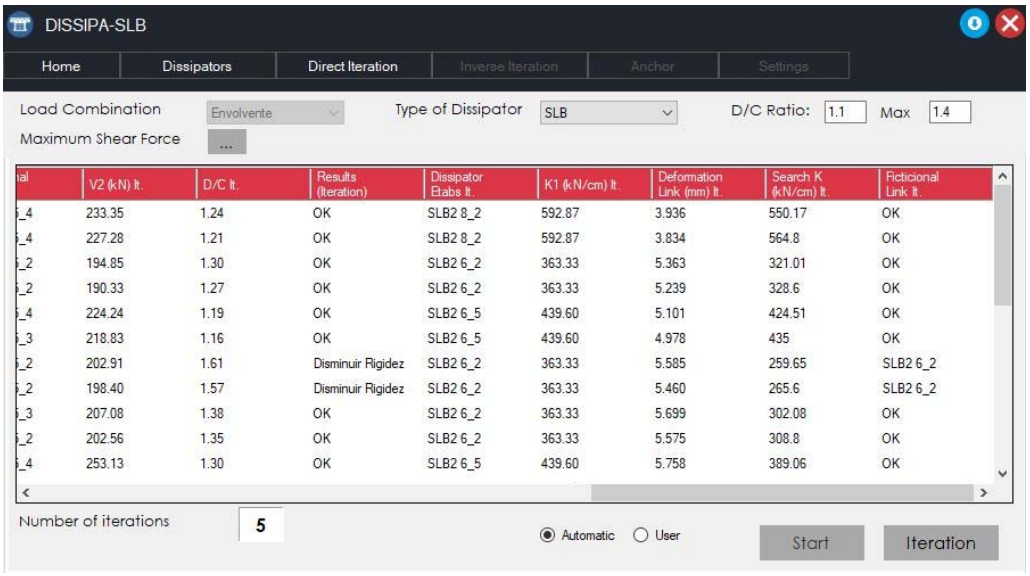

FIGURE 4.4 INVERSE ITERATION PROCEDURE IMPLEMENTED IN THE PLUG-IN ETABS

Through the inverse iteration procedure based ona linear spectral modal analysis, the behavior of the device is elastic, this means thatit doesn't take into account a threshold or a maximum shear force that the device can transfer to the supporting wall, for this reason, thetarget force is set in each link. The second stage of this procedure consists of verifying the results through a Non-Linear Time-History analysis considering the model with the type of SLB that has to be installed in reality. In this case,it is necessary to verify the level of displacement requested in each device, for which it is necessary to obtain the hysteretic curve.

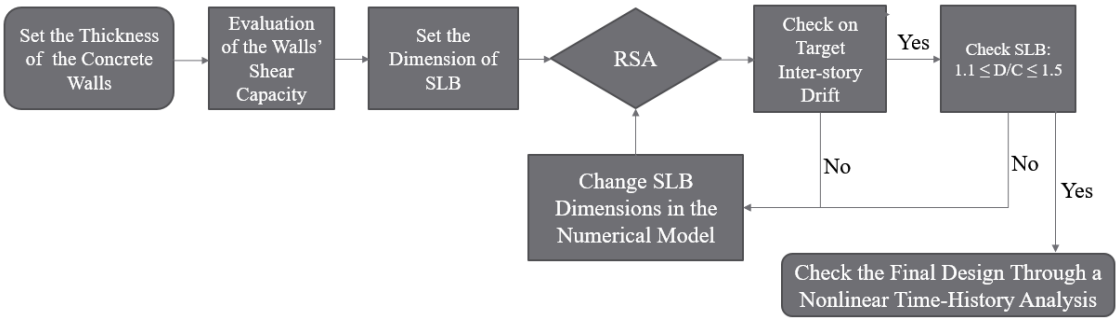

FIGURE 4.5 FLOW-CHART INVERSE ITERATION

4.2.1.1 NON-LINEAR TIME-HISTORY

The time-history analysis is a step-by-step analysis of the dynamical response of a structure to a specified loading that may vary with time.The dynamic equilibrium equations to be solved are given by:

$$\boldsymbol{K}\boldsymbol{u}(t) + \boldsymbol{C}\dot{\boldsymbol{u}}(t) + \boldsymbol{M}\ddot{\boldsymbol{u}}(t) = \boldsymbol{r}(t)$$

where $\boldsymbol{K}$ is the stiffness matrix; $\boldsymbol{C}$ is the damping matrix; $\boldsymbol{M}$ is the diagonal mass matrix; $\boldsymbol{u}$, $\dot{\boldsymbol{u}}$, and $\ddot{\boldsymbol{u}}$ are the displacements, velocities, and accelerations of the structure; and $\boldsymbol{r}$ is the applied load. If the load includes ground acceleration, thedisplacements, velocities, and accelerations are relative to this ground motion.

In a nonlinear analysis, the stiffness, damping, and load may all depend upon the displacements, velocities, and time. This requires an iterative solution to the equations of motion.The load, $\boldsymbol{r}(t)$, applied in a given time-history case may be an arbitrary function of space and time. It can be written as a finite sum of spatial load vectors, $\boldsymbol{p}_i$ multiplied by time functions, $f_i(t)$, as:

$$\boldsymbol{r}(t) = \sum_i f_i(t)\boldsymbol{p}_i$$

Direct integration results are extremely sensitive to time-step size in a way that isnot true for modal superposition. It is necessary to decrease time-step sizes until the step size is small enough that results are no longer affected by it.

The advantages to using direct integration are that full damping that couples the modes can be considered, the impact and wave propagation problems that might excite a large number of modes may be more efficiently solved by direct integration and all types of nonlinearity may be included in a nonlinear direct integration analysis.

The types of nonlinearity to consider may be:

Material nonlinearity

– Various type of nonlinear properties in Link/Support elements

– Tension and/or compression limits in Frame elements

Geometric nonlinearity

– P-delta effects

– Large displacement effects

To set a Non-Linear Time-History analysis it is necessary to set the initial conditions, in the specific it has to continue from a non–linear static analysis or another direct-integration time-history nonlinear analysis.

In direct-integration time-history analysis, damping in the structure is modeled using a full damping matrix. Unlike modal damping in linear and nonlinear modal analysis, this allows coupling between the modes to be considered. Direct-integration damping has two types of damping: *proportional damping* and *modal damping*.The effects of the specified proportional damping and modal damping are simultaneously considered in the analysis.

The direct-integration time history analysis is performed with the "Hilber-Hughes-Taylor alpha" (HHT) method, it uses a single parameter called alpha. This parameter may take values between 0 and -1/3.

For alpha = 0, the method is equivalent to the Newmark method with gamma = 0.5and beta = 0.25, which is the same as the average acceleration method (also called the trapezoidal rule.) Using alpha = 0 offers the highest accuracy of the available methods but may permit excessive vibrations in the higher frequency modes, i.e., those modes with periods of the same order as or less than the time-step size.

The nonlinear equations are solved using event-to-event stepping and/or equilibrium iteration in each time step. This may require reforming and resolving the stiffness and damping matrices at each step or iteration.

4.3 EVALUATION OF THE EQUIVALENT DAMPING

Once defined the dimensions of the SLB and the geometry of the elements of support, such as walls of concrete or diagonals chevron, the next step is to design the structure. The structural design is provided through a response spectrum analysis, in order to reduce the computational time. To take into account the dissipative effects of the hysteretic devices installed, it is necessary to evaluate an equivalent value of damping ratio. While it is easy to calculate this ratio for a complete cycle of loading and unloadingof the device, the more complex the calculation on the complete structure protected by additional energy dissipation devices inserted in the structure. The procedure described in this paragraph has the aim to estimate an equivalent damping value for structures equipped with dissipative energy devices, to reduce the spectral ordinates and consequently reduce the effects on the structure optimizing the structural design.

The lack of robust and validated methods that allow the evaluation of the effective damping ratio of a damped structure represents a strong limitation to the widespread use of energy dissipation systems. The Federal Emergency Management Agency (FEMA) included draft guidelines for the implementation of passive energy dissipation devices in new buildings in the 1994 edition of the NEHRP Recommended Provisions for the Seismic Regulations for New Buildings (BSSC1994). FEMA 273 NEHRP Guidelines for the Seismic Rehabilitation of Buildings (1997) and its commentary FEMA 274 convey suggestions for the employment of passive energy dissipation devices in retrofit construction. In particular, they propose linear and nonlinear methods in order to define the effective damping ratio of structures equipped with energy dissipation devices.Linear procedures proposed are referred to static and dynamic analysis, theyare only permitted if it can be demonstrated that the framing system exclusive of the energy dissipation devices remains essentially linearly elastic for the level of earthquake demand of interest after the effects of added damping are considered. Further, the effective damping afforded by the energy dissipation shall not exceed 30% of critical in the fundamental mode. For the purpose of evaluating the regularity of a building, the energy dissipation devices shall be included in the mathematical model. The linear procedures proposed by FEMA 273 are distinguished in linear static procedure and

linear dynamic procedure. According to FEMA 273, nonlinear procedures may be used to implement passive energy dissipation devices without restriction, allowing the use of two alternative methods in order to perform a nonlinear static procedure.

From previous research (*Ventajas Empleo Dissipadores SLB en Proyecto OAK 58 en Puebla – L.M. Bozzo - 2018*) it was highlighted that the employment of more complex and accurate analysis, such as the nonlinear dynamic analysis, led to a better estimation of the real behavior of a structure equipped with hysteretic metallic devices, thus giving the possibility of realizing cheaper constructions. For this reason, the main idea of this research is to calibrate the results of the linear dynamic analysis over the results of the nonlinear dynamic analyses, which take into account the hysteretic behavior of the devices, modifying the damping parameters. The procedure provided is based on the comparison of the results in terms of inter-story drift and story shear between linear time-history analysis and nonlinear time-history analysis. The damping value of the linear analysis has to be increase iteratively up to obtain a good correlation of the results between the two analyses. For each seismic signal considered will be evaluated the equivalent damping value in order that the results of the linear and nonlinear analysis are compatible. The equivalent damping estimated, considering the mean value reduced for the standard deviation, can be applied to the design response spectrum, reducing the ordinates and consequently the effects on the structure, leading to economical advantages in the structural design.

According to ASCE/SEI 7-16,which provides detailed information regards the use of time-history analyses, a suite of not less than 11 ground motions shall be selected for the target spectrum allowing the use of the mean value of story drift and elements demand to evaluate the acceptability criteria.

The procedure can be summarized in the few steps described below and has to be repeated for each signal considered:

1. Afterward a “Direct Iteration”procedure of design, the model to use to run the nonlinear time-analysis and the linear time-history analysis is the same.
   Afterward an “Inverse Iteration” procedure of design, two different models have to be considered, one characterized by the properties of the links corresponding to the dissipators that have been chosen in reality and a second model with the

properties of the equivalent dissipators determined by means of the inverse iteration.

- For the first model, a Non-Linear Time-History Analysis with Direct Integration has to be run considering the nonlinearity concentrated just in the devices.
- For the second model has to be run Linear Time-History Analyses with Direct Integration.

  As described in the previous paragraph, the damping parameters of the time-history analyses must be set depending on the period, the first period is referred to the first mode, the second period is the period for which 90% participating mass is reached in both translational directions. The gravitational loads have to be combined with the results of the linear analysis while for the nonlinear case they have to be applied at the initial step of the analysis as a nonlinear static case.

2. The procedure proposed is an iterative procedure in which the damping value in the linear analysis has to be increased, starting from the initial value of 5%, until the inter-story drift and the story shear reached values similar to the correspondent nonlinear analysis. Have to be considered the distributions of the results for all the stories for the maximum and the minimum peaks of the signal, in both directions x and y.

   The correlation of the results has to be done considering the trends of the results for all the height of the structure, for the maximum and the minimum peaks of the acceleration, and their maximum values, in both directions. This has to be done separately for the story shear and for the inter-story drift. A good correlation of the results is reached when at least one of the maximum values considered reachedadifference range of 10% between the results of the linear analysis and nonlinear analysis.

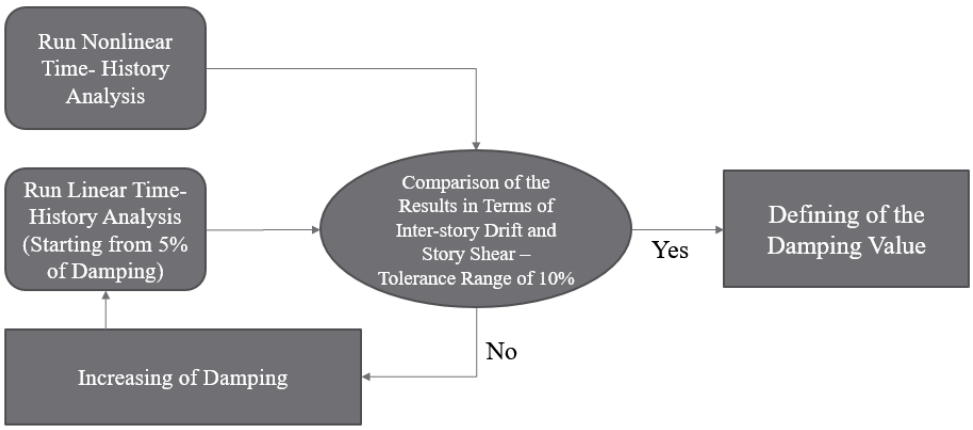

FIGURE 4.6FLOW-CHART EVALUATION OF EQUIVALENT DAMPING PROCEDURE

This procedure could lead to the definition of two different damping values, one obtained from the comparison of the drift and a second from the comparison of the shear. At the end of all the procedures, the designer could choose the damping value to use depending on his valuation.

The iterative procedure has to be applied for each signal, defining, for each of them, the damping values that give the best correlation of the results.To define the modal damping parameter to reduce the design spectrum ordinates, it will be evaluated the mean value and its standard deviation allowing to estimate of a conservative value reducing the mean value for the standard deviation.

The structural design will be computed through a response spectrum analysis whose design spectrum is reduced for damping and for ductility. To operate in a conservative area it could be appropriate to adopt the increase of damping evaluated just for the seismic design of the beams, the columns have to be designed considering the conventional damping value of 5 %. It is important to specify that the final design has to be checked through a complete nonlinear analysis, defining the plastic hinges in all the elements and verify that none of them reached the critical state.

5 CASE OF STUDY: LANDMARK PROJECT

5.1 DESCRIPTION OF THE BUILDING

The case-study concerns a new building situated in the city of Guadalajara (Mexico), the project is developed in collaboration with a second engineering company.

Landmark is a residential building of 38 floors plus other 5 stories at the basement for a total height of 177m, of whom 155m over the ground. The shape of the building is approximately squared, with a total surface area of 1200m^2 which has to be divided into8 apartments. The building has a reinforced concrete structure with large bays until to 11 meters in length and, because of the discontinuity of some floors, from level 20 up to 22, it presentsdouble-height columns and significantvariations of the mass between consecutive floors.

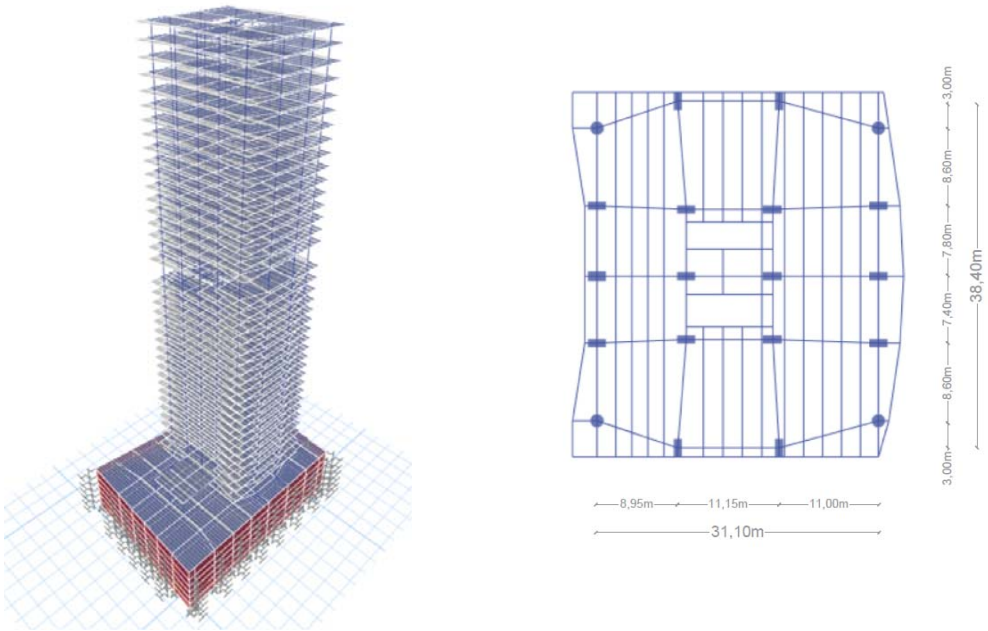

FIGURE 5.1 GEOMETRY OF THE MODEL

All the element's sections and the properties of the materials have been just defined by the previous company. Hereinafter, the elements cross-section dimensionsand the relative concrete compressive strengthare reported below, for each floor:

Levels	Rectangula Columns (BXH)cm	Circular Columns (D)cm	Internal Beams (BXH)cm	Perimetral Beams (BXH)cm
AZO	80X120-50Mpa	100-50Mpa	50X90-35Mpa	40X90-35Mpa
N37	80X120-50Mpa	100-50Mpa	50X90-35Mpa	40X90-35Mpa
N36	80X120-50Mpa	100-50Mpa	50X90-35Mpa	40X90-35Mpa
N35	80X120-50Mpa	100-50Mpa	50X90-35Mpa	40X90-35Mpa
N34	80X120-50Mpa	100-50Mpa	50X90-35Mpa	40X90-35Mpa
N33	80X120-50Mpa	100-50Mpa	50X90-35Mpa	40X90-35Mpa
N32	80X120-50Mpa	100-50Mpa	50X90-35Mpa	40X90-35Mpa
N31	80X120-50Mpa	100-50Mpa	50X90-35Mpa	40X90-35Mpa
N30	80X120-50Mpa	100-50Mpa	50X90-35Mpa	40X90-35Mpa
N29	80X140-50Mpa	100-50Mpa	50X90-35Mpa	40X90-35Mpa
N28	80X140-50Mpa	120-50Mpa	50X90-35Mpa	40X90-35Mpa
N27	80X140-50Mpa	120-50Mpa	50X90-35Mpa	40X90-35Mpa
N26	80X140-50Mpa	120-50Mpa	50X90-35Mpa	40X90-35Mpa
N25	80X140-50Mpa	120-50Mpa	50X90-35Mpa	40X90-35Mpa
N24	80X160-50Mpa	120-50Mpa	50X90-35Mpa	40X90-35Mpa
N23	80X180-50Mpa	120-50Mpa	50X90-35Mpa	40X90-35Mpa
N22	80X180-50Mpa	120-50Mpa	50X120-35Mpa	50X120-35Mpa
N21	80X180-50Mpa	120-50Mpa	50X120-35Mpa	50X120-35Mpa
N20	80X180-50Mpa	120-50Mpa	50X120-35Mpa	50X120-35Mpa
N19	80X180-50Mpa	120-50Mpa	50X90-35Mpa	40X90-35Mpa
N18	80X180-50Mpa	120-50Mpa	50X90-35Mpa	40X90-35Mpa
N17	80X180-50Mpa	120-50Mpa	50X90-35Mpa	40X90-35Mpa
N16	80X180-50Mpa	120-50Mpa	50X90-35Mpa	40X90-35Mpa
N15	80X180-50Mpa	120-50Mpa	50X90-35Mpa	40X90-35Mpa
N14	80X180-50Mpa	120-50Mpa	50X90-35Mpa	40X90-35Mpa
N13	90X200-50Mpa	140-50Mpa	50X90-35Mpa	40X90-35Mpa
N12	90X200-50Mpa	140-50Mpa	50X90-35Mpa	40X90-35Mpa
N11	90X200-50Mpa	140-50Mpa	50X90-35Mpa	40X90-35Mpa
N10	90X200-50Mpa	140-50Mpa	50X90-35Mpa	40X90-35Mpa
N9	90X200-65Mpa	140-65Mpa	50X90-45Mpa	40X90-45Mpa
N8	90X200-65Mpa	140-65Mpa	50X90-45Mpa	40X90-45Mpa
N7	90X200-65Mpa	140-65Mpa	50X90-45Mpa	40X90-45Mpa
N6	90X200-65Mpa	140-65Mpa	50X90-45Mpa	40X90-45Mpa
N5	100X200-65Mpa	140-65Mpa	50X90-45Mpa	40X90-45Mpa
N4	100X200-65Mpa	140-65Mpa	50X90-45Mpa	40X90-45Mpa
N3	120X200-65Mpa	160-65Mpa	60X120-45Mpa	60X120-45Mpa
N2	120X200-65Mpa	160-65Mpa	60X120-45Mpa	60X120-45Mpa
N1	120X200-65Mpa	160-65Mpa	60X140-45Mpa	60X140-45Mpa
PB	120X200-65Mpa	160-65Mpa	40X80-45Mpa	40X80-45Mpa
SOT1	120X200-65Mpa	160-65Mpa	PTR 45-35Mpa	PTR 45-35Mpa
SOT2	120X200-65Mpa	160-65Mpa	PTR 45-35Mpa	PTR 45-35Mpa
SOT3	120X200-65Mpa	160-65Mpa	PTR 45-35Mpa	PTR 45-35Mpa
SOT4	120X200-65Mpa	160-65Mpa	PTR 45-35Mpa	PTR 45-35Mpa
SOT5	120X200-65Mpa	160-65Mpa	PTR 45-35Mpa	PTR 45-35Mpa

TABLE 5-1 SECTION PROPERTIES

The main goal was to provide a solution based on the architectural project with the purpose to control the structural behavior under the seismic actions andoptimizing the structural design. In this regard, the solution proposed was to use passive energy dissipation systems SLB typeconnected to the structure with decoupled concrete walls.The use of dissipatorsincreases the stiffness of the structure, reducing the inter-story drift, and provides the capacity to dissipate energy in correspondence of the devices, reducing the structural damage.

5.2 REFERENCE CODE

- "*REGLAMENTO DE CONSTRUCCIONES Y DESARROLLO URBANO DEL MUNICIPIO DE ZAPOPAN, JALISCO Y NORMAS TÉCNICAS COMPLEMENTARIAS PARA DISEÑO POR SISMO"*- Reference code took into account for the definition of the criteria for the calculation of seismic forces in the city of Guadalajara.
- ASCE/SEI 7-16 – Reference code for the use of Time-History Analyses.

5.2.1 GRAVITY LOADS

The gravitational loads are defined as static loads. According to the code, have been defined the dead loads, consisting of the weight of all materials of construction incorporated into the structural elements of the building, the permanent non-structural loads, consisting of the weight of the non-structural elements of the building, and live loads, consisting of the load produced by the use and occupancy of the building or environmental loads, such as wind load, snow load, rain load, earthquake load.
For the case of study representing a residential building has been considered:
Dead Loads (DL): 2400kg/m^3
Permanent Non-structural loads (SCM): 200kg/m^2
Live Loads (LL): 190kg/m^2
Basic Combination:
1.4DL+1.4SCM
1.2DL+1.2SCM+1.6LL

Basic Combinations with Seismic Load Effects:

$1.4(DL+SCM)+1.0LL \pm E_h$

$0.7(DL+SCM) \pm E_h$

5.2.2 Definition of the Response Spectrum

To introduce, it is important to explain that the Mexican territory is divided into four seismic zones, two of low seismicity and two of high seismicity. To determine the seismic zone is provided a simple criterion based on the value of the maximum rock acceleration. Considering the site of Guadalajara, it falls in zone C. It is, therefore, characterized by an high seismicity, with maximum rock-bed accelerations between 100cm/sec^2 (0.1g) and 200cm/sec^2 (0.2g).

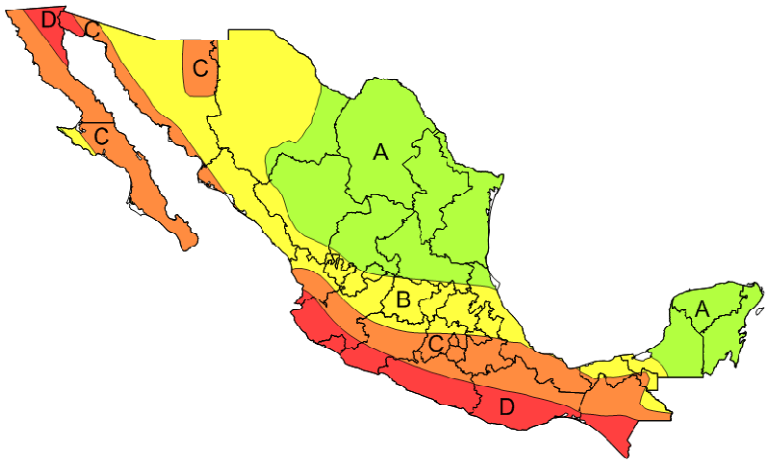

Figure 5.2 Hazard Map of Mexico

Aceleración máxima en roca, a_0^r (cm/s^2), correspondiente al nivel de referencia ER	Zona	Intensidad sísmica
$a_0^r \geq 200$	D	Muy Alta
$100 \leq a_0^r < 200$	C	Alta
$50 \leq a_0^r < 100$	B	Moderada
$a_0^r < 50$	A	Baja

Table 5-2 Bedrock Acceleration

The type of soil is determined considering the dynamic parameters of the soil,modeled as a means stratified. The parameters to take into account are the depth of the soil and the speed of propagation of the shear waves through the soil. The code provides the classification of the soil type considering three different types. The prescriptions are shown in the tab. 6.

Type	Description
I	(a) Rock or similar material characterised by a shear wave propagation velocity greater than 700 metres per second. (b) Medium-dense to dense or medium-rigid to stiff soils, with depth to rock less than 50 metres, characterised by a shear wave propagation velocity between 400 and 700 metres per second.
II	(a) A predominantly medium-dense to dense or medium-stiff to stiff soil profile, with depth greater than 50 metres, characterised by a shear wave propagation velocity between 400 and 700 metres per second. (b) Medium-dense soils with depth greater than 8 metres and less than 35 metres, characterised by a shear wave propagation velocity between 150 and 400 metres per second.
III	(a) Low dense or loose granular soils. (b) A soil profile containing more than 6 metres of soft to medium-stiff clay but not more than 12 metres of soft clay.

TABLE 5-3 TYPE OF SOIL

According to Guadalajara's local Code, the structures are classified into two main groups depending on their function:

Group A: Buildings whose operation is essential in case of urban emergency, as well as buildings whose structural failure could result in the loss of a large number of lives or exceptionally high economic or cultural losses.

Group B:Common buildings for housing, offices and commercial premises, hotels, and commercial and industrial buildings not included in Group A.

Landmark is a residential building, therefore, belongs to the group B and, in the specific, to the subgroup B1 referred to buildings over 15 m high or with more than 3,000 m² of total built area.

To apply the dynamic modal analysis, the design elastic response spectrum has to be developed adopting the following expressions:

- $T < Ta$ $\quad Sa = c \cdot (1 + 1.5\,T/Ta) \,/\, 2.5$
- $Ta \leq T \leq Tb$ $\quad Sa = c$
- $T > Tb$ $\quad Sa = c \cdot (Ta/T)^r$

where $\boldsymbol{S_a}$ represents the spectral acceleration, ***c***is a seismic coefficient site-dependent, ***T*** is the period of the SDOF system, $\boldsymbol{T_a}$ and $\boldsymbol{T_b}$ are the periods according to which the constant acceleration curve of the spectra respectively starts and ends, and, finally, ***r*** defines the spectral acceleration drop starting from ***Tb***. ***Ta***, $\boldsymbol{T_b}$, and ***r***are given by Guadalajara's local code according to the soil type, as reported in Tab.7. The seismic coefficient, ***c***, is the quotient of the horizontal shear force to be considered as acting on the base of the structure due to the effect of the earthquake, divided by the weight of the structure at that level, for the structure of Group B shall be taken equal to ***0.36***. The response spectrum obtained is determined considering a damping value of 5%.

Tipo de Suelo*	T_a	T_b	r
I	0.15	0.50	2/3
II	0.15	0.80	2/3
III	0.20	1.10	2/3

TABLE 5-4 - SPECTRAL PARAMETERS

In the current case, the building's site is characterized by the following properties:

TABLE 5-5 RESPONSE SPECTRUM PARAMETERS

Seismic Zone	Soil Type	Group	T_a(s)	T_b(s)	r	c	a_0(g)
C	II	B1	0.15	0.80	0.66	0.36	0.144

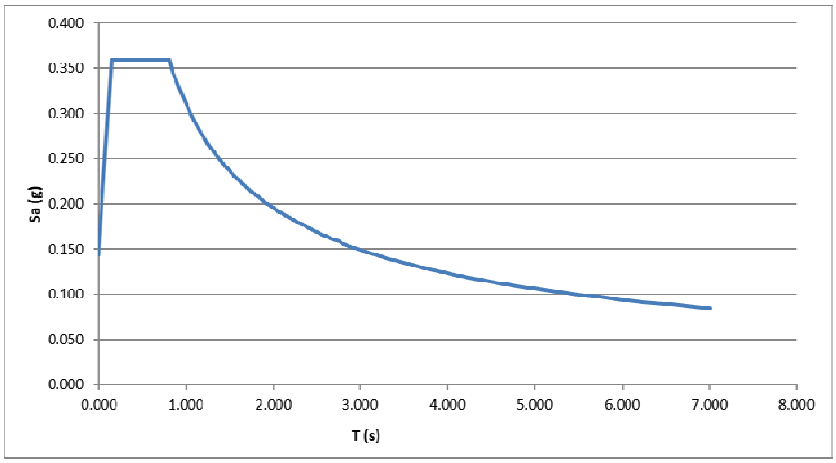

FIGURE 5.3 ELASTIC RESPONSE SPECTRUM

For design purposes, when using the dynamic modal analysis method, the seismic forces may be reduced by dividing by the reduction factor **Q'**. In the seismic design of regular structures Q' shall be calculated as follows:

$$Q' = 1 + (T/T_a)\,(Q - 1) \qquad T < Ta$$

$$Q' = Q \qquad T \geq Ta$$

T shall be taken equal to the natural period of vibration of the mode to be considered, ***Ta*** is a characteristic period of the design spectrum and ***Q*** is the seismic behavior factor defined by the code for a different type of structural systems. For common structures in which lateral forces are resisted at each level by continuous frames, by diaphragms or walls, or by a combination of these, the factor ***Q***can be assumed equal to ***3.00***.

In the seismic design of structures containing just vertical irregularities or horizontal irregularities listed, Q' shall be multiplied by *0.8*, except where there are both the types of irregularities, in which case Q' shall be multiplied by a value of *0.75*. According to the code, the case-study presents vertical irregularity due to the variation of the mass, this led to consider a ductility factor ***Q'***reduced equal to ***2.4***.

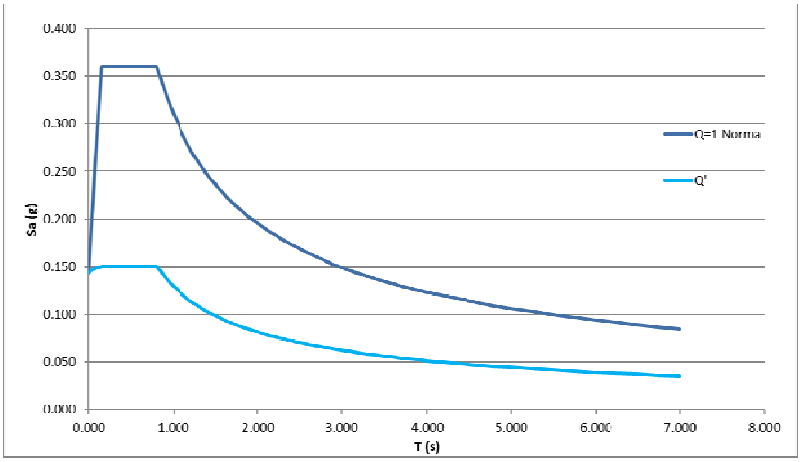

FIGURE 5.4 ELASTIC-INELATIC RESPONSE SPECTRUM

5.2.3 SEISMIC SIGNALS

According to ASCE/SEI 7 code, a suite of not less than 11 ground motions shall be selected for the target spectrum allowing the use of the mean value of story drift and elements demand to evaluate the acceptability criteria. In the 2016 edition of the standard, the minimum number of motions was increased to 11. The requirement for this larger number of motions was not based on detailed statistical analyses but rather was judgmentally selected to balance the competing objectives of more reliable estimates of mean structural responsesagainst computational effort. The signals considered are characterized by perfect compatibility with the reference spectrum, this is principally due to the fact that the signals are artificial.

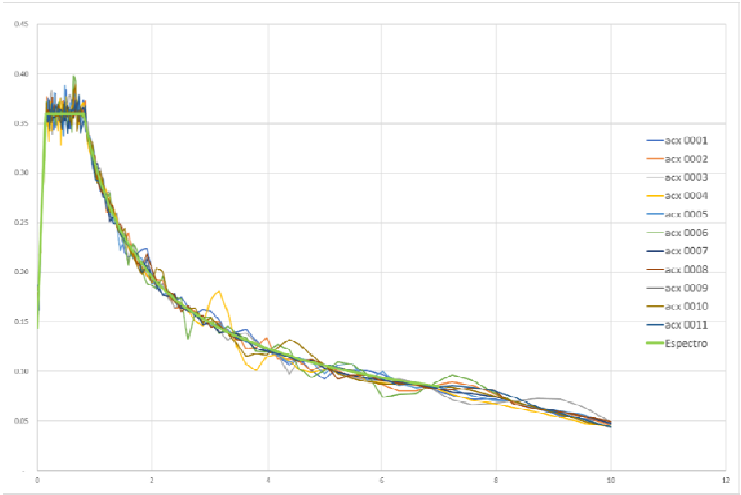

FIGURE 5.5 GROUND MOTIONS RESPONSE SPECTRA

The 11 accelerograms used in the analysis are reported below:

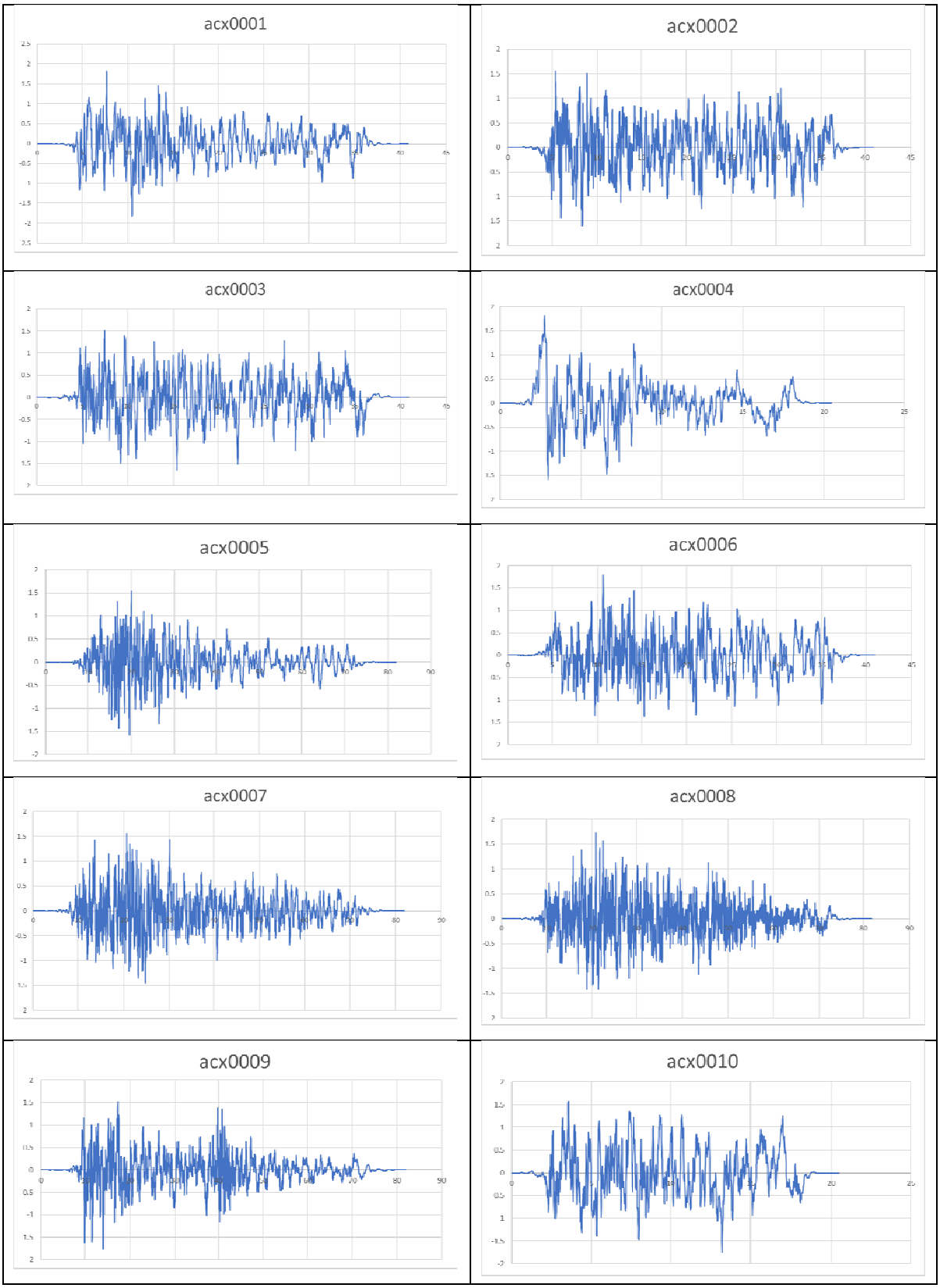

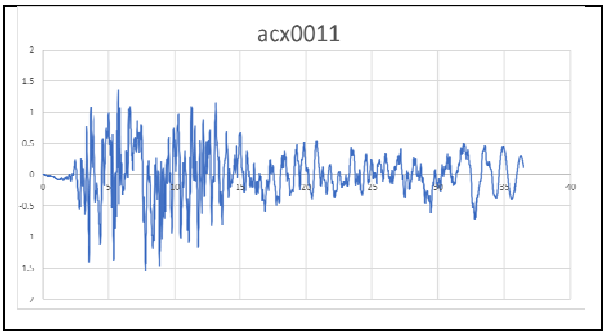

TABLE 5-6 SEISMIC SIGNALS

5.2.4 REQUIREMENTS OF THE CODE

According to the Guadalajara's Local Code, every structure and each part of them shall be designed to comply with the following basic requirements:

- Be adequately safe against the occurrence of all possible limit state failures under the most unfavorable combinations of actions that may occur during its expected life.
- Not exceed any serviceability limit state under combinations of actions corresponding to normal operating conditions.

A limit state of failure shall be considered to be any situation corresponding to the exhaustion of the load-bearing capacity of the structure or of any of its components, including the foundation, or the occurrence of irreversible damage that significantly affects the resistance to new load applications.

- At the limit state of failure, the inter-story drift shall not exceed 0.015 or 0.005Q times the height of the between storey for structures having a fundamental period of less than 0.7 seconds. For structures having a fundamental period of 0.7 seconds or greater, the calculated inter-story distortion shall not exceed 0.011 or 0.004Q times the height of the inter-story.

The serviceability limit state shall be considered to be the occurrence of deformation, cracking, vibration or damage affecting the proper functioning of the construction, but not impairing its load-bearing capacity.

- Atthe limit state of serviceability, the relative horizontal displacement between two successive levels of the structure shall be lower or equal to the inter-story height divided by 500 for buildings in which the non-structural elements have

low displacements capacity; in other cases, the limit shall be equal to the inter-story height divided by 250.

Considering the case-study, the SLB design has to be referred to the limit state of failure with the limit equal to 0.011.

5.3 STRUCTURAL BEHAVIOR OF THE BARE STRUCTURE

In order to study the structural behavior of the building, it has been run a modal analysis in order to have information about the first modes of vibration of the structure and their participating mass ratio. The results of the modal analysis are reported in tab.10.

Modal Participating Mass Ratios										
Mode	Period	UX	UY	UZ	SumUX	SumUY	SumUZ	RX	RY	RZ
	sec									
1	6.675	0.5147	0.00002218	0	0.5147	2.22E-05	0	1.95E-05	0.485	0.0002
2	6.36	0.00003501	0.4507	0	0.5148	0.4507	0	0.4353	2.61E-05	0.0725
3	6.108	0.0009	0.0585	0	0.5157	0.5092	0	0.0563	0.0008	0.2577

TABLE 5-7 MODAL ANALYSIS RESULTS

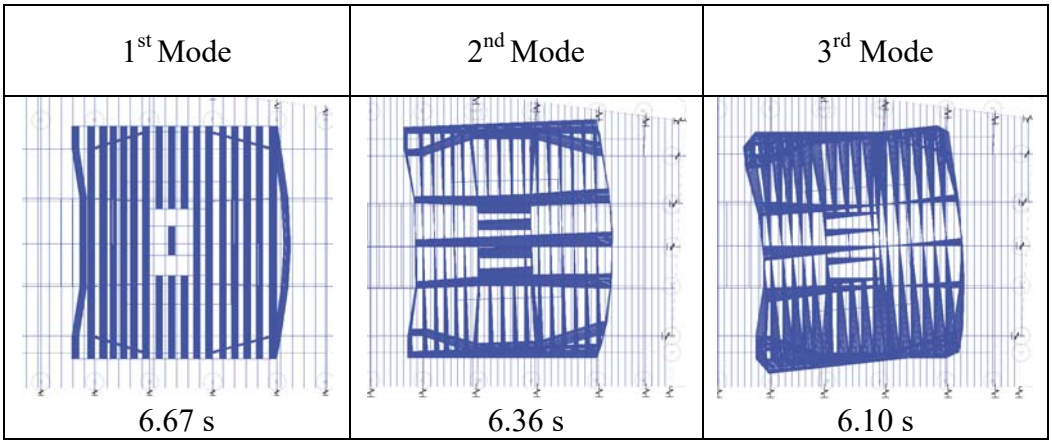

FIGURE 5.6 MODAL ANALYSIS RESULTS

The modal results showed that the structure is characterized by a large fundamental period of 6,67sec, corresponding to the first mode of vibration translational in direction x, with a participating mass of 50% of the total mass.

The results of the response spectrum analysis in terms of inter-story drift at the limit state of prevention of collapse are shown in the fig.5.7. In both directions the structure

doesn't satisfy the requirements of the code, reaching a maximum drift of 0.014 in direction x, the most deformable direction, and a maximum drift of 0.012 in direction y.

FIGURE 5.7BARE STRUCTURE - INTER-STORY DRIFT

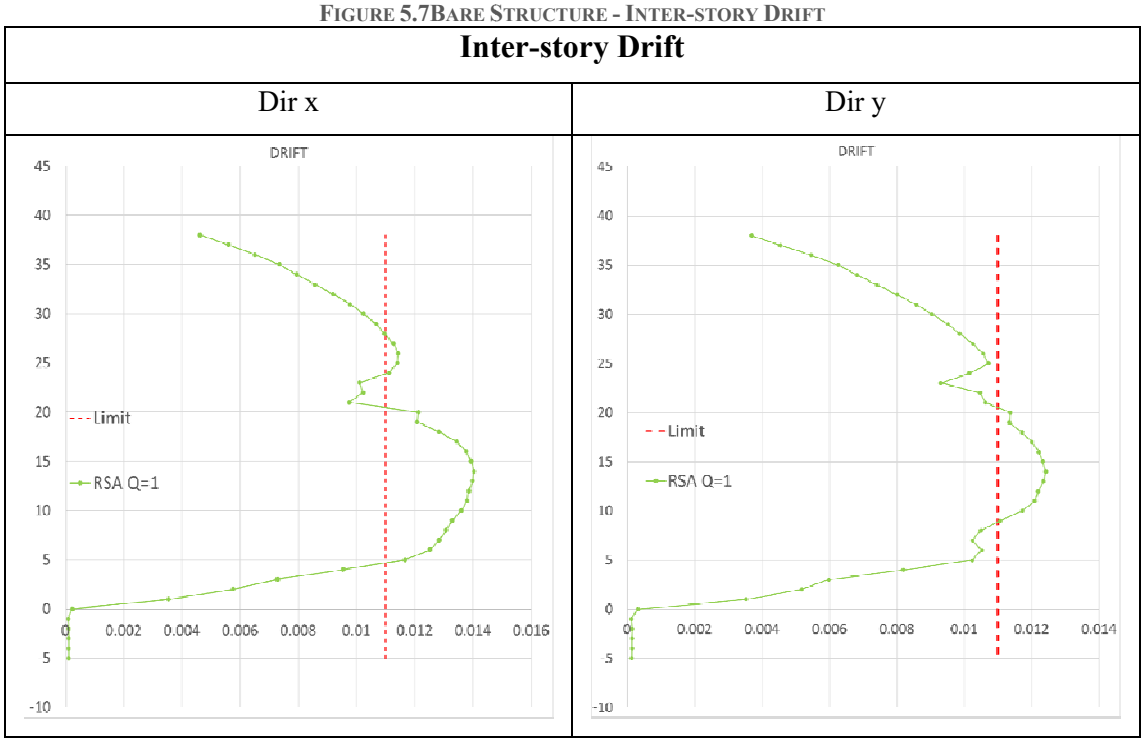

FIGURE 5.8BARE STRUCTURE - ABSOLUTE DISPLACEMENTS

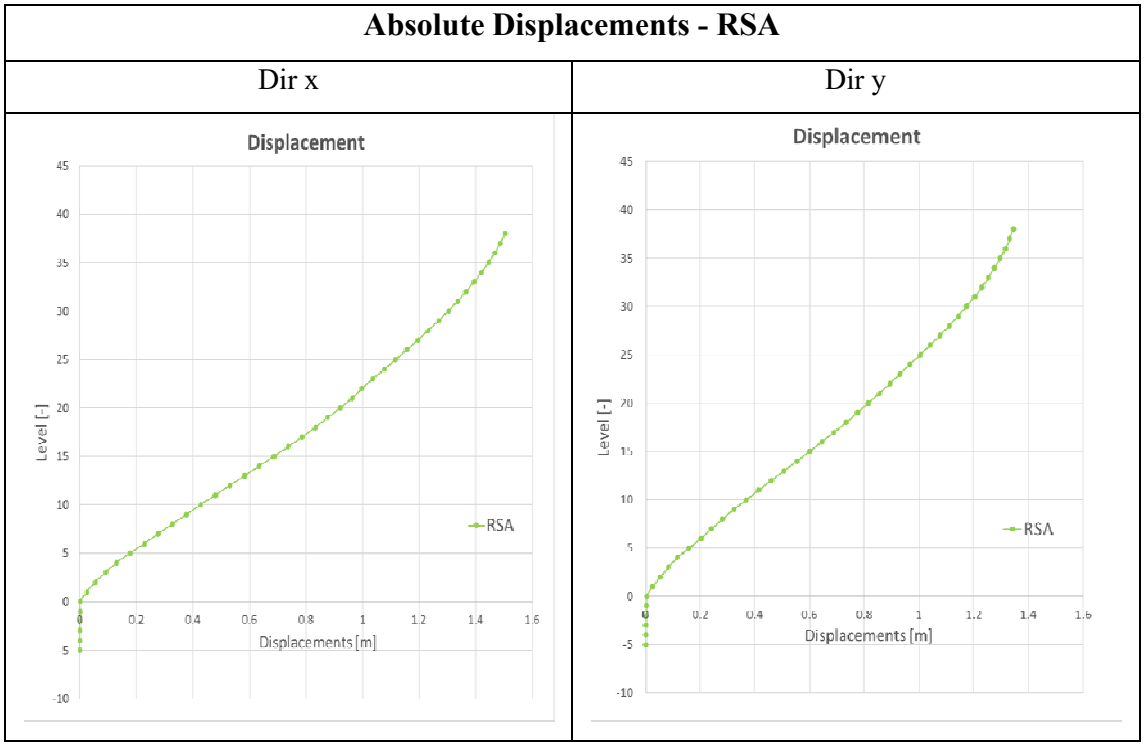

5.4 SLB DESIGN

5.4.1 INVERSE ITERATION

The design of the intervention has been done taking into account the architectural limitation imposed regarding the disposition of the decoupled walls on plane, fig., and their thickness, limited at *25cm.* According to the procedure of the "Inverse Iteration" described in paragraph *3.4.2*, to limit the size of the decoupled walls, the dimension of the dissipatorshas to be fixed according to the shear capacity of the walls and to the technological space for the anchorage of the dissipator to the wall. Therefore the device is selected by means of the table of SLB devices in such a way that its $F_y$is the one immediately below$F_{max,SLB}$.

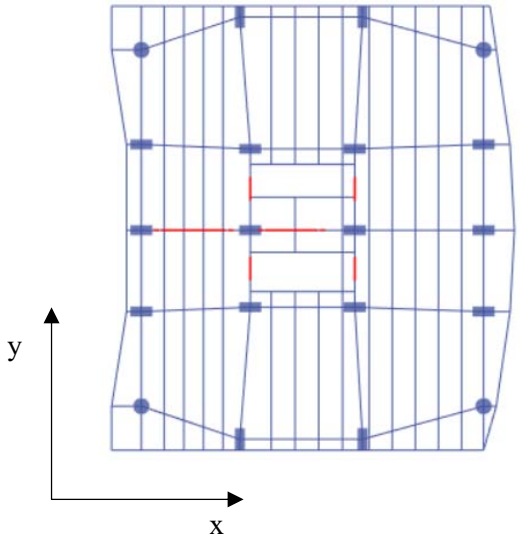

FIGURE 5.9 DISPOSITION OF THE CONCRETE WALLS

The scheme in the fig.5.9 shows that according to the architectural restrictions is possible to place a maximum of 2 walls of concrete in direction x, with a total length of 6 meters, to equipped with two devices each one, and a total of 4 walls of concrete in direction y, of 2,30 meters of length, to equipped with a single device each one.

For Landmark Project has been planned to use the fourth generation of the SLB devices, described in detail in paragraph *3.2.4*. This generation is characterized by a higher deformation capacity compared to the previous generation of devices, the properties of the SLB devices belonging to the fourth generation are reported in the following table.

Parámetros de diseño para los disipadores SHEAR LINK BOZZO de 4a generación					
Dispositivo	K_1 (KN/cm)	K_2 (KN/cm)	D_y (mm)	F_y (KN)	$F_{MÁX}$ (KN)
SLB4_10_5	2026.65	21.62	0.749	151.79	250.00
SLB4_10_6	2163.53	22.90	0.742	160.54	265.78
SLB4_15_5	2472.60	24.85	0.720	177.92	293.72
SLB4_15_6	2761.73	26.96	0.706	195.09	320.62
SLB4_15_7	3021.88	28.76	0.697	210.76	345.09
SLB4_20_6	3361.00	33.09	0.687	230.93	381.61
SLB4_20_7	3700.15	35.28	0.673	248.98	410.70
SLB4_25_6	4260.80	42.53	0.654	278.74	468.96
SLB4_25_7	4767.68	46.51	0.638	304.31	512.31
SLB4_25_8	5238.65	50.43	0.626	327.73	552.76
SLB4_30_7	5785.96	57.25	0.619	358.28	611.14
SLB4_30_8	6419.52	62.36	0.608	390.28	665.17
SLB4_30_9	6994.22	66.79	0.601	420.37	716.61
SLB4_30_10	7535.22	70.90	0.596	449.29	764.52
SLB4_40_7	7797.49	78.07	0.596	464.68	807.56
SLB4_40_8	8718.88	86.41	0.588	512.48	890.20
SLB4_40_9	9580.18	93.66	0.582	557.71	966.06
SLB4_40_10	10439.63	101.20	0.576	601.31	1043.20
SLB4_40_11	11253.53	109.93	0.571	643.06	1117.73
SLB4_40_12	12033.64	115.64	0.570	685.73	1191.30
SLB4_50_9	12289.99	120.57	0.578	709.95	1236.23
SLB4_50_10	13421.60	130.96	0.572	768.20	1340.09
SLB4_50_11	14537.41	141.39	0.569	827.48	1443.52
SLB4_50_12	15599.37	150.54	0.567	884.08	1540.02
SLB4_60_5	8891.13	91.74	0.598	531.45	932.94
SLB4_60_6	10457.28	106.25	0.586	613.19	1078.09
SLB4_60_11	17684.45	174.36	0.562	993.08	1746.50
SLB4_60_12	19029.62	185.88	0.560	1065.32	1868.98
SLB4_65_11	19829.08	194.60	0.562	1113.76	1957.04
SLB4_65_12	21326.70	209.74	0.560	1194.73	2103.54
SLB4_65_13	22872.65	223.05	0.558	1276.57	2245.62
SLB4_65_14	24379.36	235.06	0.556	1356.52	2382.04
SLB4_65_15	25869.86	249.17	0.554	1433.77	2519.93
SLB4_65_16	27331.55	261.77	0.553	1511.96	2654.85
SLB4_65_18	30180.37	286.67	0.554	1671.12	2912.47
SLB4_65_20	32951.18	306.56	0.553	1822.60	3157.88

TABLE 5-8 DESIGN TABLE PROVIDED BY THE SLB MANUAL

Calculating the shear capacity of the walls, according to the provisions of the ACI which depend on its length, thickness and characteristic resistance of concrete according to the expression (units MPa):

$$V_d = 0.75 \cdot 0.83 \cdot \sqrt{f_{ck}} \cdot L \cdot t$$

L[m]	*T[m]*	*f_{ck}[MPa]*	*V_d [kN]*
6,00	*0,25*	*45*	*6263,80*
2,3	*0,25*	*45*	*2401,12*

TABLE 5-9 CONCRETE WALLS PROPERTIES

Considering the shear capacity of the walls, it would be possible to install devices up to 65cm of width, in reality it is necessary to consider the technological space needed to anchor the device to the wall. For this reason, for a thickness of 25 cm, the maximum dimension of the device possible to install is the SLB of 40cm of width. Therefore, as first tempt, has been supposed to installall devices of type SLB4_40_7.

The SLB devices are inserted in the model as links characterized by a nonlinear behavior compatible with the plasticity model of Wen and a linear behavior defined by the effective stiffness of the device, as specified in paragraph *3.3*, while the decoupled walls were modeled as shell elements.

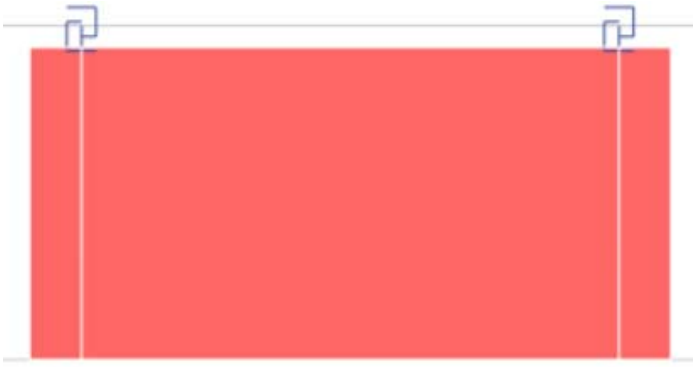

FIGURE 5.10 MODEL OF THE DECOUPLED WALLS

According to the inverse iteration procedure,in order to launch a linear analysis, the model has to be calibrated to ensure that in each device the acting shear doesn't exceed the limit demand/capacity established from 1.1-1.4. The solution is to reduce "fictitiously" in the RSA numerical model the size of the device and repeat the analysis

until obtaining a shear force within the stated range.It is important to specify that the iterative procedure for the calibration of the model is automatized in the ETABS plug-in, DissipaSLB.

Once the model has been calibrated, the inter-story drift has been checked, and,where the requirements of the code were not satisfied, the number of devices has been increased.

5.4.2 Optimized SLB Design

It is important to consider that the project was in a phase of development, this means that many architectural changes occurred leading to variations of the solution.

The SLB design has been optimized in terms of economic advantages and performances, ensuring the fulfillment of verifications reported by the code. The optimized solution proposed consists of the installation of 236 SLB devices, type SLB4_30_7, with decoupled walls of 20cm of thickness.

The details of the solution proposed are shown below:

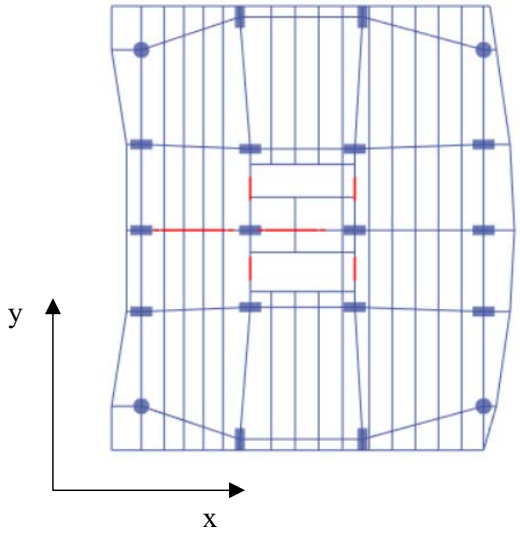

Figure 5.11 Disposition of the Concrete Walls on Plane

It has been planned the installation of up to four devices for each direction at the levels most deformable, considering two decoupled walls of concrete of 6,00 m of length and 20cm of thickness in direction x, equipped with two devices SLB4_30_7 each one, and four decoupled walls of concrete of 2,30 m of length and 20cm of thickness, equipped with a single device SLB4_30_7 each one. All the supporting walls are characterized by a concrete compressive strength of 45MPa. The details of the intervention for each floor have been reported in the next tables. It is important to highlight that because of the "toothed" connection of the devices, that doesn't transfer axial forces, they can be freely placed on plane and in height, stiffening them specifically whereit is needed and where architecturally possible.

FIGURE 5.12 DETAILS OF THE OPTIMIZED SOLUTION

Dir x

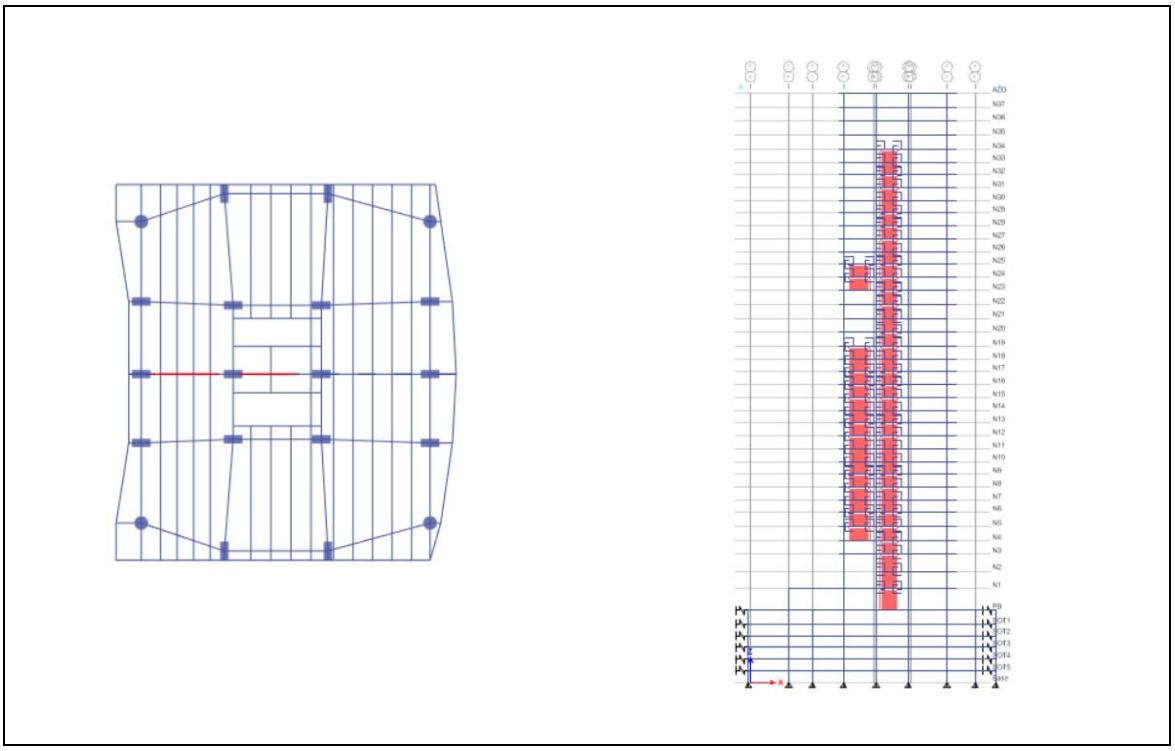

Dir y

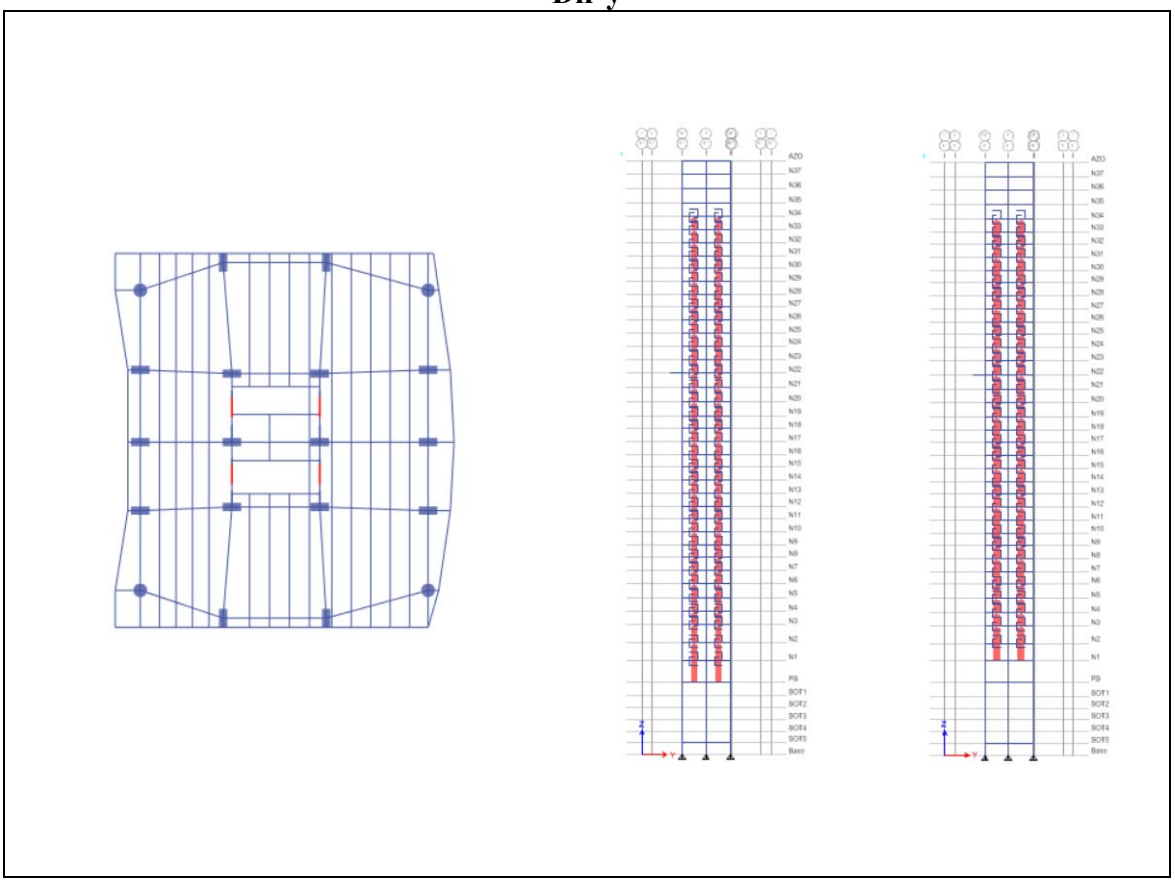

In fig.5.12 are shown the results of the modal analysis in comparison with the results of the bare structure, it can be noticed that the solution proposed shows a fundamental period lower than the original structure, and this is justified by the fact that the stiffness of the structure has been increased, but the first mode is a rotational mode. This may be due to the disposition on plane of the dissipators, closely linked to the architectural restrictions. In spite of this, the structure can be controlled and designed with significant advantages due to the solution applied.

	Landmark without SLB	**Landmark_SLB4_30_7**
1st Mode	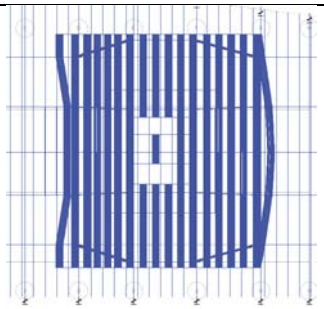 6.67 s	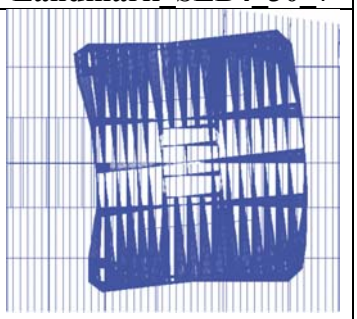 6.00 s
2nd Mode	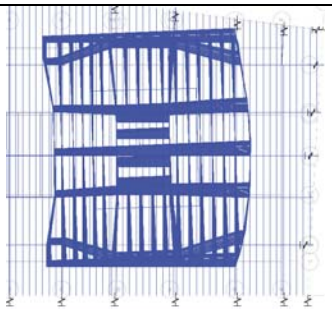 6.36 s	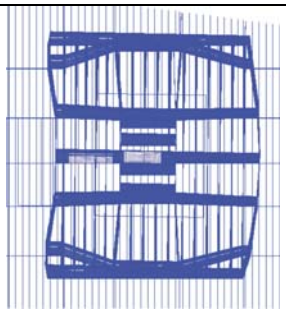 5.48 s
3rd Mode	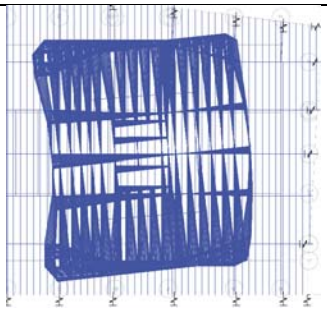 6.10 s	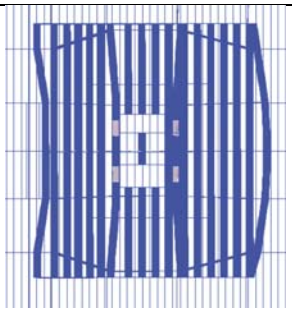 5.20s

FIGURE5.13 MODAL ANALYSIS RESULTS

Landmark without SLB

Modal Participating Mass Ratios										
Mode	Period	UX	UY	UZ	SumUX	SumUY	SumUZ	RX	RY	RZ
	sec									
1	6.675	0.5147	0.00002218	0	0.5147	2.22E-05	0	1.95E-05	0.485	0.0002
2	6.36	0.00003501	0.4507	0	0.5148	0.4507	0	0.4353	2.61E-05	0.0725
3	6.108	0.0009	0.0585	0	0.5157	0.5092	0	0.0563	0.0008	0.2577

TABLE 5-10 MODAL ANALYSIS RESULTS

Landmark_SLB4_30_7

Modal Participating Mass Ratios										
Mode	Period	UX	UY	UZ	SumUX	SumUY	SumUZ	RX	RY	RZ
	sec									
1	6.008	0.0004	0.0158	0	0.0004	0.0158	0	0.0155	0.0004	0.3302
2	5.481	0.0003	0.4935	0	0.0006	0.5093	0	0.4763	0.0002	0.0004
3	5.207	0.5007	0.0001	0	0.5014	0.5095	0	0.0001	0.4981	0.0006

TABLE 5-11 MODAL ANALYSIS RESULTS

The results of the response spectrum analysis are reported below in order to check the inter-story drift at the limit state of failure according to the Guadalajara's Local Code, with a maximum inter-story drift allow equal to 0.011.

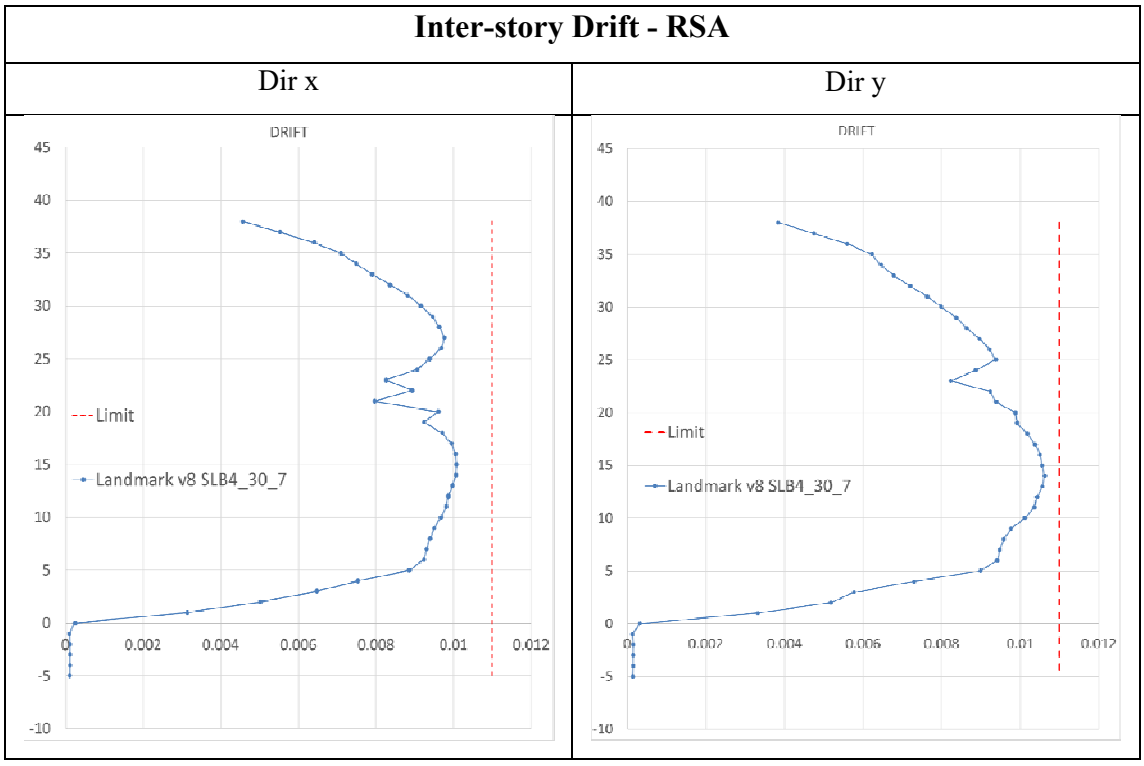

FIGURE 5.14RSA-INTER-STORY DRIFT

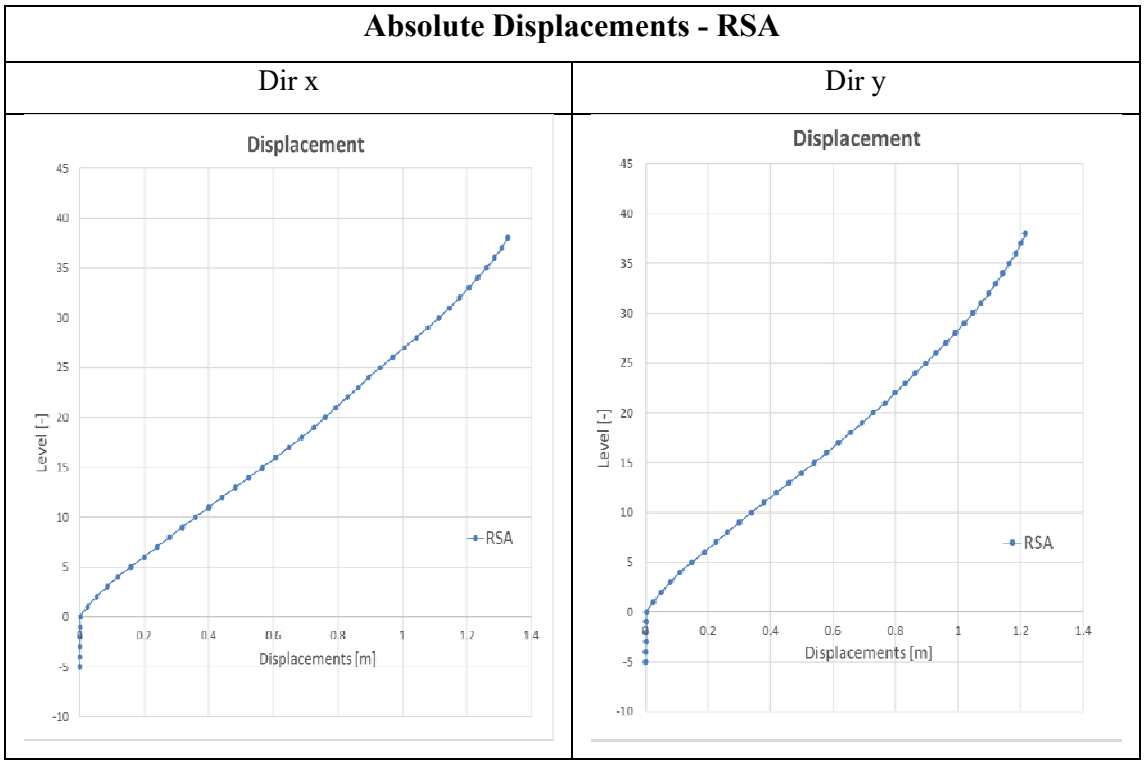

FIGURE 5.15RSA-ABSOLUTE DISPLACEMENTS

In order to assess the effective seismic performance of the structure during strong earthquake ground motions and to properly consider the elastoplastic behavior of dissipators, nonlinear time-history analyses have been performed according to Guadalajaa's Local Code and with reference to American Code ASCE/SEI 7-16. Ground motions inputs have properly been selected in order to satisfy spectrum-compatibility criteria. A group of 11 ground motions have been selected, as described in the previous paragraph, allowing the use of the mean value of story drift and elements demand to evaluate the acceptability criteria.

The use of nonlinear analyses allows to consider the hysteretic properties of the links, characterized by the plasticity model of Wen described in paragraph *3.3,* and to check the displacement capacity of the devices. Through the software ETABS it was possible to run Non-Linear Time History Analyses with Direct Integration (paragraph *3.4.2*), considering the nonlinearity concentrated just in the dissipators, in this case the model has to be set with the properties of the device chosen in the reality, the SLB4_30_7. The load cases have been set considering the nonlinear properties in Links/Support elements and the geometric nonlinearity P-Delta. The gravitational loads have been applied at the

initial step of the analysis as a nonlinear static case. In each load case, the accelerations have been combined in directions U1 and U2, in order to evaluate the nonlinear behavior of the structure.

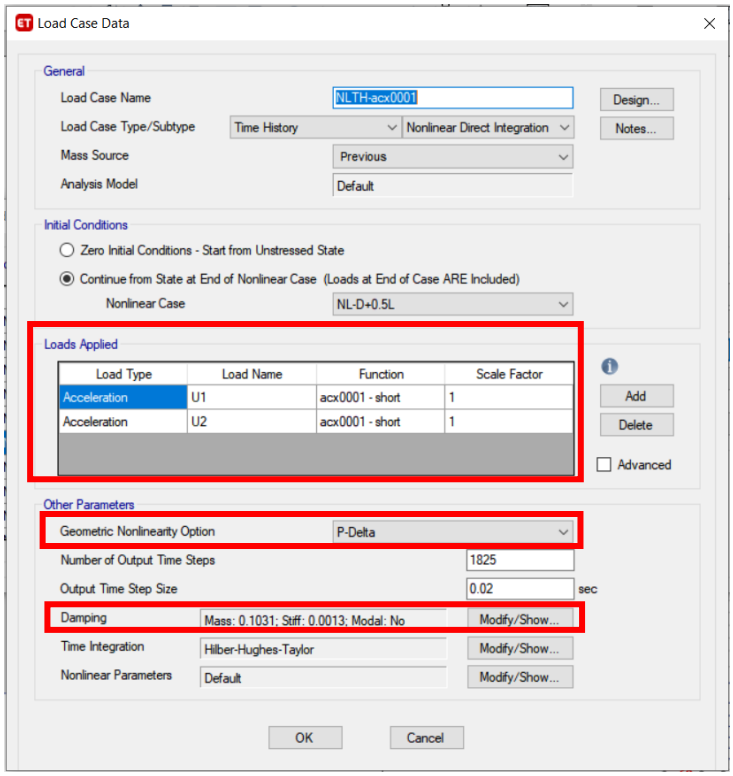

FIGURE 5.16 SETTING NONLINEAR TIME-HISTORY ANALYSIS - ETABS

The Damping parameters were set depending on the period, the first period is considered as the fundamental period and the second period is the period for which 90% participating mass is reached in both translational directions. The damping is conventionally specified for reinforced concrete at 0.05.

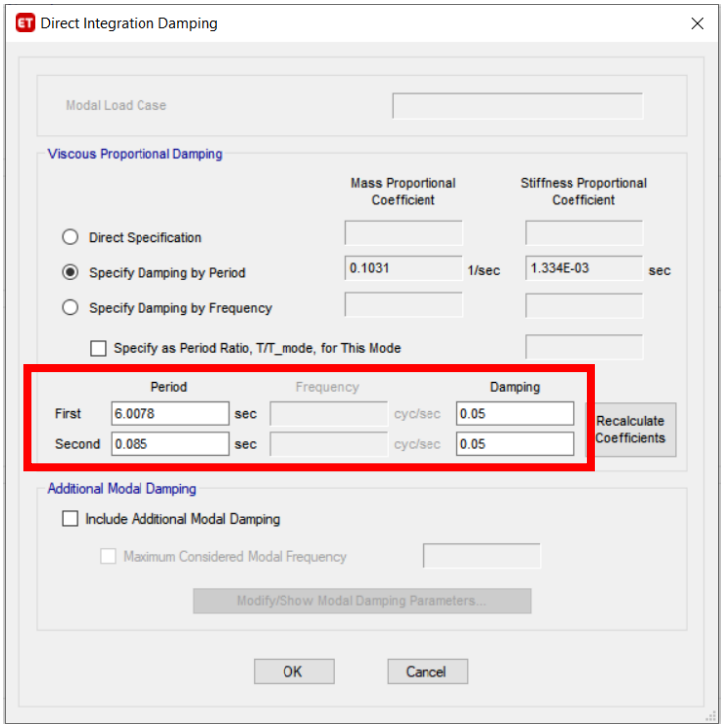

FIGURE 5.17 SETTING DAMPING PARAMETERS OF NONLINEAR ANALYSIS - ETABS

In the fig. are shown the results in terms of inter-story drift of the nonlinear stime-history analyses for all the 11 signals and their mean value.

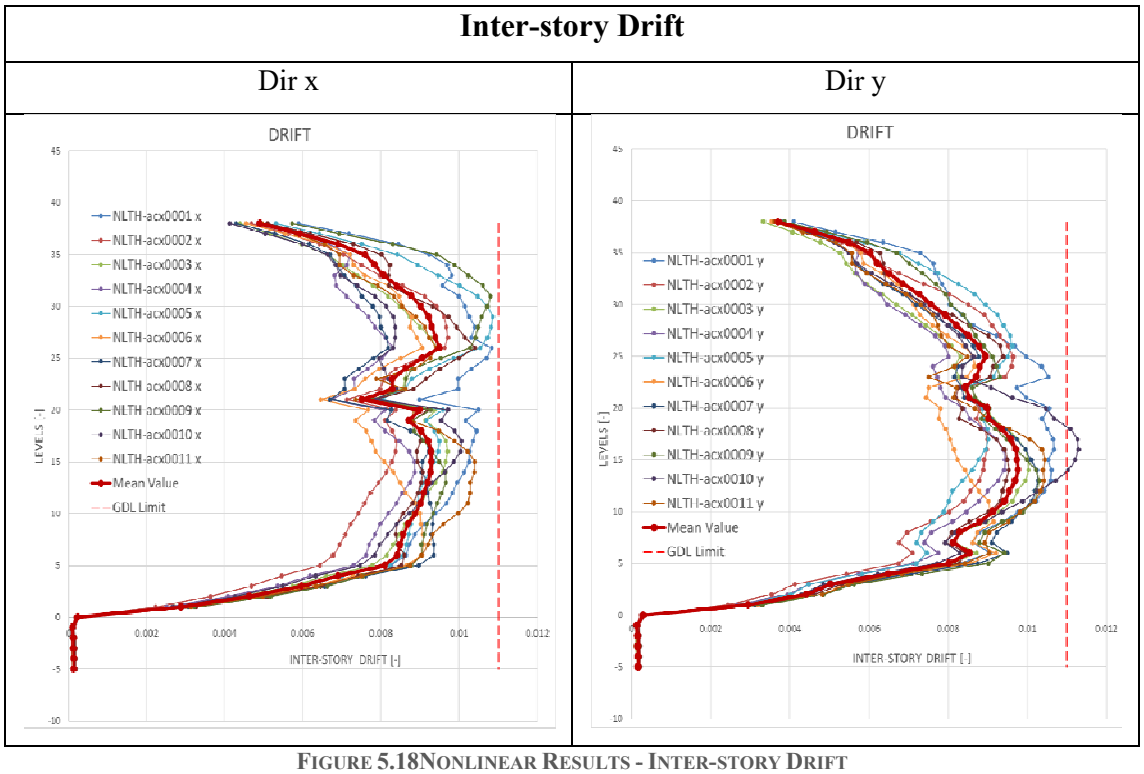

FIGURE 5.18NONLINEAR RESULTS - INTER-STORY DRIFT

In the next figure it is shown the hysteretic curve of the device in corrispodence of the level with the maximum value of dirft. It is possible to check the maximum displacement and the maximum force reached by the dissipator in order to be compatible with the property of the device (SLB4_30_7).

SLB4_30_7	
F_{MAX}[kN]	611,14
Δ_{MAX} [mm]	48

FIGURE 5.19 SLB PROPERTIES

The displacement capacity of SLB ofthe fourth generation has been set on the results of the experimental tests at the University of Cantabria (2020), it is to specify that the device is in a phase of development in order to reach a greater level of deformation.

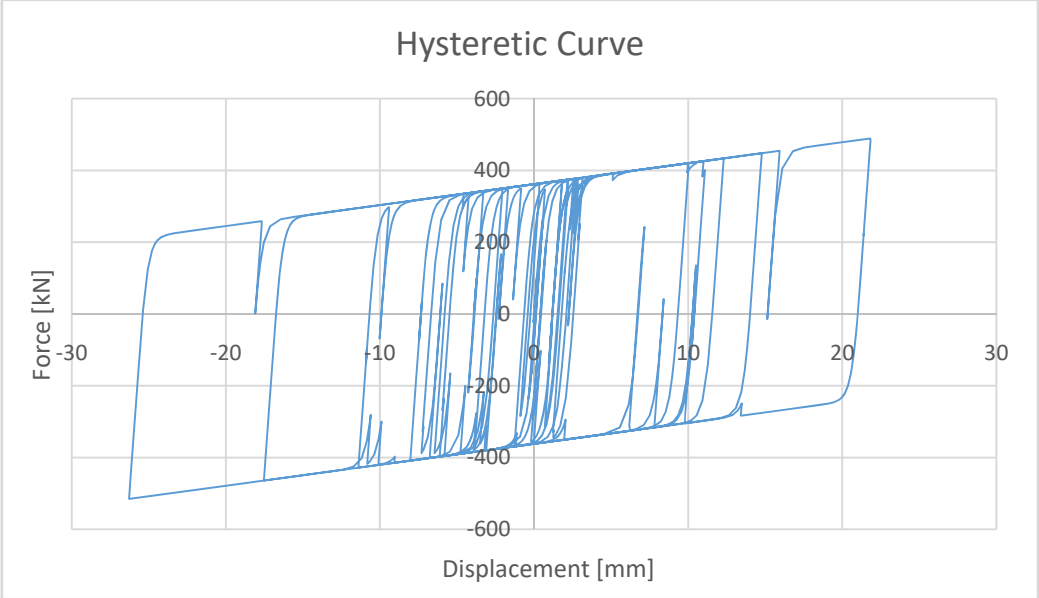

FIGURE 5.20 SLB HYSTERETIC CYCLE - NONLINEAR ANALYSIS TIME-HISTORY

In order to provide a complete comparison between the behavior of the structure before and after the intervention, the next figures are shown the comparison of the mean of the results in terms of drift, absolute displacements and story shear obtained from time-history analyses considering all the 11 signals available.

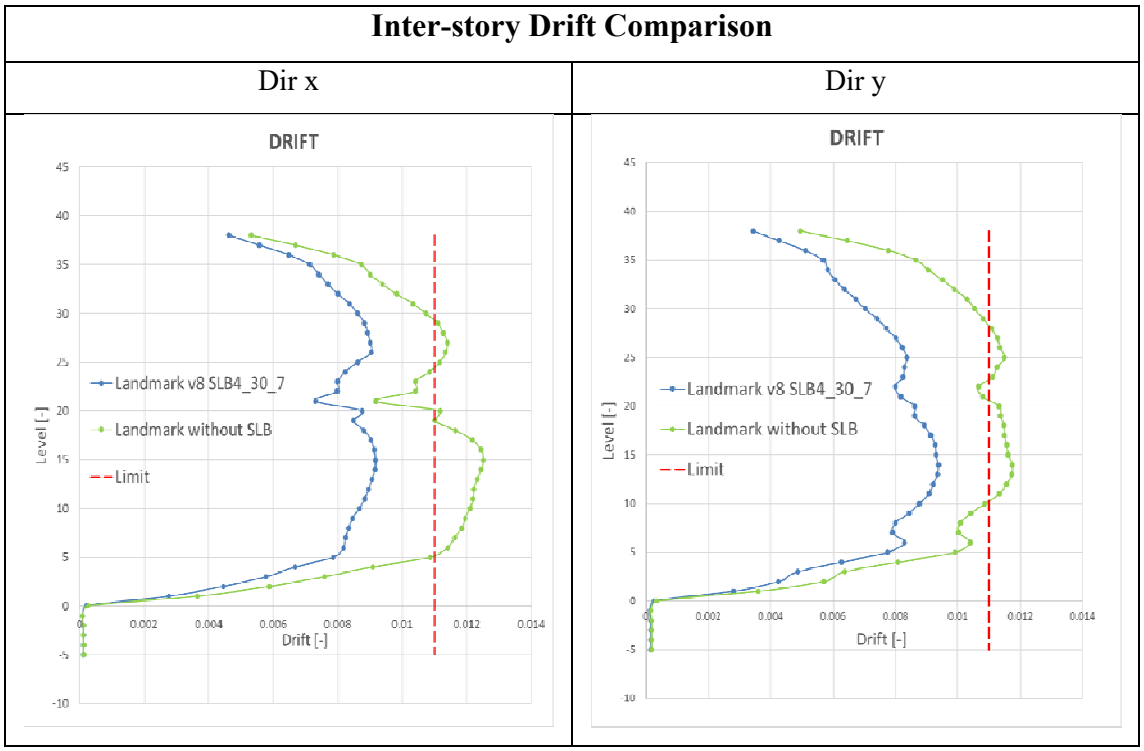

FIGURE 5.21 INTER-STORY DRIFT – COMPARISON

As it is possible to see from the fig.5.21 the installation of the devices led to a reduction of the inter-story drift of 27% in direction x and of 20% in direction y.

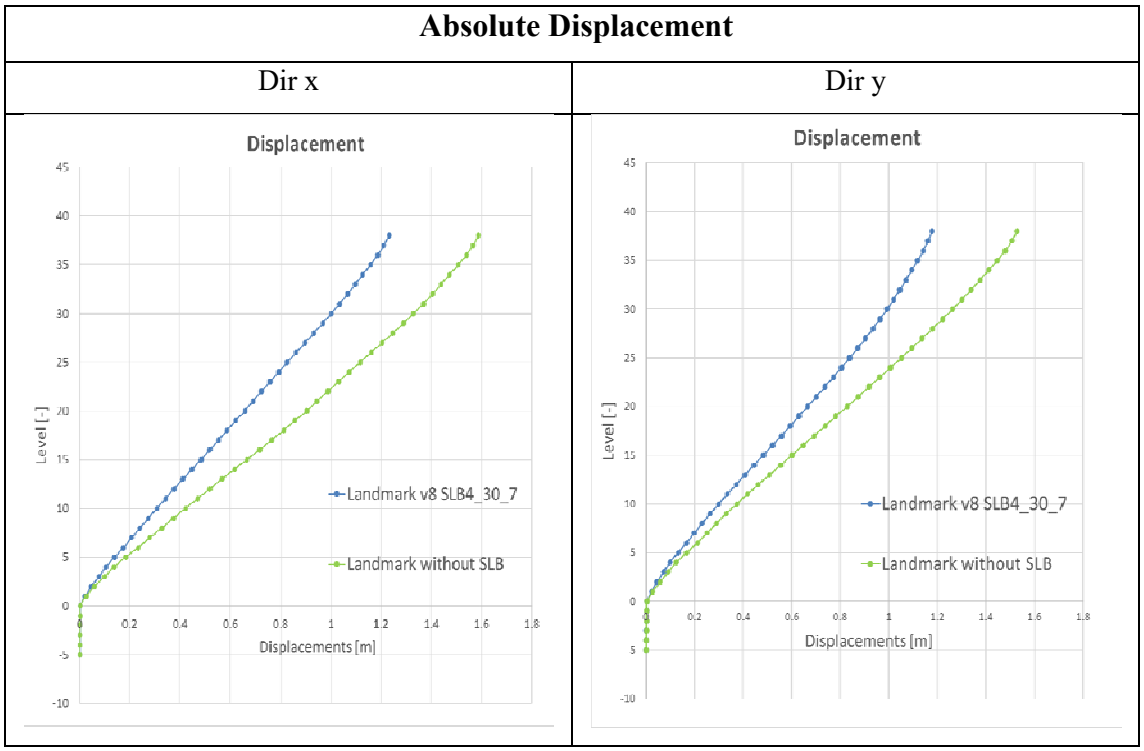

FIGURE 5.22 ABSOLUTE DISPLACEMENTS - COMPARISON

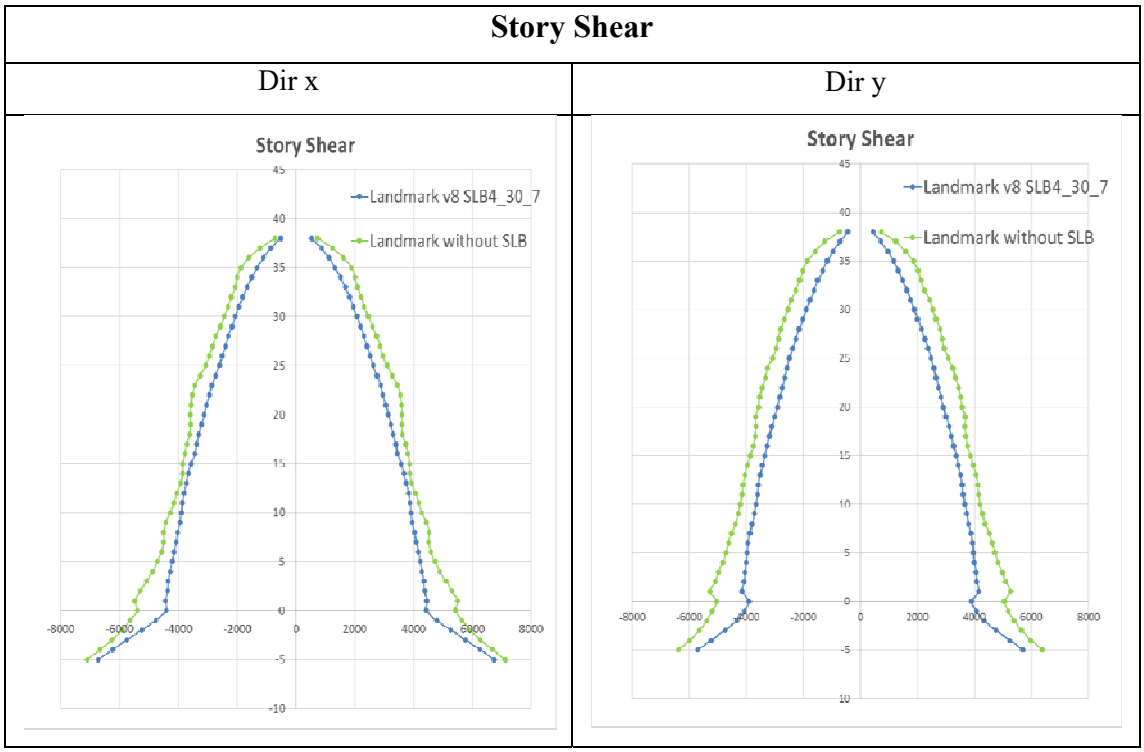

FIGURE 5.23 STORY SHEAR – COMPARISON

Comparing the distribution of the story shear, it is possible to observe that the installation of the SLB devices produces a reduction of the maximum shear of almost 20%, as shown below for the two main directions:

X	Whitout SLB	With SLB4_30_7	**Reduction**
Shear MAX	**5488,39 tonf**	**4444,33 tonf**	**19%**

Y	Whitout SLB	With SLB4_30_7	**Reduction**
Shear MAX	**5269,87 tonf**	**4146,63 tonf**	**21%**

5.5 EVALUATION OF EQUIVALENT DAMPING

Comparing the results obtained for the optimized solution between the response spectrum analysis, with 5% of damping, and the mean value of the nonlinear time-history analysis, it is possible to see that the first gives more conservative results, the relative difference is shown in fig. 5.24; 5.25; 5.26.

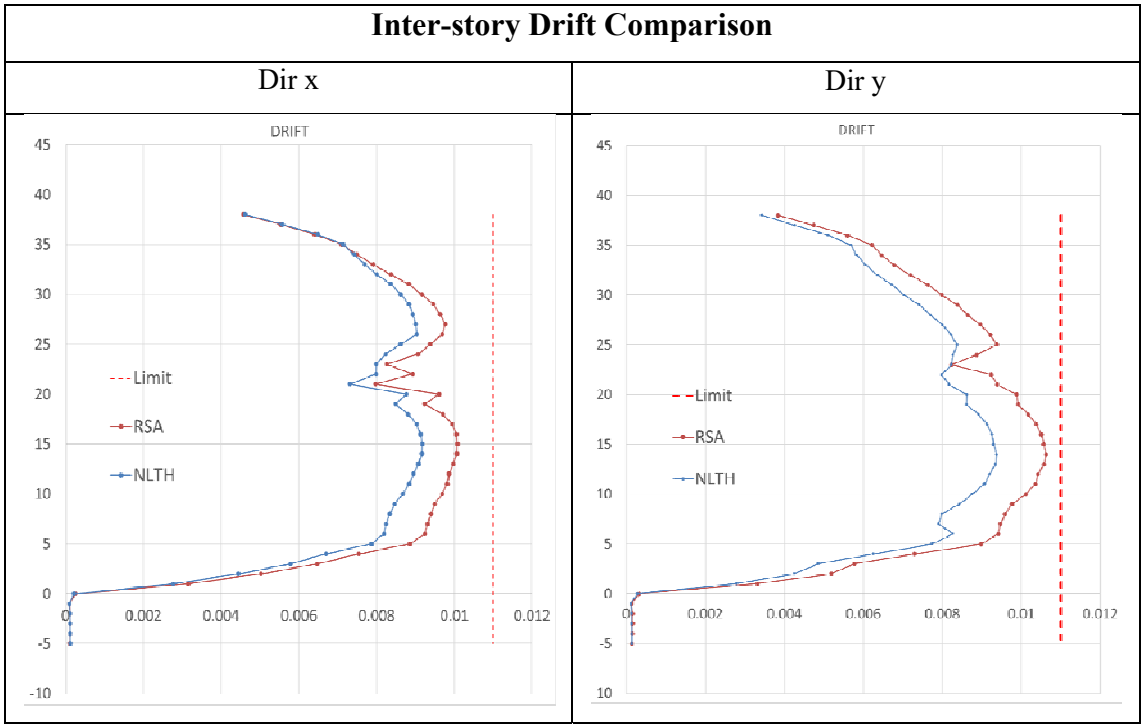

FIGURE 5.24 INTER-STORY DRIFT RSA - MEAN VALUE OF NONLINEAR ANALYSES RESULTS

X	RSA	NLTH	Reduction
Max Drift	**0,01008**	**0,00917**	**9%**

Y	RSA	NLTH	Reduction
Max Drift	**0,01062**	**0,00937**	**12%**

Absolute Displacement	
Dir x	Dir y
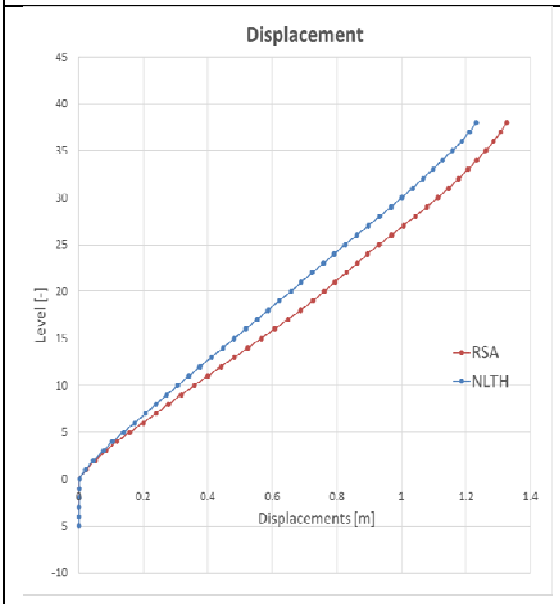	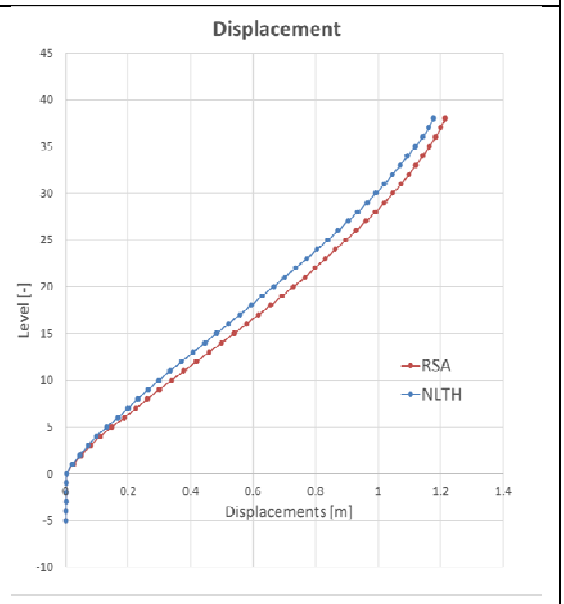

FIGURE 5.25 ABSOLUTE DISPLACEMETS RSA –MEAN VALUE OF NONLINEAR ANALYSES

X	RSA	NLTH	Reduction
Max Displacement	**1,32m**	**1,23m**	**7%**

Y	RSA	NLTH	Reduction
Max Displacement	**1,21m**	**1,17m**	**3%**

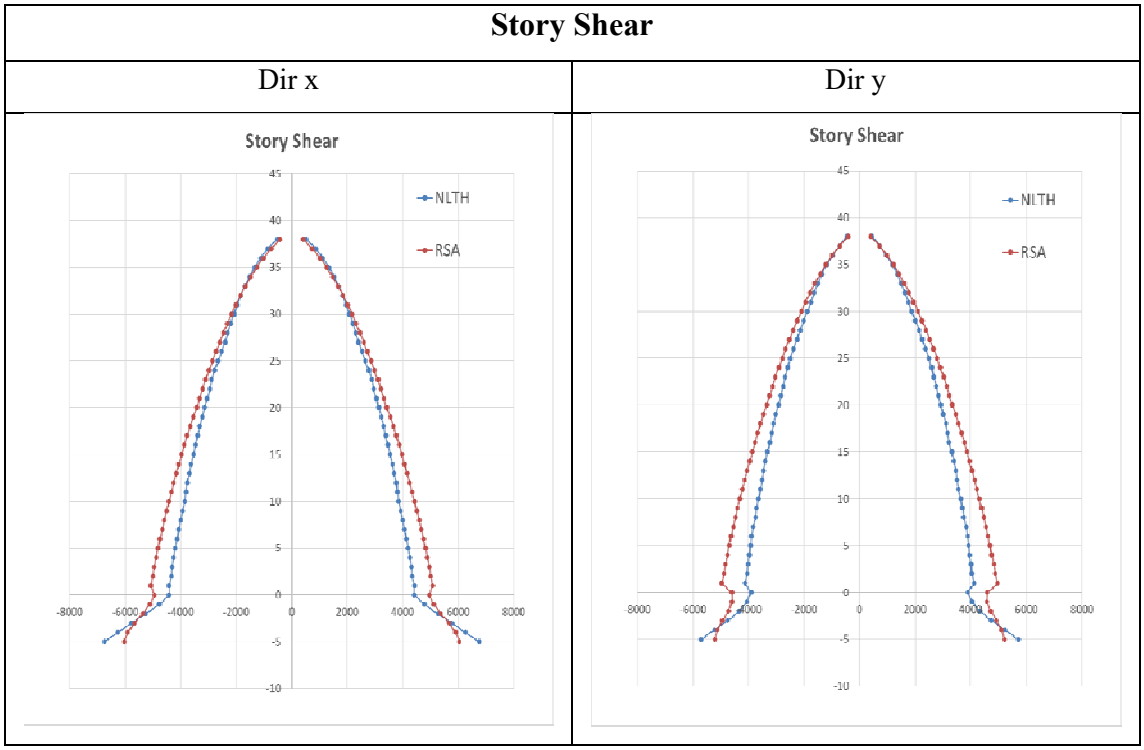

FIGURE 5.26 STORY SHEAR RSA- MEAN VALUE OF NONLINEAR ANALYSES

X	RSA	NLTH	Reduction
Base Shear	**5059,76 tonf**	**4386,24 tonf**	**13%**

Y	RSA	NLTH	Reduction
Base Shear	**4965,63 tonf**	**4116,80 tonf**	**17%**

From the previous results, it is possible to see that the two analyses can give significant differences in the results, especially in terms of drift and story shear. This can be justified by the fact that the linear analysis cannot take into account the hysteretic behavior of the devices.

Following the procedure described in paragraph *4.3*, it was possible to evaluate an equivalent value of damping in order to take into account the dissipation of energy due to the presence of hysteretic devices in the structure.

The procedure is iterative and based on the comparison of the results obtained from time-history analyses in order to estimate the effects of the nonlinear behavior of the devices on the structure through an increase of damping value in the linear analyses.

The linear and nonlinear analyses can’t be performed on the same model for modeling problems of the links. Therefore two equivalent models have been considered, the one defined through the inverse iteration and the second set with the properties of the real device (SLB4_30_7). Having the results of the nonlinear time-history analysis available from the previous study, in this case have been run theLinear Time-History Analyses with Direct Integration starting from an initial value of 5% of damping. As described also in the previous paragraph, the damping parameters of the time-history analyses must be set depending on the periodand the gravitational loads have to be combined with the results of the linear. To have a detailed comparison of the results have been considered the distributions of the results for all the stories for the maximum and the minimum peaks of the signal, in both directions x and y. The procedure hasbeen repeated for tries until to reach a good correlation of the results, this has been done for each of the 11 signals available.

To show a practical example, in the next table are reported the plots of the results referred to the signal acx0001, in terms of inter-story drift for the maximum and the minimum peaks, in both the directions. In this case,a good correlation has been reached for the 8% of damping, the main criteria was initially to compare the maximum values for all the four graphs, reducing the difference up to an error of 10%, then, to confirm the correlation, has been checked that along all the storeys the linear analyses didn’t give results lower than the nonlinear analyses, with a tolerance of the 20%.

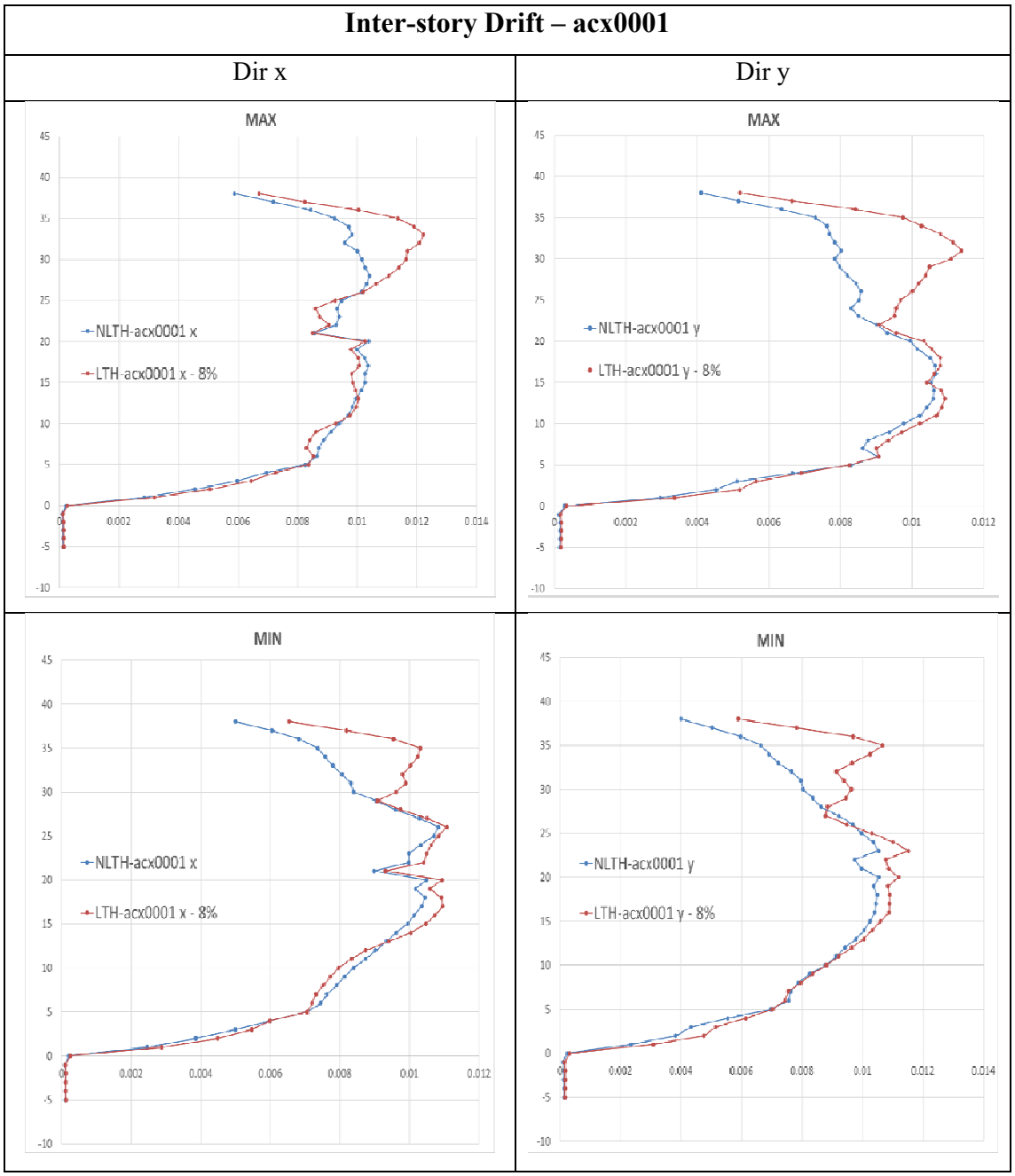

FIGURE 5.27 COMPARISON INTER-STORY DRIFT – MAXIMUM AND MINIMUM PEAKS

			DRIFT			SHEAR	
			NLTH	LTH SLB Damping 8%		NLTH	LTH SLB Damping 10%
Acx0001	X	MAX	0.010402	0.012227	X	4127.2983	4289.0339
		MIN	0.010836	0.011073		-4634.1132	-5172.4633
		Difference		18%		Difference	4%
				2%			12%
	Y	MAX	0.010669	0.011384	Y	3724.8887	4321.6033
		MIN	0.010554	0.011532		-4382.4529	-4896.9109
		Difference		7%		Difference	16%
				9%			12%

FIGURE 5.28INTER-STORY DRIFT - MINIMUM DIFFERENCE OBTAINED

In the fig.5.28 are reported all the maximum values of the distributions. For a damping of 8%, the difference between the two types of analyses is reduced up to 2% for the distribution referred to the minimum peaks in direction x. Increasing the damping, the linear value of the drift would be reduced further giving values lower than the nonlinear analyses. For this reason, the 8% of damping was considered a reasonable value to obtain a good correlation of the results.To have confirmation of this, have been checked also the differences for all the storeys in order to not have values of the "linear" drift much lower than the "nonlinear" drift. In this case, the maximum reduction of the "linear" drift was of 8% lower than the "nonlinear" drift. In order to repeat the same procedure for a total of 11 signals, the correlation was considered acceptable.

Regarding the comparison in terms of story shear, the criteria followed was the same, with the difference that have been reached higher values of damping.For this reason, it was decided to provides two different values of damping, one referred to the comparison of the drift and the other referred to the comparison of shear.

From the next table it is possible to see the comparison of the story shear for a damping value of 10%.

Story Shear – acx0001	
Dir x	Dir y
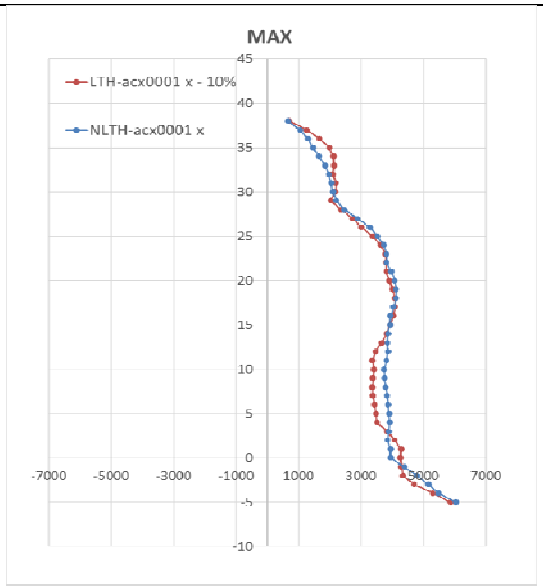	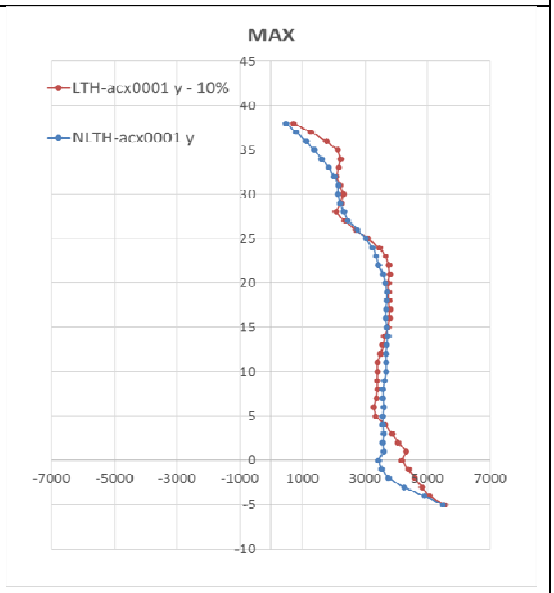
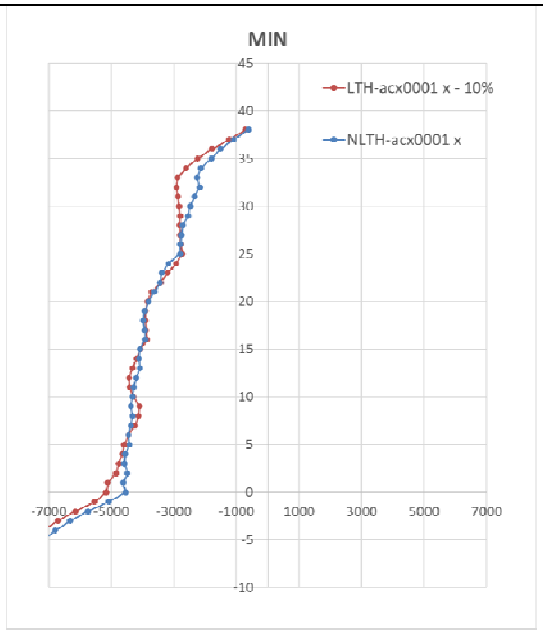	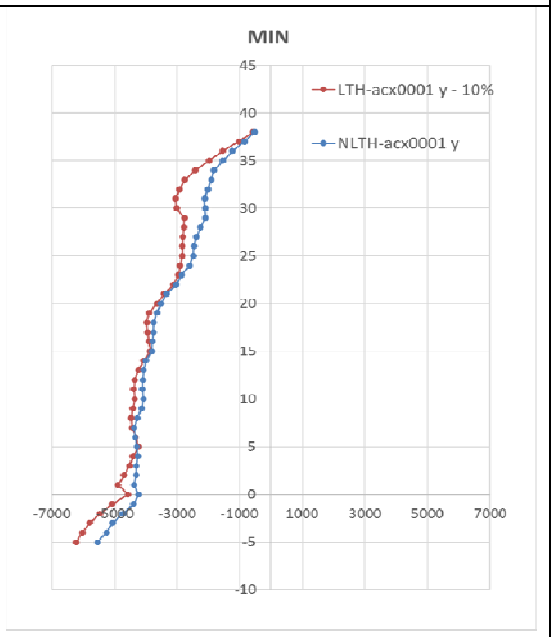

FIGURE 5.29 COMPARISON STORY SHEAR – MAXIMUM AND MINIMUM PEAKS

			DRIFT			SHEAR	
			NLTH	LTH SLB Damping 8%		NLTH	LTH SLB Damping 10%
Acx0001	X	MAX	0.010402	0.012227	X	4127.2983	4289.0339
		MIN	0.010836	0.011073		-4634.1132	-5172.4633
			Difference	18%		Difference	4%
				2%			12%
	Y	MAX	0.010669	0.011384	Y	3724.8887	4321.6033
		MIN	0.010554	0.011532		-4382.4529	-4896.9109
			Difference	7%		Difference	16%
				9%			12%

FIGURE 5.30 STORY SHEAR - MINIMUM DIFFERENCE OBTAINED

In this case, the difference between the maximum values of the distributions reached the 4%. Also in this case, to confirmthe damping value, have been checked the differences for all the storeys in order to not have values of the “linear” shear much lower than the “nonlinear” shear, but with a tolerance of 15%, because the distributions in terms of story shear are more comparable. In this case, the maximum reduction of the “linear” shear was 12% lower then the “nonlinear” shear. Also in this case the correlation has been considered acceptable.

Afterward have been reported the results also for the signal acx0005, because of the process has been the same, there will be shown just the results.

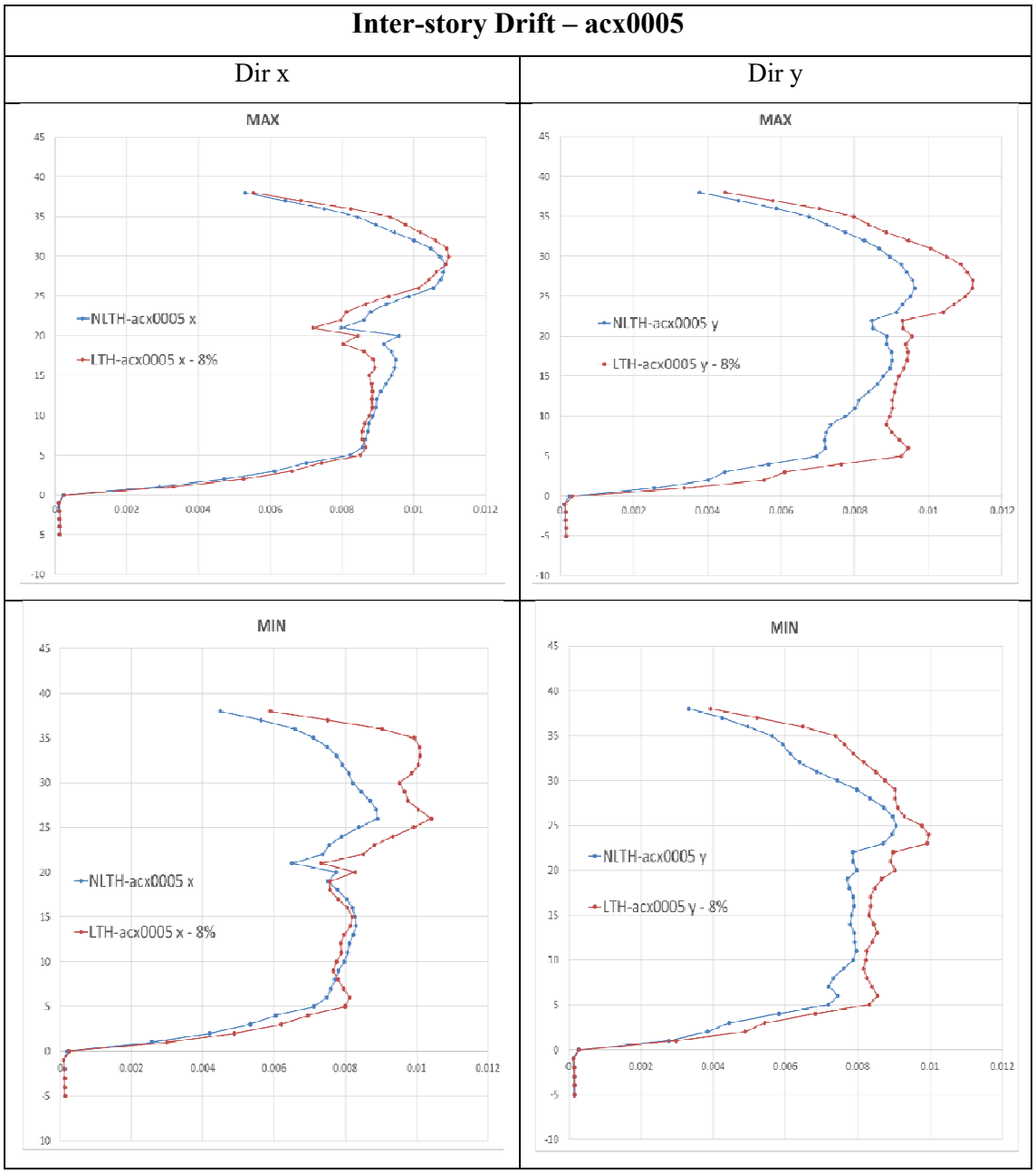

FIGURE 5.31 COMPARISON INTER-STORY - MAXIMUM AND MINIMUM PEAKS

			DRIFT			SHEAR	
			NLTH	LTH SLB Damping 8%		NLTH	LTH SLB Damping 10%
Acx0005	X	MAX	0.010864	0.010971	X	4519.644	4319.6989
		MIN	0.008904	0.010414		-4750.623	-4833.8295
		Difference		1%		Difference	-4%
				17%			2%
	Y	MAX	0.009619	0.011201	Y	4165.8303	4204.8665
		MIN	0.009055	0.009964		-3790.7377	-4713.663
		Difference		16%		Difference	1%
				10%			24%

FIGURE 5.32 INTER-STORY DRIFT - MINIMUM DIFFERENCE OBTAINED

Story Shear– acx0005	
Dir x	Dir y
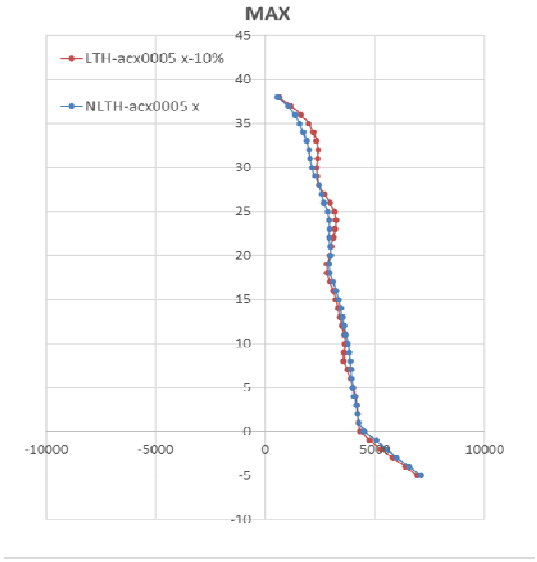	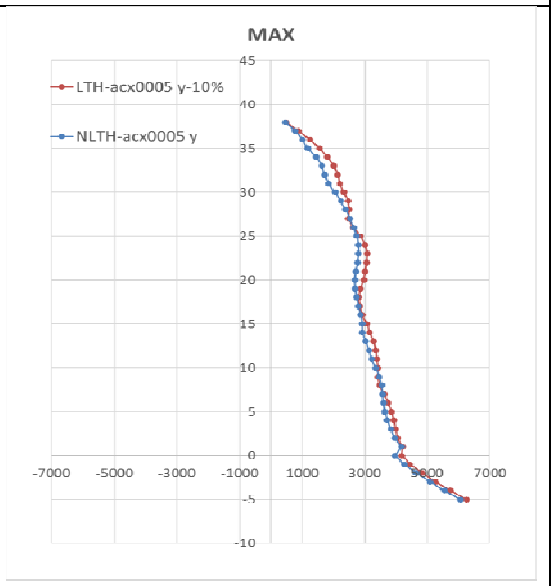
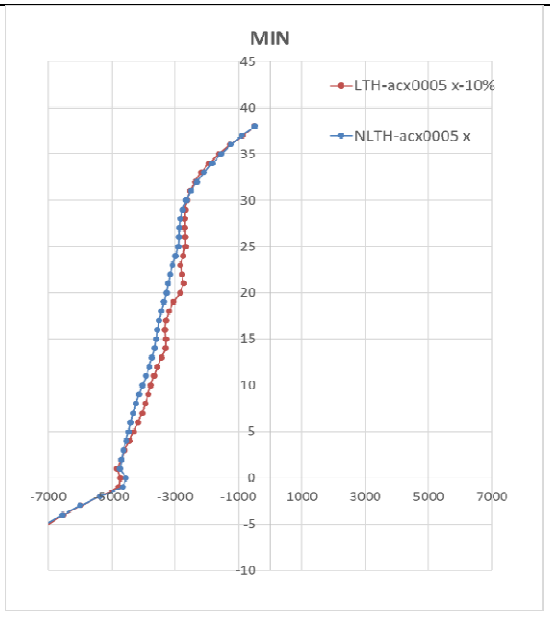	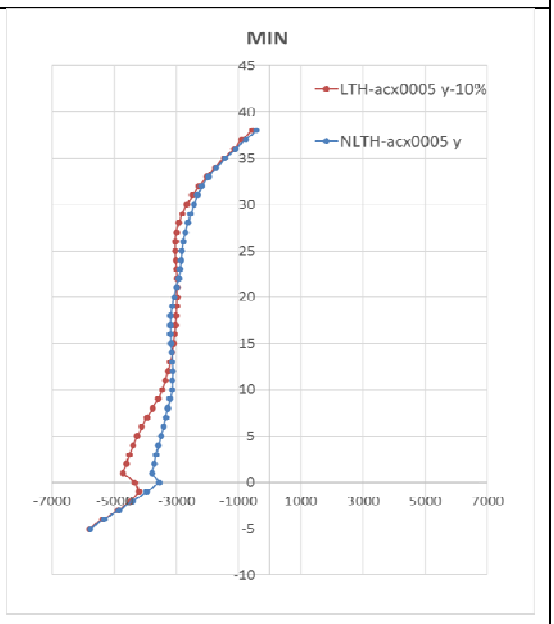

FIGURE 5.33 COMPARISON STORY SHEAR – MAXIMUM AND MINIMUM PEAKS

			DRIFT			SHEAR	
			NLTH	LTH SLB Damping 3%		NLTH	LTH SLB Damping 10%
Acx0005	X	MAX	0.010864	0.010971	X	4519.644	4319.6389
		MIN	0.008904	0.010414		-4750.623	-4833.8295
			Difference	1%		Difference	4%
				17%			2%
	Y	MAX	0.009619	0.011201	Y	4165.8303	4204.8665
		MIN	0.009055	0.009964		-3790.7377	-4713.663
			Difference	16%		Difference	1%
				10%			24%

FIGURE 5.34 STORY SHEAR – MINIMUM DIFFERECE OBTAINED

According to the criteria described before, in the fig.5.34is possible to see the comparison of the results for each signal, in terms of drift and story shear, reporting the relative parameter of damping chosen and the difference obtainedbetween the maximum values of the results of the analyses.

TABLE 5-12 SUMMARY OF THE COMPARISON VALUES FOR ALL THE 11 SEISMIC SIGNALS CONSIDERED

			DRIFT			SHEAR	
			NLTH	LTH SLB Damping 8%		NLTH	LTH SLB Damping 10%
Acx0001	X	MAX	0.010402	0.012227	X	4127.2983	4289.0339
		MIN	0.010836	0.011073		-4634.1132	-5172.4633
		Difference		18%		Difference	4%
				2%			12%
	Y	MAX	0.010669	0.011384	Y	3724.8887	4321.6033
		MIN	0.010554	0.011532		-4382.4529	-4896.9109
		Difference		7%		Difference	16%
				9%			12%
			NLTH	LTH SLB Damping 10%		NLTH	LTH SLB Damping 13%
Acx0002	X	MAX	0.008204	0.008524	X	3695.3305	3661.8124
		MIN	0.009716	0.010571		-3473.7641	-3623.3595
		Difference		4%		Difference	-1%
				9%			4%
	Y	MAX	0.007923	0.008597	Y	3458.5424	3811.7327
		MIN	0.009647	0.010496		-3265.659	-3387.1725
		Difference		9%		Difference	10%
				9%			4%
			NLTH	LTH SLB Damping 8%		NLTH	LTH SLB Damping 8%
Acx0003	X	MAX	0.009708	0.010891	X	3382.3341	5075.1488
		MIN	0.007243	0.008732		-4329.1475	-4097.9935
		Difference		12%		Difference	50%
				21%			-5%
	Y	MAX	0.010038	0.011171	Y	3186.98	4299.8332
		MIN	0.008046	0.008344		-4059.8003	-4605.6188
		Difference		11%		Difference	35%
				4%			13%
			NLTH	LTH SLB Damping 8%		NLTH	LTH SLB Damping 8%
Acx0004	X	MAX	0.00886	0.007973	X	4187.0718	4232.1677
		MIN	0.008332	0.008703		-4030.3812	-4541.3372
		Difference		-10%		Difference	1%
				4%			13%
	Y	MAX	0.0091735	0.008869	Y	3968.2301	4847.9755
		MIN	0.0085295	0.008547		-3700.4059	-4425.4431
		Difference		-3%		Difference	22%
				0%			20%
			NLTH	LTH SLB Damping 8%		NLTH	LTH SLB Damping 10%
Acx0005	X	MAX	0.010864	0.010971	X	4519.644	4319.6989
		MIN	0.008904	0.010414		-4750.623	-4833.8295
		Difference		1%		Difference	-4%
				17%			2%
	Y	MAX	0.009619	0.011201	Y	4165.8303	4204.8665
		MIN	0.009055	0.009964		-3790.7377	-4713.663
		Difference		16%		Difference	1%
				10%			24%

			NLTH	LTH SLB Damping 10%		NLTH	LTH SLB Damping 10%
Acx0006	X	MAX	0.008359	0.007886	X	5143.8423	5468.9601
		MIN	0.009084	0.009566		-4433.5789	-4600.2032
			Difference	-6%		Difference	6%
				5%			4%
	Y	MAX	0.008405	0.008222	Y	4867.9837	5580.5826
		MIN	0.009199	0.009275		-4365.7123	-4557.9552
			Difference	-2%		Difference	15%
				1%			4%

			NLTH	LTH SLB Damping 8%		NLTH	LTH SLB Damping 9%
Acx0007	X	MAX	0.008646	0.008789	X	5041.6763	5059.5546
		MIN	0.009358	0.009292		-4310.2767	-4385.8865
			Difference	2%		Difference	0%
				-1%			2%
	Y	MAX	0.009432	0.009384	Y	4637.2297	5529.7929
		MIN	0.010275	0.010187		-4163.3189	-4616.9109
			Difference	-1%		Difference	19%
				-1%			11%

			NLTH	LTH SLB Damping 5%		NLTH	LTH SLB Damping 8%
Acx0008	X	MAX	0.010414	0.010398	X	5088.6931	5538.3961
		MIN	0.009066	0.010614		-6042.8961	-6368.5317
			Difference	0%		Difference	9%
				17%			5%
	Y	MAX	0.009388	0.010862	Y	4215.1059	5503.728
		MIN	0.009535	0.011474		-5141.4891	-5891.0579
			Difference	16%		Difference	31%
				20%			15%

			NLTH	LTH SLB Damping 9%		NLTH	LTH SLB Damping 8%
Acx0009	X	MAX	0.0108	0.011022	X	5038.1257	5139.6597
		MIN	0.009271	0.009836		-5181.1439	-5144.0777
			Difference	2%		Difference	2%
				6%			-1%
	Y	MAX	0.010312	0.010757	Y	4586.3449	5143.6902
		MIN	0.009407	0.010066		-4799.2604	-5211.7303
			Difference	4%		Difference	12%
				7%			9%

			NLTH	LTH SLB Damping 8%		NLTH	LTH SLB Damping 8%
Acx0010	X	MAX	0.009503	0.009451	X	4633.5094	5044.4058
		MIN	0.01006	0.010376		-3997.6314	-4132.9674
			Difference	-1%		Difference	9%
				3%			3%
	Y	MAX	0.009578	0.009941	Y	4303.252	5003.9618
		MIN	0.011293	0.011146		-3720.4234	-4657.6908
			Difference	4%		Difference	16%
				-1%			25%

			NLTH	LTH SLB Damping 8%		NLTH	LTH SLB Damping 8%
Acx0011	X	MAX	0.010402	0.01015	X	4230.6355	4807.831
		MIN	0.008693	0.00903		-4714.2794	-5592.3532
			Difference	-2%		Difference	14%
				4%			19%
	Y	MAX	0.010438	0.010701	Y	4000.4288	4363.1567
		MIN	0.009217	0.009018		-4444.8434	-5708.7959
			Difference	3%		Difference	9%
				-2%			28%

To summarize, the damping values evaluated for each signal analyzed are reported in the next table. (table 16)

	DAMPING	
	Drift	Shear
SEÑAL-acx0001	8%	10%
SEÑAL-acx0002	10%	13%
SEÑAL-acx0003	8%	8%
SEÑAL-acx0004	8%	8%
SEÑAL-acx0005	8%	10%
SEÑAL-acx0006	10%	10%
SEÑAL-acx0007	8%	9%
SEÑAL-acx0008	5%	8%
SEÑAL-acx0009	9%	8%
SEÑAL-acx0010	8%	8%
SEÑAL-acx0011	8%	8%

μ	9%	10%
б	2%	2%
μ-б	7%	8%

TABLE 5-13 DAMPING VALUES OBTAINED

- *Mean value:* $\boldsymbol{\mu} = \frac{\sum_{i=1}^{N} x_i}{N}$

- *Standard Deviation:* $\boldsymbol{\sigma} = \sqrt{\frac{\sum_{i=1}^{N} (x_i - \mu)^2}{N}}$

As specified in the description of the procedure, paragraph *4.3*, to define the modal damping parameter to reduce the design spectrum ordinates, it has been evaluated the mean value and its standard deviation from the values obtained for all the 11 signals,this

allowed to estimate a conservative value reducing the mean value for the standard deviation, as shown in the Tab.16.

For a first tempt, it has been chosen the highest damping value obtained from the procedure andit has been applied to the elastic design spectrum in order to run a response spectrum analysis. The results in terms of drift and story shear have been plotted and compared with the mean results of the nonlinear time-history analyses of all the signals.

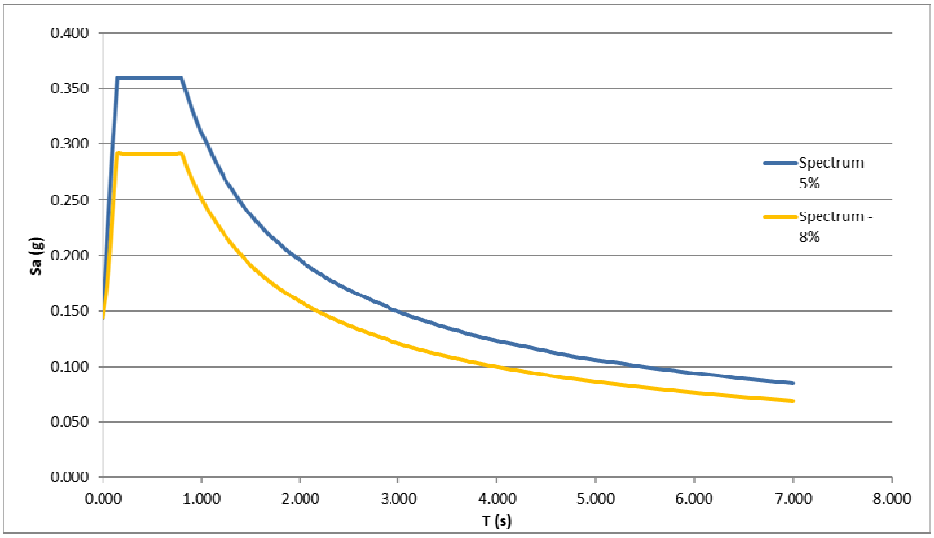

FIGURE 5.35 ELASTIC RESPONSE SPECTRUM – 8% DAMPING

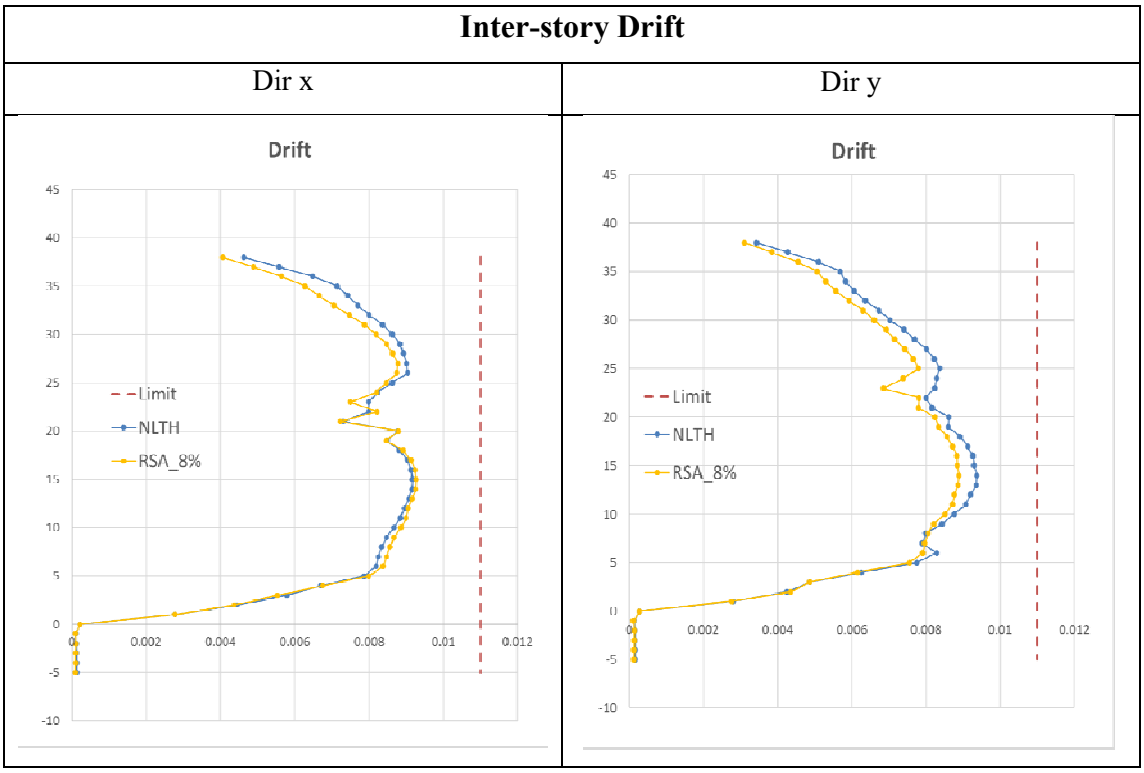

FIGURE 5.36 INTER-STORY DRIFT [RSA_8% - MEAN VALUE OF NONLINEAR ANALYSES]

X	RSA_8%	NLTH	Difference
Max Drift	**0,00926**	**0,00917**	**1%**

Y	RSA_8%	NLTH	Difference
Max Drift	**0,00889**	**0,00937**	**-5%**

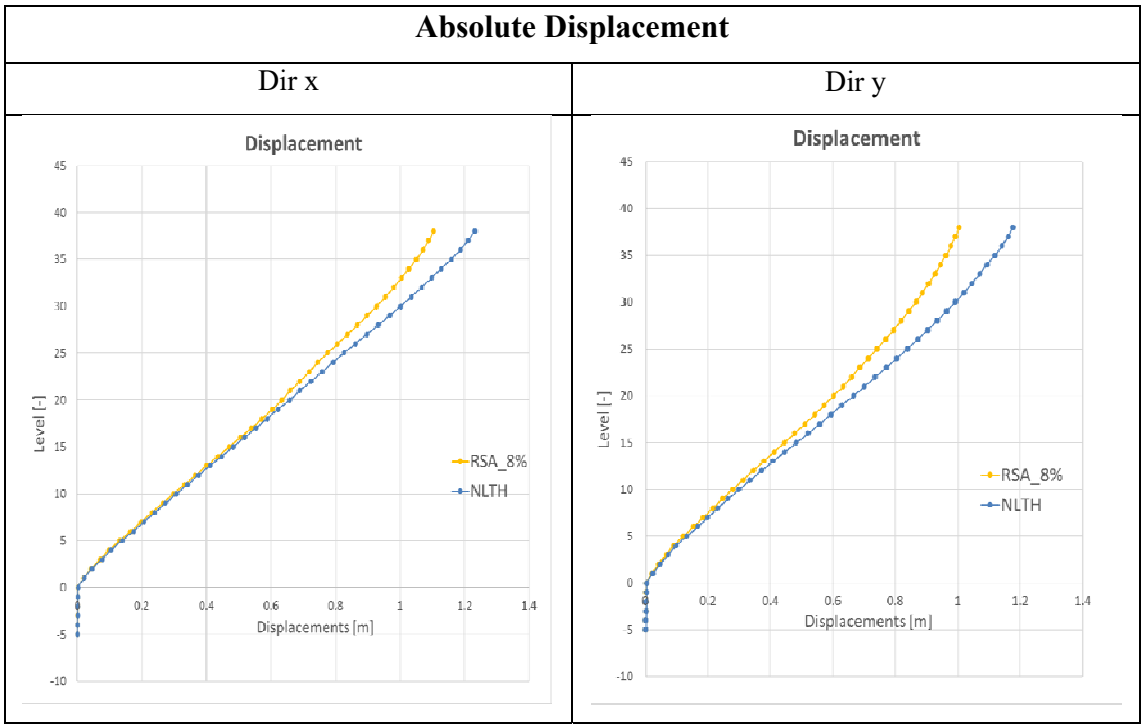

FIGURE 5.37 ABSOLUTE DISPLACEMENTS [RSA_8% - MEAN VALUE OF NONLINEAR ANLAYSES]

X	RSA_8%	NLTH	Difference
Max Displacement	**1,10m**	**1,23m**	**-12%**

Y	RSA_8%	NLTH	Difference
Max Displacement	**1,00m**	**1,17m**	**-17%**

Story Shear	
Dir x	Dir y
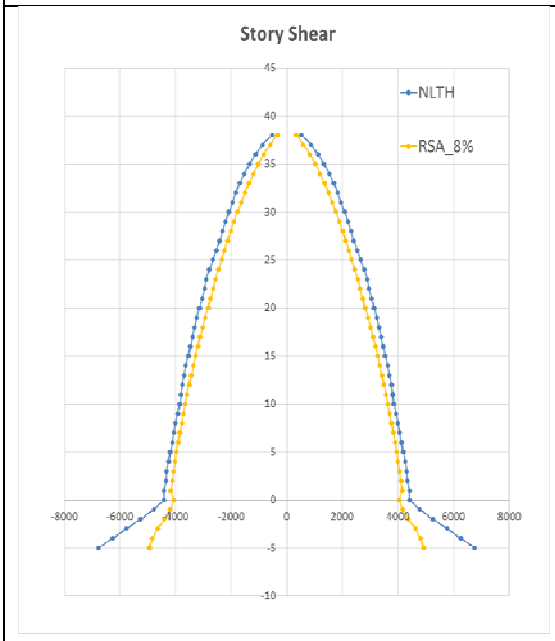	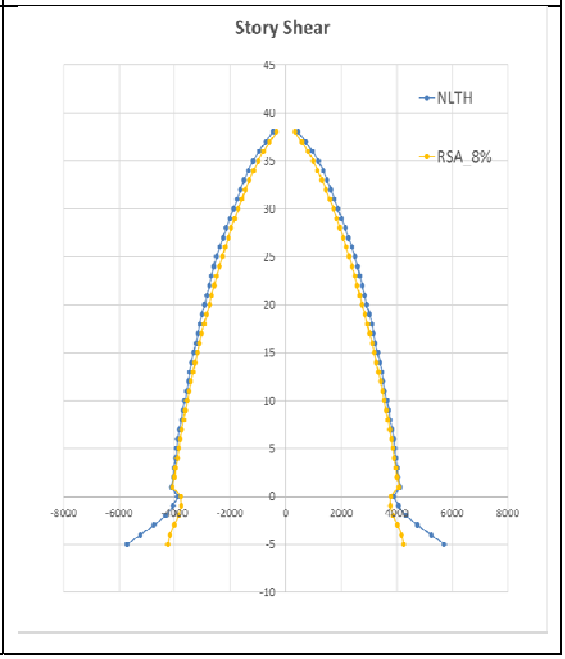

FIGURE 5.38 STORY SHEAR [RSA_8% - MEAN VALUE OF NONLINEAR ANLAYSES]

X	RSA_8%	NLTH	Difference
Base Shear	**4174,67 tonf**	**4386,24 tonf**	**-5%**

Y	RSA_8%	NLTH	Difference
Base Shear	**4078,30 tonf**	**4116,80 tonf**	**-1%**

The results obtained from the combination of the effects of the response spectrum analysis set with equivalent damping of 8% show a better correlation in terms of story shear but less in terms of drift and displacements, the trends of the results present some difference even though the difference range for the maximum value is just of 5%. This difference in terms of relative displacements can be justified by the fact that, to have a good correlation, it has to be used a damping value of 7%. For this reason,have been considered the results of the response spectrum analysis with 7% of damping whose results are shown below.

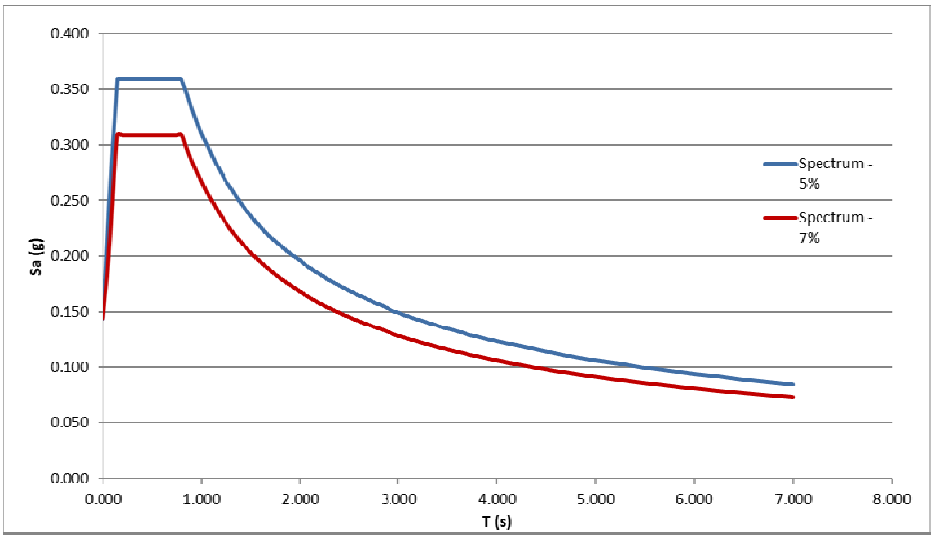

FIGURE 5.39 ELASTIC RESPONSE SPECTRUM – 7% DAMPING

Inter-story Drift

Dir x	Dir y

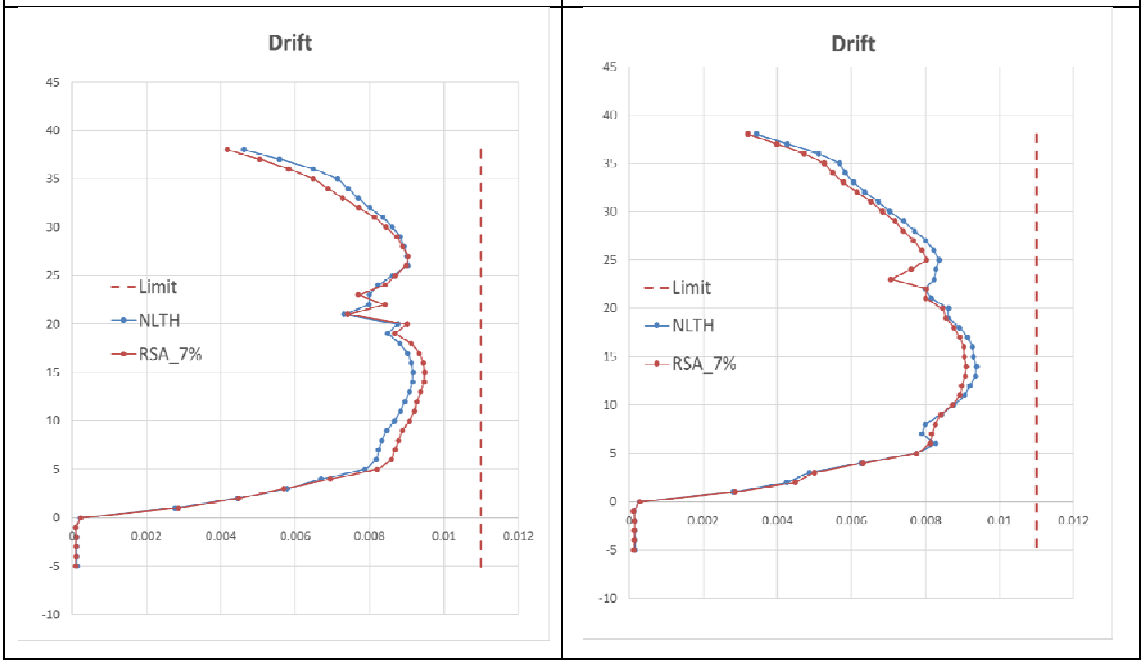

FIGURE 5.40 INTER-STORY DRIFT [RSA_7% - MEAN VALUE OF THE NONLINEAR ANALYSES]

X	RSA_7%	NLTH	**Difference**
Max Drift	**0,00948**	**0,00917**	**3%**

Y	RSA_7%	NLTH	**Difference**
Max Drift	**0,00910**	**0,00937**	**-3%**

Absolute Displacement	
Dir x	Dir y

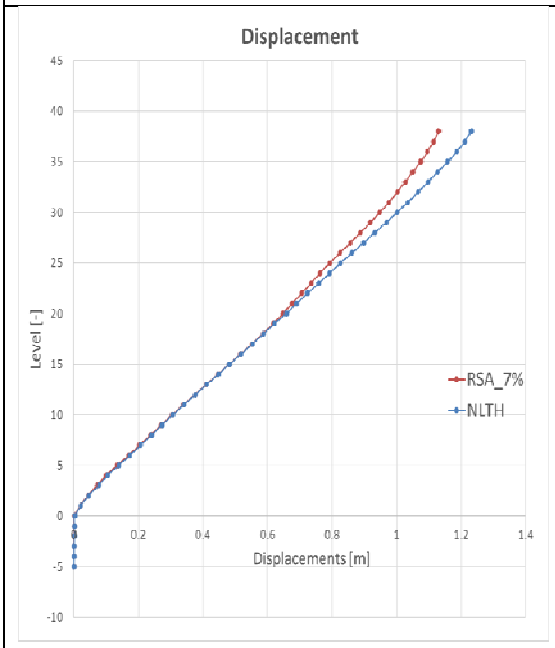

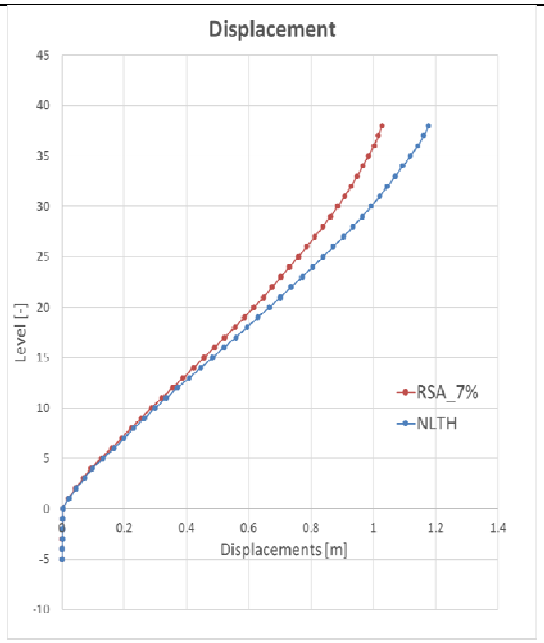

FIGURE 5.41 ABSOLUTE DISPLACEMENTS [RSA_7% - MEAN VALUE OF NONLINEAR ANALYSES]

X	RSA_7%	NLTH	Difference
Max Displacement	**1,13m**	**1,23m**	**-9%**

Y	RSA_7%	NLTH	Difference
Max Displacement	**1,03m**	**1,17m**	**-15%**

Story Shear	
Dir x	Dir y
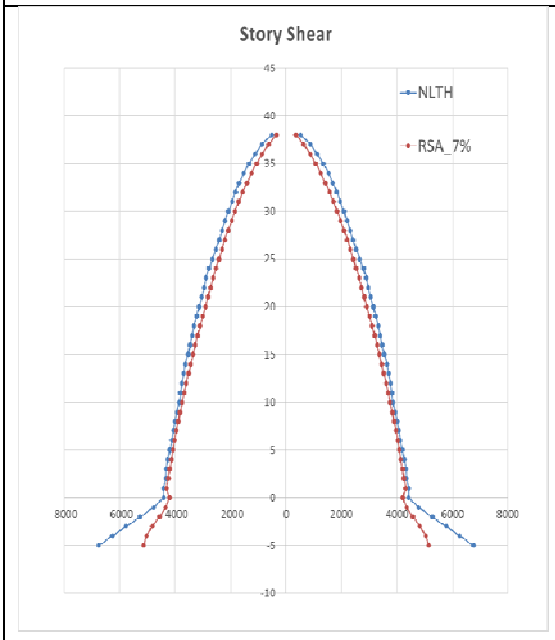	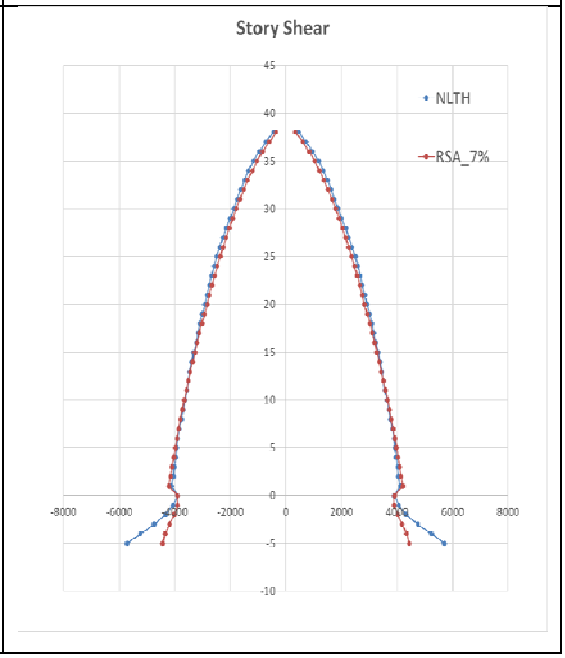

FIGURE 5.42 STORY SHEAR [RSA_7% - MEAN VALUE OF NONLINEAR ANALYSES]

X	RSA_7%	NLTH	**Difference**
Base Shear	**4304,13 tonf**	**4386,24 tonf**	**-2%**

Y	RSA_7%	NLTH	**Difference**
Base Shear	**4217,30 tonf**	**4116,80 tonf**	**2%**

The results obtained from the combination of the effects of the response spectrum analysis set with 7% of damping show a good correlation both in terms of drift and story shear, reducing the difference of the maximum values up to 3% for the inter-story drift and 2% for the base shear.

Regarding the absolute displacements in both the case, the analyses gave a large difference from the results of the nonlinear analysis, up to 15%.

The next step is to design the structure on the basis of the results obtained and afterward check the design performance through a complete nonlinear analysis, considering the material and geometric nonlinearity.

5.6 STRUCTURAL DESIGN

Considering the results of theprocedure explained in paragraph *4.3*, the designer has to choose and justify the modal damping value to use for the response spectrum analysis in order to design the structure. For the case study, based on the results obtained from the previous analyses, it has been chosen to adopt equivalent damping of 7%. It is suggested, to operate in a conservative area, to adopt this procedure for the seismic design of the beams, while columns have to be designed considering the conventional damping value of 5 %. Anyway, it is necessary, as reported in paragraph *4.3*, to check the performance of the design of the structure obtained considering the complete nonlinear behavior of the structure. For this reason, both material and geometric nonlinearities have to be considered in the model. The execution of a complete nonlinear time-history analysis with direct integration iscomputationally intensive, for this reason, it requires long computational time and, especially for irregular structures, it could give problems of convergence.

The purpose of this paragraph is to show a simplified example of the application of the results obtained from the previous study, designing a single frame of the structure and verifying its performance through a complete nonlinear analysis.

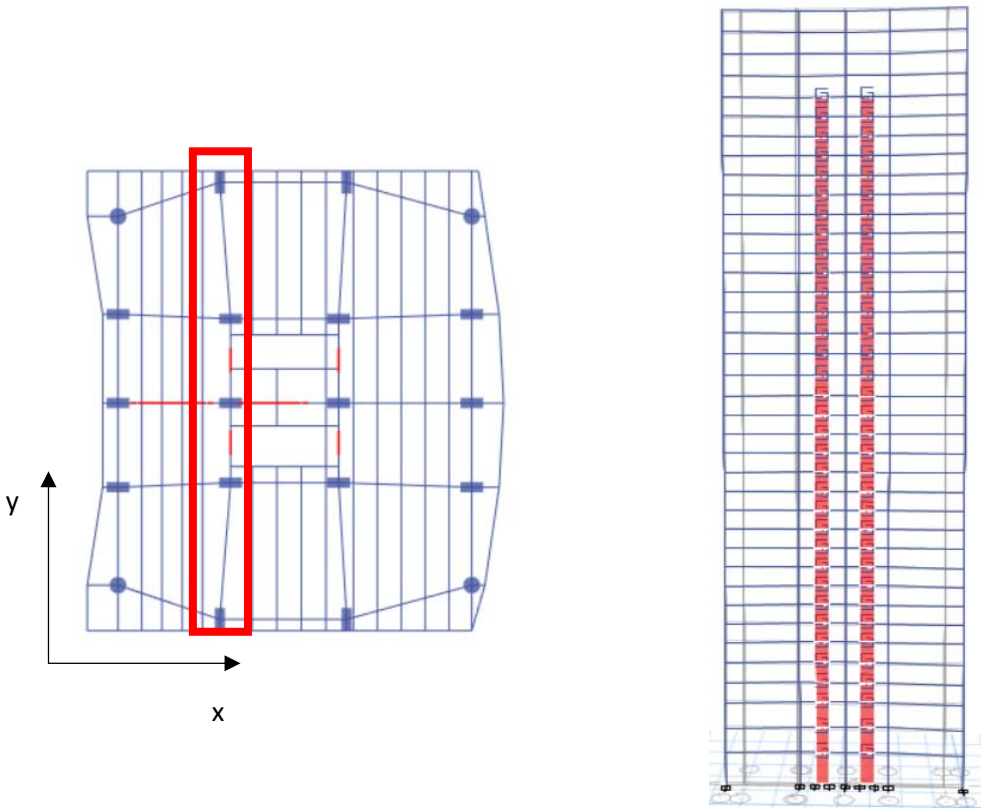

FIGURE 5.43 FRAME SELECTED

For the analyses, it has been selected one of the frames equipped with SLB devices in direction y, which is the most deformable direction of the structure. The frame has been studied as a bidimensional frame, fixing the degree of freedom in the direction x, and, in order to obtain stresses equivalent to those acting on the complete structure, it has been increased the mass until to reach the same period of the structure.

Modal Participating Mass Ratios											
Case	Mode	Period	UX	UY	UZ	SumUX	SumUY	SumUZ	RX	RY	RZ
		sec									
Modal	1	6.008	0	0.71	0	0	0.7096	0	0.3007	0	7.33E-06

TABLE 5-14 MODAL ANALYSIS RESULTS

The first step was to design the frame through the modal response spectrum analysis. The aim is to design the beams using equivalent damping of 7% and the columns adopting the 5% damping.The design response spectra used are shown infig. 5.44 and

5.45, obtained reducing the elastic spectral ordinates through a ductility factor ***Q'***equal to***2,4***, as specified in paragraph *5.2.2.*

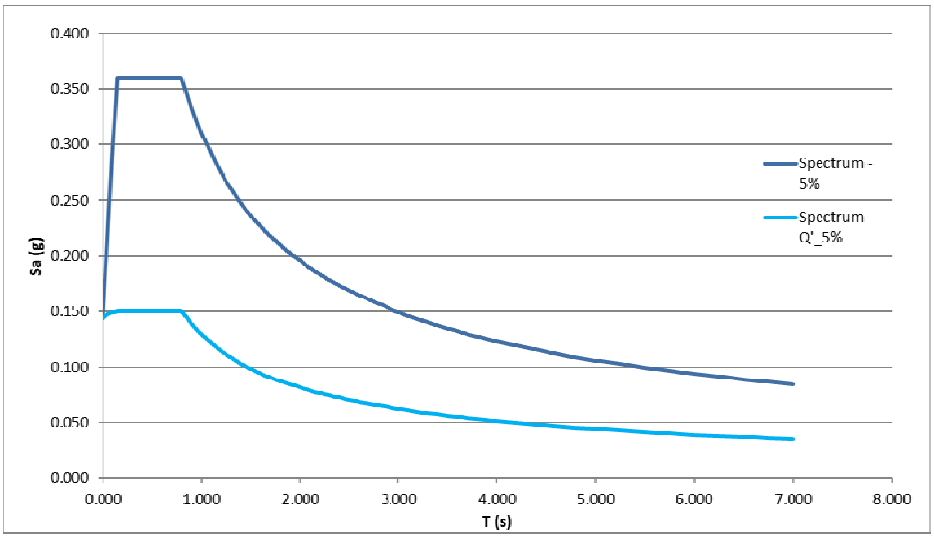

FIGURE 5.44 RESPONSE SPECTRUM - 5% DAMPING

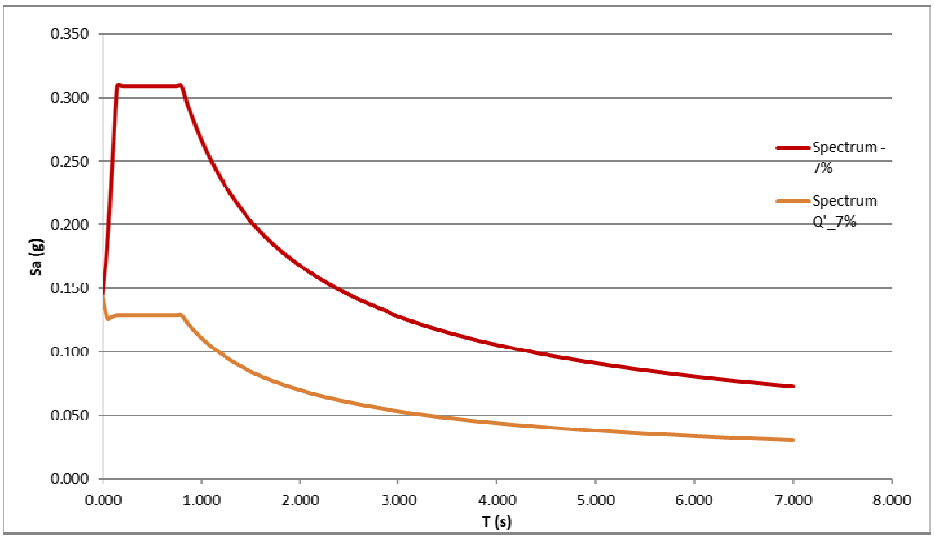

FIGURE 5.45 RESPONSE SPECTRUM - 7% DAMPING

The columns of the frame have been designed according to the building code requirements (ACI 318-14) usingthe design response spectrumwith 5% of damping, reduced for Q'.Have been considered the maximum effects from the basic combinations with the seismic load effects according to Guadalajara's Local Code, as shown in paragraph *5.2.1*.

Basic Combinations with Seismic Load Effects:

$1.4(DL+SCM)+1.0LL \pm E_y$

$0.7(DL+SCM) \pm E_y$

The design procedure provided by the software ETABS led to the definition of the amount of steel needed for all the elements of the frame, in order to satisfy the requirements of the code in terms of capacity design and resistence. The amount of steel provided for the columns has been used to define the number of longitudinal barsand the transversereinforcements, (tab. 19).In order to simplify the design, the distribution of the shear reinforcements has been assumed constant for all the length of the element.

According to the American code (ACI 318-14), the steel used for the calculation oflongitudinal and transverse rebars is*ASTM A615Grade 60*, whose properties are shown below.

Steel	$f_{y,d}$ [Mpa]	f_u[Mpa]	E_s[Mpa]
A615Grade 60	413,69	620,53	200000

TABLE 5-15 MATERIAL PROPERTIES

TABLE 5-16 COLUMNS STEEL REINFORCEMENTS

Levels	Column line 49			Column line 36			Column line 33			Column line 27			Column line 22		
	Size [cm]	N. Long. Reb.	Shear Reinf.	Size [cm]	N. Long. Reb.	Shear Reinf.	Size [cm]	N. Long. Reb.	Shear Reinf.	Size [cm]	N. Long. Reb.	Shear Reinf.	Size [cm]	N. Long. Reb.	Shear Reinf.
AZO	80X120	14 ϕ32	7 ϕ12/150	80X120	14 ϕ32	7 ϕ12/150	80X120	14 ϕ32	7 ϕ12/150	80X120	14 ϕ32	7 ϕ12/150	80X120	14 ϕ32	7 ϕ12/150
N37	80X120	14 ϕ32	7 ϕ12/150	80X120	14 ϕ32	7 ϕ12/150	80X120	14 ϕ32	7 ϕ12/150	80X120	14 ϕ32	7 ϕ12/150	80X120	14 ϕ32	7 ϕ12/150
N36	80X120	14 ϕ32	7 ϕ12/150	80X120	14 ϕ32	7 ϕ12/150	80X120	14 ϕ32	7 ϕ12/150	80X120	14 ϕ32	7 ϕ12/150	80X120	14 ϕ32	7 ϕ12/150
N35	80X120	14 ϕ32	7 ϕ12/150	80X120	14 ϕ32	7 ϕ12/150	80X120	14 ϕ32	7 ϕ12/150	80X120	14 ϕ32	7 ϕ12/150	80X120	14 ϕ32	7 ϕ12/150
N34	80X120	14 ϕ32	7 ϕ12/150	80X120	14 ϕ32	7 ϕ12/150	80X120	14 ϕ32	7 ϕ12/150	80X120	14 ϕ32	7 ϕ12/150	80X120	14 ϕ32	7 ϕ12/150
N33	80X120	14 ϕ32	7 ϕ12/150	80X120	14 ϕ32	7 ϕ12/150	80X120	14 ϕ32	7 ϕ12/150	80X120	14 ϕ32	7 ϕ12/150	80X120	14 ϕ32	7 ϕ12/150
N32	80X120	14 ϕ32	7 ϕ12/150	80X120	14 ϕ32	7 ϕ12/150	80X120	14 ϕ32	7 ϕ12/150	80X120	14 ϕ32	7 ϕ12/150	80X120	14 ϕ32	7 ϕ12/150
N31	80X120	16 ϕ32	8 ϕ12/150	80X120	14 ϕ32	7 ϕ12/150	80X120	14 ϕ32	7 ϕ12/150	80X120	14 ϕ32	7 ϕ12/150	80X120	14 ϕ32	7 ϕ12/150
N30	80X140	16 ϕ32	8 ϕ12/150	80X120	14 ϕ32	7 ϕ12/150	80X120	14 ϕ32	7 ϕ12/150	80X120	14 ϕ32	7 ϕ12/150	80X140	16 ϕ32	7 ϕ12/150
N29	80X140	16 ϕ32	8 ϕ12/150	80X140	16 ϕ32	8 ϕ12/150	80X140	16 ϕ32	8 ϕ12/150	80X140	16 ϕ32	8 ϕ12/150	80X140	16 ϕ32	8 ϕ12/150
N28	80X140	16 ϕ32	8 ϕ12/150	80X140	16 ϕ32	8 ϕ12/150	80X140	16 ϕ32	8 ϕ12/150	80X140	16 ϕ32	8 ϕ12/150	80X140	16 ϕ32	8 ϕ12/150
N27	80X140	16 ϕ32	8 ϕ12/150	80X140	16 ϕ32	8 ϕ12/150	80X140	16 ϕ32	8 ϕ12/150	80X140	16 ϕ32	8 ϕ12/150	80X140	16 ϕ32	8 ϕ12/150
N26	80X140	16 ϕ32	8 ϕ12/150	80X140	16 ϕ32	8 ϕ12/150	80X140	16 ϕ32	8 ϕ12/150	80X140	16 ϕ32	8 ϕ12/150	80X140	16 ϕ32	8 ϕ12/150
N25	80X140	18 ϕ32	8 ϕ12/150	80X140	18 ϕ32	8 ϕ12/150	80X140	18 ϕ32	8 ϕ12/150	80X140	18 ϕ32	8 ϕ12/150	80X140	16 ϕ32	8 ϕ12/150
N24	80X160	18 ϕ32	8 ϕ12/150	80X160	18 ϕ32	8 ϕ12/150	80X160	18 ϕ32	8 ϕ12/150	80X160	18 ϕ32	8 ϕ12/150	80X160	18 ϕ32	8 ϕ12/150
N23	80X160	20 ϕ32	8 ϕ12/150	80X180	20 ϕ32	8 ϕ12/150	80X180	20 ϕ32	8 ϕ12/150	80X180	20 ϕ32	8 ϕ12/150	80X160	18 ϕ32	8 ϕ12/150
N22	80X180	20 ϕ32	8 ϕ12/150	80X180	20 ϕ32	8 ϕ12/150	80X180	20 ϕ32	8 ϕ12/150	80X180	20 ϕ32	8 ϕ12/150	80X180	20 ϕ32	8 ϕ12/150
N21	80X180	20 ϕ32	8 ϕ12/150	80X180	20 ϕ32	8 ϕ12/150	80X180	20 ϕ32	8 ϕ12/150	80X180	20 ϕ32	8 ϕ12/150	80X180	20 ϕ32	8 ϕ12/150
N20	80X180	20 ϕ32	8 ϕ12/150	80X180	20 ϕ32	8 ϕ12/150	80X180	20 ϕ32	8 ϕ12/150	80X180	20 ϕ32	8 ϕ12/150	80X180	20 ϕ32	8 ϕ12/150
N19	80X180	20 ϕ32	8 ϕ12/150	80X180	20 ϕ32	8 ϕ12/150	80X180	20 ϕ32	8 ϕ12/150	80X180	20 ϕ32	8 ϕ12/150	80X180	20 ϕ32	8 ϕ12/150
N18	80X180	20 ϕ32	8 ϕ12/150	80X180	20 ϕ32	8 ϕ12/150	80X180	20 ϕ32	8 ϕ12/150	80X180	20 ϕ32	8 ϕ12/150	80X180	20 ϕ32	8 ϕ12/150
N17	80X180	20 ϕ32	8 ϕ12/150	80X180	20 ϕ32	8 ϕ12/150	80X180	20 ϕ32	8 ϕ12/150	80X180	20 ϕ32	8 ϕ12/150	80X180	20 ϕ32	8 ϕ12/150
N16	80X180	20 ϕ32	8 ϕ12/150	80X180	20 ϕ32	8 ϕ12/150	80X180	20 ϕ32	8 ϕ12/150	80X180	20 ϕ32	8 ϕ12/150	80X180	20 ϕ32	8 ϕ12/150
N15	80X180	20 ϕ32	8 ϕ12/150	80X180	20 ϕ32	8 ϕ12/150	80X180	20 ϕ32	8 ϕ12/150	80X180	20 ϕ32	8 ϕ12/150	80X180	20 ϕ32	8 ϕ12/150
N14	80X180	20 ϕ32	8 ϕ12/150	80X180	20 ϕ32	8 ϕ12/150	80X180	20 ϕ32	8 ϕ12/150	80X180	20 ϕ32	8 ϕ12/150	80X180	20 ϕ32	8 ϕ12/150
N13	80X180	24 ϕ32	8 ϕ12/150	90X200	24 ϕ32	8 ϕ12/150	80X180	24 ϕ32	8 ϕ12/150	90X200	24 ϕ32	8 ϕ12/150	80X180	24 ϕ32	8 ϕ12/150
N12	90X200	24 ϕ32	8 ϕ12/150	90X200	24 ϕ32	8 ϕ12/150	90X200	24 ϕ32	8 ϕ12/150	90X200	24 ϕ32	8 ϕ12/150	90X200	24 ϕ32	8 ϕ12/150
N11	90X200	24 ϕ32	8 ϕ12/150	90X200	24 ϕ32	8 ϕ12/150	90X200	24 ϕ32	8 ϕ12/150	90X200	24 ϕ32	8 ϕ12/150	90X200	24 ϕ32	8 ϕ12/150
N10	90X200	24 ϕ32	8 ϕ12/150	90X200	24 ϕ32	8 ϕ12/150	90X200	24 ϕ32	8 ϕ12/150	90X200	24 ϕ32	8 ϕ12/150	90X200	24 ϕ32	8 ϕ12/150
N9	90X200	24 ϕ32	8 ϕ12/150	90X200	24 ϕ32	8 ϕ12/150	90X200	24 ϕ32	8 ϕ12/150	90X200	24 ϕ32	8 ϕ12/150	90X200	24 ϕ32	8 ϕ12/150
N8	90X200	24 ϕ32	8 ϕ12/150	90X200	24 ϕ32	8 ϕ12/150	90X200	24 ϕ32	8 ϕ12/150	90X200	24 ϕ32	8 ϕ12/150	90X200	24 ϕ32	8 ϕ12/150
N7	90X200	24 ϕ32	8 ϕ12/150	90X200	24 ϕ32	8 ϕ12/150	90X200	24 ϕ32	8 ϕ12/150	90X200	24 ϕ32	8 ϕ12/150	90X200	24 ϕ32	8 ϕ12/150
N6	90X200	24 ϕ32	8 ϕ12/150	90X200	24 ϕ32	8 ϕ12/150	90X200	24 ϕ32	8 ϕ12/150	90X200	24 ϕ32	8 ϕ12/150	90X200	24 ϕ32	8 ϕ12/150
N5	90X200	24 ϕ32	8 ϕ12/150	100X200	26 ϕ32	8 ϕ12/150	90X200	24 ϕ32	8 ϕ12/150	100X200	26 ϕ32	8 ϕ12/150	90X200	24 ϕ32	8 ϕ12/150
N4	90X200	24 ϕ32	8 ϕ12/150	100X200	26 ϕ32	8 ϕ12/150	90X200	24 ϕ32	8 ϕ12/150	100X200	26 ϕ32	8 ϕ12/150	90X200	24 ϕ32	8 ϕ12/150
N3	120X200	32 ϕ32	8 ϕ12/150	120X200	32 ϕ32	8 ϕ12/150	120X200	32 ϕ32	8 ϕ12/150	120X200	32 ϕ32	8 ϕ12/150	120X200	32 ϕ32	8 ϕ12/150
N2	120X200	32 ϕ32	8 ϕ12/150	120X200	32 ϕ32	8 ϕ12/150	120X200	32 ϕ32	8 ϕ12/150	120X200	32 ϕ32	8 ϕ12/150	120X200	32 ϕ32	8 ϕ12/150
N1	120X200	32 ϕ32	8 ϕ12/150	120X200	32 ϕ32	8 ϕ12/150	120X200	32 ϕ32	8 ϕ12/150	120X200	32 ϕ32	8 ϕ12/150	120X200	32 ϕ32	8 ϕ12/150

Similarly, the beams of the frame have been designed according to the building code requirements (ACI 318-14), using the design response spectrum with 7% of damping, reduced for the ductility factor Q'.

The amount of steel provided by the software for the beam elements has been used to define the longitudinal bars and the shear reinforcements whose distribution has been assumed constant for all the length of the beam, tab. 20.

TABLE 5-17 BEAMS STEEL REINFORCEMENTS

Levels	Size [cm]	As Top	As Bot	Shear Reinf.
AZO	50X90	8 ϕ32	4 ϕ32	2 ϕ12/100
N37	50X90	9 ϕ32	5 ϕ32	2 ϕ12/100
N36	50X90	10 ϕ32	5 ϕ32	2 ϕ12/100
N35	50X90	10 ϕ32	5 ϕ32	2 ϕ12/100
N34	50X90	10 ϕ32	5 ϕ32	2 ϕ12/100
N33	50X90	10 ϕ32	5 ϕ32	2 ϕ12/100
N32	50X90	10 ϕ32	5 ϕ32	2 ϕ12/100
N31	50X90	11 ϕ32	5 ϕ32	2 ϕ12/100
N30	50X90	11 ϕ32	5 ϕ32	2 ϕ12/100
N29	50X90	11 ϕ32	5 ϕ32	2 ϕ12/100
N28	50X90	11 ϕ32	5 ϕ32	2 ϕ12/100
N27	50X90	11 ϕ32	5 ϕ32	2 ϕ12/100
N26	50X90	11 ϕ32	5 ϕ32	2 ϕ12/100
N25	50X90	11 ϕ32	5 ϕ32	2 ϕ12/100
N24	50X90	11 ϕ32	5 ϕ32	2 ϕ12/100
N23	50X90	11 ϕ32	5 ϕ32	2 ϕ12/100
N22	50X120	10 ϕ32	5 ϕ32	2 ϕ12/100
N21	50X120	10 ϕ32	5 ϕ32	2 ϕ12/100
N20	50X120	10 ϕ32	5 ϕ32	2 ϕ12/100
N19	50X90	11 ϕ32	6 ϕ32	2 ϕ12/100
N18	50X90	11 ϕ32	6 ϕ32	2 ϕ12/100
N17	50X90	11 ϕ32	6 ϕ32	2 ϕ12/100
N16	50X90	11 ϕ32	7 ϕ32	2 ϕ12/100
N15	50X90	11 ϕ32	7 ϕ32	4 ϕ12/150
N14	50X90	11 ϕ32	7 ϕ32	4 ϕ12/150
N13	50X90	11 ϕ32	7 ϕ32	4 ϕ12/150
N12	50X90	10 ϕ32	8 ϕ32	4 ϕ12/150
N11	50X90	10 ϕ32	8 ϕ32	4 ϕ12/150
N10	50X90	10 ϕ32	8 ϕ32	4 ϕ12/150
N9	50X90	11 ϕ32	9 ϕ32	4 ϕ12/150
N8	50X90	11 ϕ32	9 ϕ32	4 ϕ12/150
N7	50X90	11 ϕ32	9 ϕ32	4 ϕ12/150
N6	50X90	11 ϕ32	9 ϕ32	4 ϕ12/150
N5	50X90	11 ϕ32	9 ϕ32	4 ϕ12/150
N4	50X90	10 ϕ32	9 ϕ32	4 ϕ12/150
N3	60X120	11 ϕ32	10 ϕ32	4 ϕ12/150
N2	60X120	11 ϕ32	10 ϕ32	4 ϕ12/150
N1	60X140	10 ϕ32	8 ϕ32	2 ϕ12/100

The beams design obtained for 7% of damping can provide a reduction of the amount of steel for longitudinal rebars up to 15% for each beam, this evidence a great economic advantage, especially for tall buildings.

5.6.1 CHECKING OF STRUCTURAL DESIGN

The steel reinforcements calculated has to be assigned to the frame section of the model in order to define the plastic hinges for each element.

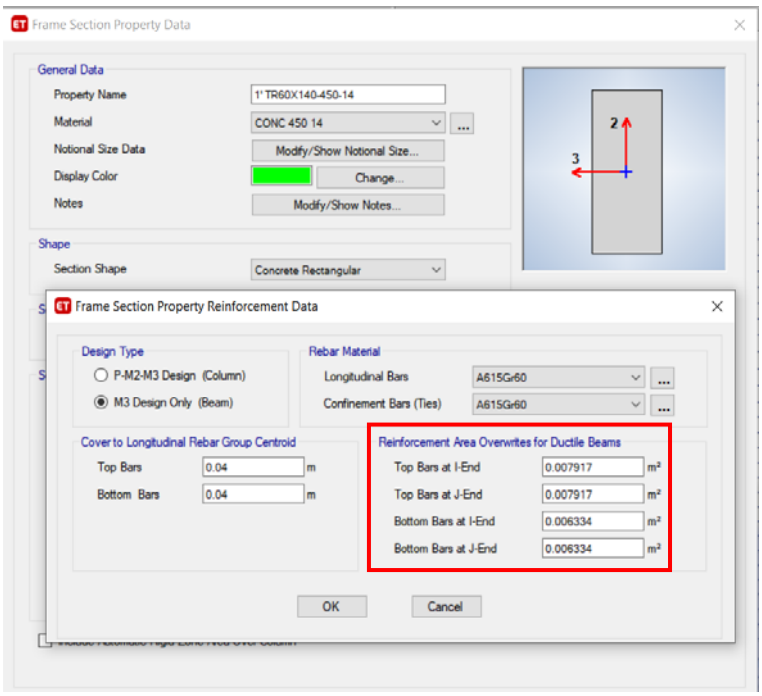

FIGURE 5.46 ASSIGNING STEEL REINFORCEMENTS TO THE FRAME - ETABS

5.6.1.1 DEFINITION OF THE HINGE PROPERTIES

Each plastic hinge is modeled as a discrete point hinge. All plastic deformation, whether it be displacement or rotation, occurs within the point hinge. For this reason, it is necessary to assume a length for the hinge over which the plastic strain or plastic curvature is integrated.

For each force or moment degree of freedom, it has to be defined a force-displacement (moment-rotation) curve that gives the yield value and the plastic deformation after yield. This is done in terms of a curve with values at five points, A-B-C-D-E, as shown in fig.5.47.

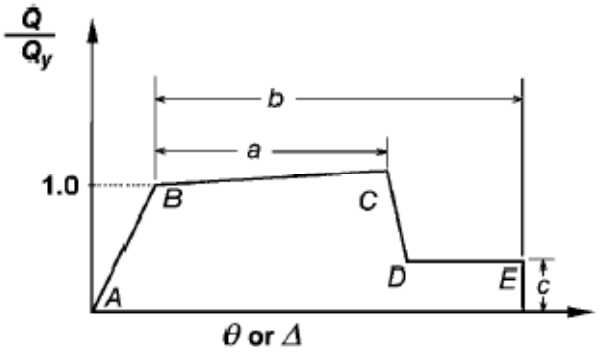

FIGURE 5.47 PLASTIC HINGE CURVE DEFINITION

• Point A is always the origin.

• Point B represents yielding. No deformation occurs in the hinge up to point B, regardless of the deformation value specified for point B. The displacement (rotation) at point B will be subtracted from the deformations at points C, D, and E. Only the plastic deformation beyond point B will be exhibited by the hinge.Prior to reaching point B, all deformation is linear and occurs in the frame element itself, not the hinge. Plastic deformation beyond point B occurs inthe hinge in addition to elastic deformation that may occur in the element.

In the software ETABS, the plastic hinges can be assigned through the automatic method based on Tables 6-7 and 6-8 in FEMA-356 implemented in the structural program Etabs through Table 10-8 of ASCE 41-13. The deformation is expressed with rotation and the parameters “a” and “b” refer to plastic deformation that occurs after yield. The parameter “c” is the residual strength ratio. The parameters “a”, “b” and “c” are defined numerically as shown in the following table.

Table 10-8. Modeling Parameters and Numerical Acceptance Criteria for Nonlinear Procedures—Reinforced Concrete Columns

		Modeling Parameters[a]			Acceptance Criteria[a]		
		Plastic Rotations Angle (radians)		Residual Strength Ratio	Plastic Rotations Angle (radians)		
					Performance Level		
Conditions		a	b	c	IO	LS	CP
Condition i.[b] $\frac{P}{A_g f'_c}$[c]	$\rho = \frac{A_v}{b_w s}$						
≤0.1	≥0.006	0.035	0.060	0.2	0.005	0.045	0.060
≥0.6	≥0.006	0.010	0.010	0.0	0.003	0.009	0.010
≤0.1	=0.002	0.027	0.034	0.2	0.005	0.027	0.034
≥0.6	=0.002	0.005	0.005	0.0	0.002	0.004	0.005

TABLE 5-18 [TABLE 10-8 ASCE 41-13]

Before performing a nonlinear analysis,the reinforcing steel must be explicitly defined, or else the section must have already been designed by the program.

The results of the nonlinear analysis shown the plastic displacements and/or rotations in terms of the most extreme state experienced by the hinge in any degree of freedom. These states are indicated as:

- A to B
- B to C
- C to D
- D to E
- >E

The hinges are plotted as colored dots indicating their most extreme state or status, immediate occupation (IO), life safety (LS), or collapse prevention (CP):

• B to IO

• IO to LS

• LS to CP

• CP to C

• C to D

• D to E

• > E

5.6.1.2 IMPLEMENTATION OF PLASTIC HINGES

The plastic hinges have been modeled through the automatic method, automatic properties require that the program have detailed knowledge of the frame section property used by the element that contains the hinge. For the concrete beams have been generated plastic hinges type M2 or M3, for the concrete columns have been generated plastic hinges type P-M2 or P-M3 because it is a bidimensional case. To assign the plastic hinges it was necessary to define the relative distance that is a defined point

where is focused the plastic hinge. This value is the ratio between the height of the plastic hinge and the total height of the column.The length of the plastic hinge was calculated, according to ACI 318-14, as L_{c1}= max (h_{col}, L_{col}/6, 450mm).

Then have been set the parameters of the hinges regarding the reference table, the degree of freedom and the failure condition.

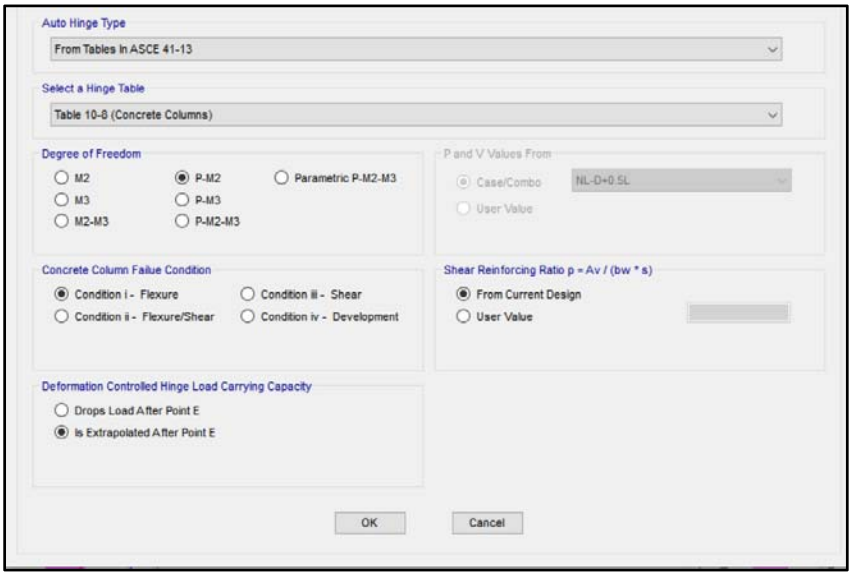

FIGURE 5.48 PLASTIC HINGE PROPERTIES SETTING - ETABS

5.6.1.3 NONLINEAR TIME-HISTORY ANALYSES OUTPUT

Afterward, nonlinear time-history analyses with direct integration have been run for two of the eleven seismic signals available, selecting the once characterized by the highest peaks of acceleration, this because the test has the purpose to check the performance of the structural design.

The output of the analyses are shown below:

NLTH – Acx0006

Development of the Plastic Hinges

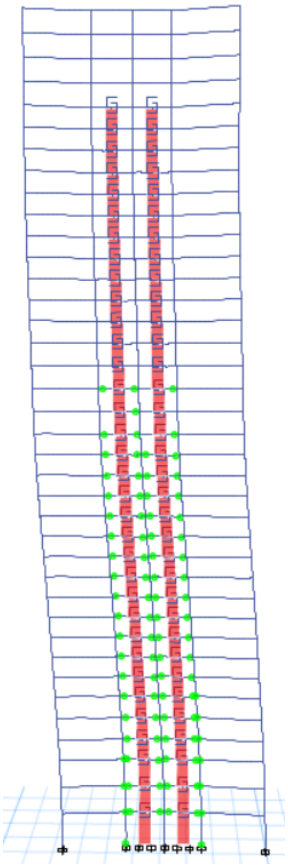

Plastic Hinge Response ***SLB Hysteretic Behavior***

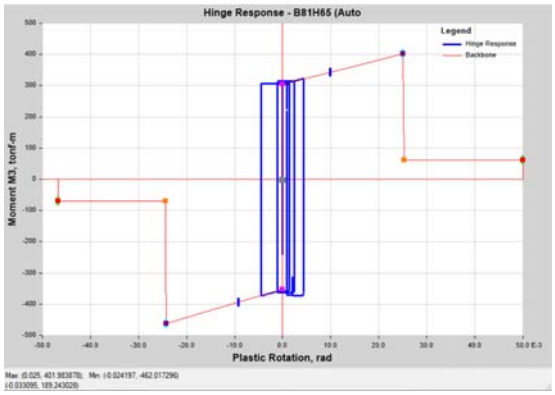

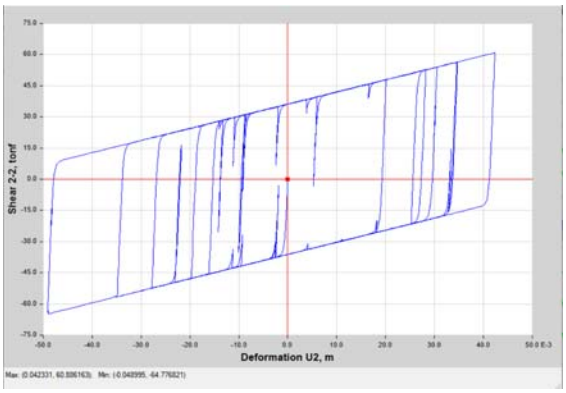

M_{max}= *401,01tonf-m* *θ=0,025rad* *V=597,23kN* Δ = *42mm*

FIGURE 5.49PERFORMANCE OF THE STRUCTURE

In the table 5.50 are reported the results of the nonlinear analysis run with the seismic signal acx0006. The plastic hinges have been developed in correspondence of the beams where have been installed the devices, this is due to the fact that the presence of the devices produces a redistribution of the stiffness in the frames of the structure. It is shown the state of the plastic hinges according to the performance levels that are immediate occupation (IO), life safety (LS), collapse prevention (CP). According to Table 10-8 of ASCE/SEI 41-13 the performance levels are related to the plastic rotation angle (radians) that depends on the failure condition and the amount of steel reinforcement.For this reason, plastic hinges developed by the structure reached the performance level of immediate occupation (IO) without reaching the level of live safety (LS). In the fig.5.49 it is shown the plastic hinge response in correspondence of the 6^{th} level, where has been registered the maximum displacement of the SLB device whose hysteretic behavior has been plotted in order to check its displacement capacity.

In order to confirm the previous results, another analysis has been run with the seismic signal acx0003 whose results are shown below:

NLTH – Acx0003

Development of the Plastic Hinges

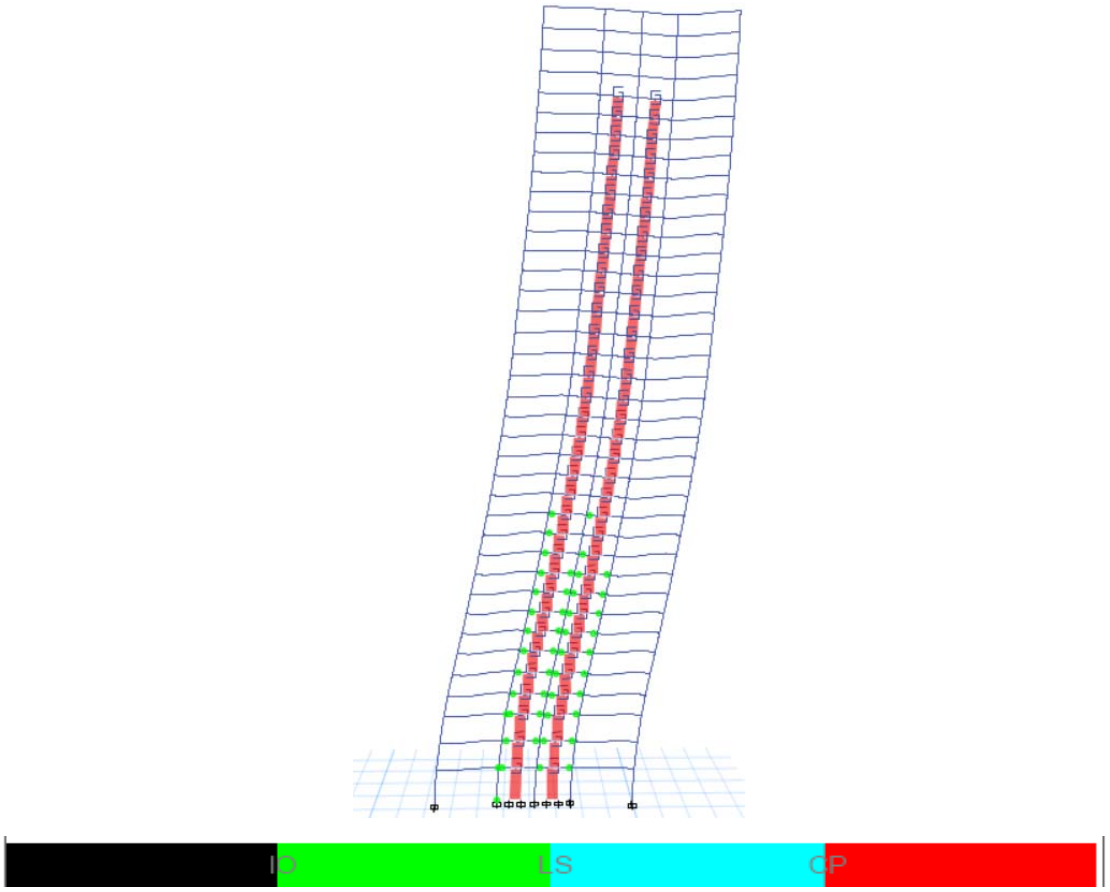

Plastic Hinge Resonse ***SLB Hysteretic Behavior***

M_{max}= *401,01tonf-m* *θ=0,025rad* *V=510,12kN* *Δ = 36mm*

FIGURE 5.50 PERFORMANCE OF THE STRUCTURE

The results of the analysis are compatible with the previous, indeed also in this case the plastic hinges have been developed in correspondence of the beams where have been installed the devices and reached the performance level of immediate occupation (IO) without reaching the level of live safety (LS). In the fig. 5.50has been shown the plastic response of the hinge and the hysteretic behavior of the device which also in this case reached the largest displacement in correspondence of the 6^{th} floor.

The results of the analyses show that the reduction of the amount of steel for flexion provided by the procedure adopted to increase the damping ratio led to an optimization of the structural design without reducing the performance. Obviously, for the case study it has been considered a simplified example, but to confirm the results it will be necessary to analyze the nonlinear behavior of the complete structure.

It is also possible to notice that in the previous analyses the structure has not developed a complete plastic response, this means that it hasn't reached the maximum optimization of the design. In order to obtain a better optimization, it could be possible to adopt the performance-based design, a more complex method and computationally intensive.

6 CONCLUSIONS

The “Shear link Bozzo” (SLB) device represents a good solution for seismic protection of buildings structures,providing a significant contribution in the reduction of the inter-story drift and a great capacity of energy dissipation due to its hysteretic behavior. It also provides the capacity to concentrate plastic deformations in the device preserving structural elements from damage.The introduction of the fourth generation of Shear Link Bozzo led to the definition of devices characterized by greater displacement capacity than the previous generation and, consequently, to greater energy dissipation capacity. In order to evaluate the effects of the dissipative capacity of the new devices on the structural behavior, it has been implemented a new procedure in order to evaluate the increase of the total damping of the structure due to the installation of SLB devices. The evaluation of the equivalent damping has been based on the calibration of the linear dynamic analysis over the results of the nonlinear time-history analysis, increasing the damping value of the linear analysis iteratively. The procedure provided has to be applied after the design of the SLB devices through one of the design procedurescommonly employed in professional practice, to specify, the “direct” iterative procedure and the “inverse” iterative procedure, both based upon the shear check acting on the dissipator.

An application of the design procedure and estimation of the equivalent damping has been shown for a complex case study situated in Guadalajara (Mexico). Thestructure analyzed has been equipped with SLB of fourth-generation designed through the inverse iterative method. The results obtainedshow an improvement of the structural behavior in terms of inter-story drift and of story shear but because of the not optimal disposition of the supporting elements on plane due to the architectural restrictions, the structure shows a torsional first mode of vibration. In the specific, it would be preferable to place the walls of concrete symmetrically respect to the center of the building.

The increase of the dissipative capacity of the structure due to the installation of the devices has been considered through the application of the procedure of evaluation of the equivalent damping.Based on the evidence of the results obtained from the comparison of the linear and nonlinear time-history analyses for 11 seismic signals and

considering a restrictive tolerance range,it has been obtained an equivalent damping value of 7%.

The next step was to design the structural elements optimizing the design taking into account the dissipative capacity of the devices installed through the use of the equivalent damping obtained from the previous analyses. To operate in a conservative range it has been decided to adopt the 7% of damping to design the beams elements and the conventional 5% of damping to design the columns.For this part of the study, it has been considered a simplified example case, in the specific, it has been considered just one of the frames of the structure, in the most deformable direction, in order to reduce the computational time. The final results led to a reduction of the amount of steel for the beams up to 15% for each floor leading to great economic advantages especially for tall buildings.

The final step of the study was to check the performance of the structural design of the frame considered in the case study through a complete nonlinear time-history analysis considering both geometric and material nonlinearities. Conducing the analyses for two of the signals provided, it has been possible to have a clear idea of the behavior of the structure designed. The output of the analyses show the development of the plastic hinges in the lower levels of the structure, in correspondence of the beams where have been installed the devices and at the base of the relative columns, this is due to the fact that the presence of the devices produces a redistribution of the stiffness in the frames of the structure.Furthermore, the results show that plastic hinges reached the performance level of immediate occupation (IO) without reaching the level of live safety (LS). Considering the plots of the plastic response of the hinges and the plots of the hysteretic cycle of the devices, it is possible to see how most part of the energy has been dissipated through the devices reducing, or avoiding in some cases, the excursion in plastic zone of the structural elements, confirming the correct functioning of the devices. In fact, the damage is concentrated mainly in the SLB devices that, after a strong earthquake, can be easily replaced and in a cheap way.

According to the results obtained it is possible to assert that the reduction of the amount of steel for flexion provided by the procedure adopted to increase the damping ratio led to an optimization of the structural design without reducing the performance.

Considering that the structure has not developed a complete plastic response, this means that it hasn't reached the maximum optimization of the design. In order to obtain a better optimization, it could be possible to increase the tolerance range of comparison adopted in the procedure of evaluation of the equivalent damping leading to adopt higher damping values or to adopt the performance-based design, a more complex method of design based on nonlinear analyses and for this reason computationally intensive.

Obviously, for the case study it has been considered a simplified example, but to confirm the results it will be necessary to analyze the nonlinear behavior of the complete structure.

It is important to specify that the definition of a procedure to adopt to optimize the structural design increasing the damping value is in a preliminary phase, it is necessary to analyze much more cases and compare all the results in order to calibrate correctly all the parameters considered and to define a complete procedure to implement in the design process.

REFERENCES

Aiken Ian D. [et al.] Testing of Passive Energy Dissipation Systems [Rivista]. - 1993.

American Society of Civil Engineers Structural Engineers Institute ASCE/41-13 Seismic Evaluation and Retrofit of Existing Buildings [Libro]. - 2013.

American Society of Civil Engineers Structural Engineers Institute. ASCE/SEI 7-16 [Libro]. - 2016.

BenaventCliment Amadeo [et al.] Estructuras con sistemas de protección sísmica [Libro]. - 2020.

Bozzo Dr. Luis M [et al.] ANÁLISIS Y DISEÑO UTILIZANDO DISIPADORES SÍSMICOS TIPO SLB EJEMPLOS DE APLICACIÓN [Rivista]. - 2019.

Bozzo Luis M. VENTAJAS EMPLEO DISIPADORES SLB EN PROYECTO OAK 58 EN PUEBLA DESEMPEÑO ESPERADO DE PROYECTO OAK 58 DURANTE SISMO DE PUEBLA DEL 17 DE SEPTIEMBRE DEL 2017 [Rapporto]. - 2018.

Constantinou Michael. C., Soong Tsu. T. e Dargush Gary. F. Passive Energy Dissipation Systems For Structural Design and Retrofit [Libro]. - 1998.

Construction American Institute of Steel AISC 327 SEISMIC DESIGN MANUAL [Libro]. - 2018.

CSi CSi Analysis Reference Manual [Libro]. - 2017.

Fernández Guillermo Bozzo Simulación de un ensayo en mesa vibrante de una estructura con dispositivos de disipación sísmica para viviendas de bajo coste [Rivista]. - 2018.

Fernández Guillermo Bozzo UNA NUEVA GENERACIÓN DE DISIPADORES SLB “SHEAR LINK” PARA EL DISEÑO SISMORRESISTENTE [Rivista]. - 2020.

Hurtado Francisco e Bozzo Luis M. NUMERICAL AND EXPERIMENTAL ANALYSIS OF A SHEAR-LINK ENERGY DISSIPATOR FOR SEISMIC PROTECTION OF BUILDINGS [Rivista]. - 2008.

Institute American Concrete ACI 318-19 Building Code Requirements [Libro]. - 2019.

Iolanda Nuzzo Daniele Losanno, Fabrizia Cilento, Nicola Caterino Analytical and numerical modelling of shear-link device for seismic energy [Rivista]. - 2020.

Iolanda Nuzzo Daniele Losanno, Giorgio Serino, Luis M. Bozzo Rotondo A Seismic-resistant Precast r.c. System equipped with Shear Link Dissipators for Residential Buildings [Rivista]. - 2015.

Iolanda Nuzzo Daniele Losanno, Nicola Caterino, Giorgio Serino, Luis M. Bozzo Rotondo Experimental and analytical characterization of steel shear links for seismic energy dissipation [Rivista]. - 2018.

L. M. Bozzo J. Ramirez, J. Bairan, G. Bozzo, E. Muñoz PRECAST BUILDINGS EQUIPPED WITH SLB SEISMIC DEVICES [Rivista]. - 2020.

LEONARDO BANDINI TECNICHE AVANZATE DI MODELLAZIONE STRUTTURALE E VERIFICHE AI SENSI DELLE NTC2008 [Atti di convegno]. - [s.l.] : CSi Italia, 2012.

M. Pantoja H. Gonzales, L.M. Bozzo, G.Bozzo, J. Ramirez EXPERIMENTAL VS NUMERICAL CORRELATION FOR A SHAKING TABLE TEST OF A CONCRETE PRECAST MODEL STRUCTURE EQUIPPED WITH SLB DEVICES [Rivista]. - 2020.

M. Pantoja M. Flores, L. Bozzo, H. Gonzales NUMERICAL ANALYSIS AND EXPERIMENTAL CORRELATION OF UNCOUPLED CONCRETE WALLS INCORPORATING SLB DEVICES [Rivista]. - 2020.

Ozcelik Ramazan, Dikiciasik Yagmur e Erdil Elif Firuze The development of the buckling restrained braceswith new end restrains [Rivista]. - 2016.

P.S.Balaji [et al.] Wire rope isolators for vibration isolation of equipment and structures [Rivista]. - 2015.

Públicas Dirección General de Obras REGLAMENTO DE CONSTRUCCIONES Y DESARROLLO URBANO DEL MUNICIPIO DE ZAPOPAN, JALISCO Y NORMAS TÉCNICAS COMPLEMENTARIAS PARA DISEÑO POR SISMO [Libro]. - 2008.

Soong T.T. e B.F. Spencer Jr Supplemental energy dissipation: state-of-the-art and state-of-thepractice [Rivista]. - 2002.

Zahraei Seyed Mehdi, Moradi Alireza e Moradi Mohammadreza Using Pall Friction Dampers for Seismic Retrofit of a 4-Story Steel Building in Iran [Rivista]. - 2013.

Rivolgo un ringraziamento speciale al Prof. Giorgio Serino per avermi guidato nella stesura del lavoro di tesi e soprattutto per avermi dato l'opportunità di vivere un'esperienza di tirocinio unica ed estremamente formativa.

All'Ing. Iolanda Nuzzo per il fondamentale contributo nello sviluppo del lavoro di tesi

Rivolgo inoltre i ringraziamenti più importanti ai miei genitori per avermi sempre supportato e spronato specialmente nei momenti più difficili.

Ai miei migliori amici Francesco, Giuseppe, Pasquale e Vincenzo per essere stati sempre presenti ed avermi regalato tanti momenti di spensieratezza.

Ai miei collegi e amici Antonio, Elsa e Santo per avermi accompagnato in questo lungo percorso di studio e per aver condiviso con me momenti di gioia e di fatica.

A special thanks to Prof. Luis Bozzo for giving me the chance to collaborate with the activities of his high qualified company improving my knowledge and giving me the opportunity to carry out the research work for my thesis. A thank you to all his collaborators especially Andres, Leonardo, Marlon, Rodrigo and Guillermo, for their availability and their help.